Characterizing the Mesolimbic Dopamine Reward Pathway in a Magel2-null Mouse, a Model of Prader-Willi Syndrome

by

Chloe Luck Gibson

A thesis submitted in partial fulfillment of the requirements for the degree of

Master of Science

Medical Sciences – Genetics

University of Alberta

Abstract

Prader-Willi Syndrome (PWS) is a genetic disorder characterized by extreme hyperphagia that can lead to severe obesity. The abnormal motivation to eat in PWS suggests a disruption in the hedonic feeding pathway, which is feeding based on reward as opposed to physiological need. Hedonic feeding is controlled by dopaminergic neurons in the ventral tegmental area (VTA) and other regions of the brain, forming a reward circuit. *Magel2* is one of the genes inactivated in PWS, and mice lacking *Magel2* have phenotypes that resemble those seen in people with PWS. The aim of this research project is to characterize the dopamine reward circuitry in a mouse model of PWS lacking the *Magel2* gene.

Regions important for motivative behaviour and reward processing were assessed. Immunohistochemistry, high-performance liquid chromatography (HPLC), and immunoblot analyses were used to identify the baseline differences within the reward pathway of *Magel2*-null mice. The responses to changes in diet which are similar to biochemical responses observed with drugs of abuse, were also measured by subjecting the mice to a high-fat diet, then withdrawing them from the high fat diet back to a standard diet. Specific molecular changes including the phosphorylation of ERK, AKT and CREB within brain regions that form the reward circuit were identified and measured in response to changes in diet. The levels of biogenic amines within the nuclei of the reward pathway were also assessed by HPLC, in response to the changes in diet. Binge feeding behavior was assessed by exposing the mice to a limited time access of high-fat food.

There was no difference between the *Magel2*-null and wildtype mice in the number of dopamine-producing cells within the nuclei of the reward pathway. However, the HPLC analysis showed a global reduction in the dopaminergic and serotonergic metabolites in the *Magel2*-null mice. The level of neurofilament was significantly increased in the hypothalamus of *Magel2*-null

mice, and the axonal calibre of forebrain projections from the VTA was significantly smaller in the *Magel2*-null animals. This could influence how much dopamine is reaching the target nuclei in response to rewarding behaviours. *Magel2*-null mice consume consistently less high-fat food when given limited access to a high-fat diet. This suggests an impaired bingeing response. This behavioural response suggests decreased dopaminergic responses to the exposure. *Magel2*-null mice show a loss of HPLC-detected differences between mice fed a chronic high-fat diet or a standard diet. *Magel2*-null also have an attenuated feeding response to the initial exposure of a HF-diet. This also suggests a decrease in dopamine signaling in response to a palatable food source.

In conclusion, *Magel2*-null mice show deficits throughout the dopamine reward pathway that indicate reduced dopamine-related activity. Deficits were observed both under baseline conditions, and in response to both acute and chronic exposure to a rewarding food source. This is consistent with the attenuated locomotive response to cocaine previously observed in mice lacking *Magel2*. This phenotype resembles the increased threshold for dopamine signaling and the subsequent feeling of reward that is observed in pathological drug users, driving the compulsive need to obtain the drug. Understanding how the loss of *Magel2* influences dopamine signaling and the molecular mechanisms driving the pathology of Prader-Willi Syndrome. This knowledge will be useful for the development or potential treatments for individuals with PWS and other forms of binge eating disorder.

Preface

Some of the results included in this thesis are part of a manuscript in press in the journal of Behavioural Neuroscience titled "Abnormal brain reward pathways in mice lacking *Magel2,* a Prader-Willi syndrome candidate gene." This manuscript includes work led by Dr. Rachel Wevrick in the Department of Medical Genetics at the University of Alberta, in collaboration with Dr. Martha H. Vitaterna at the Centre for Sleep and Circadian Biology at Northwestern University. Dr. Martha H. Vitaterna conducted the experiments on the locomotive response to cocaine included in Figure 1 of this manuscript. This experiment was conducted at Northwestern University, and influenced greatly the direction of this research project. This manuscript also includes experimental data that is also included in this thesis, and that was done by myself under the supervision of Dr. Wevrick at the University of Alberta in the Department of Medical Genetics. This includes data from Table 3.2 and results from Figures 3.4, 3.13, 3.31, 3.33, 3.38, 3.39, & 3.42-3.44. The University of Alberta Animal Care and Use Committee approved all procedures involving animals in accordance with the guidelines of the Canadian Council on Animal Care.

Acknowledgments

Throughout my time at the University of Alberta, I have met and worked with some amazing people who I would like to thank for their help along the way . I would like to acknowledge that none of this work would have been possible without the financial support received from the Department of Medical Genetics, and from Woman and Children's Research Institute (WCHRI).

First and foremost, I would like to thank my supervisor Rachel Wevrick. Thank you for accepting me into your lab and providing me with the best possible work environment. Thank you for providing me with all of the support and guidance needed to succeed. I would also like to thank my committee members for helping me through the process. Thank you Dr. Simonetta Sipione and Dr. Heather McDermid for agreeing to be on my committee and for your expertise.

I would like to thank both our lab technicians, Jocelyn Bischof and Herman Cortes for the advice they have given throughout my degree. You have helped me with everything from experimental design, to deciding which backstreet boy to have babies with. I would like to thank the other Wevrick lab members, Dila Kamaludin, Vanessa Carias, Christa Smolarchuk, Igor Pravdivyi, and Xiao Li. Thank you for working with me towards a common goal. I am lucky to have had the chance to work in such a cooperative, supportive lab.

I would like to thank Gail Rauw from Dr. Glen Baker's lab in the department of Psychiatry. Thank you for taking the time to not only performed the HPLC analysis with me, but for helping me learn the protocol step-by-step, from sample preparation to the analysis of the results, you were extremely willing to help.

I would also like to thank all the graduate students on the floor for providing an environment where students can work together and can come to each other for help. I would like to thank my peers for taking the time to help me and encourage me along the way. Thank you for being my friends and teammates in the lab and on the field. I am truly grateful.

Thank you to my support system outside of the lab. Thank you to my uncle and aunt for making Edmonton feel like home. Thank you to my mother, Angela Luck for unconditionally believing in me. I would also like to thank all of the Wolves soccer girls for providing me with the feeling of reward in the form exercise, and social interaction, along with the unnaturally huge feeling of euphoria that comes around once a year in the form of Kamloops.

Lastly I want to thank Vanessa Carias. Thank you for always having my back, and for making even the most tedious lab chores enjoyable. You are someone I admire and respect and my experience in the Wevrick lab would not have been the same without you.

Table of Contents

List of Figures

List of Tables

List of Abbreviations

α-MSH……α-Melanocortin-stimulating hormone

ΔFosB ……Delta FBJ murine osteosarcoma viral oncogene homolog B

2H3……Antibody recognizing neurofilament

3MT ……...3-Methoxytyramine

5HT ……Serotonin

5HIAA ……...5-Hydroxyindoleacetic acid

A10 ……Dopaminergic population in the ventral tegmental area

A14 ……Caudal-most dopaminergic cell population in the periventricular nucleus

A15 ……Rostral-most dopaminergic cell population in the periventricular nucleus

AADC ……...Aromatic amino acid decarboxylase

AgRP ……Agouti-related peptide

AKT ……...Protein kinase B

AMY……..Amygdala

ARC ……..Arcuate nucleus

ANOVA ……The analysis of variance (statistical test)

BDNF ……Brain-derived neurotrophic factor

BED ……...Binge eating disorder

CART ……Cocaine-and amphetamine regulated transcripts

CCK ……...Cholecystokinin

Cdk5 ……..Cyclin-dependent kinase 5

Cing ……...Cingulate cortex

COMT ……...Catechol-O-methyl transferase

CPAP …….Continuous positive airway pressure

CPu ……Caudate putamen

CRE ……...cAMP response element

CREB ……cAMP response element-binding protein

CSF ……Cerebral spinal fluid

D1,D2,D3,D4,D5 ……..Dopamine receptors

DA ……Dopamine

DAT ……..Dopamine transporter

DAPI ……4', 6-diamidino-2-phenylindole

DBH ……..Dopamine β-hydroxylase

DLPO ……Dorsolateral preoptic nucleus

DMH ……..Dorsomedial hypothalamus

DOPAC ……Dihydroxyphenylacetic acid

DYN ……..Dynorphin

E18.5 ……..Embryonic day 18.5

ERK ……...Extracellular signal-regulated kinases

fMRI ……..Functional magnetic resonance imaging

GABA ……Gamma-aminobutyric acid

GFAP …… Glial fibrillary acidic protein

GH ……Growth hormone

GLP-1…….Glucagon-like peptide-1

GluR2…….....Glutamate receptor 2

HIAO …….Hypothalamic injury-induced obesity

HPLC ….....High-performance liquid chromatography

HF …….High-fat

HVA ……..……Homovanillic acid

HYP ……...Hypothalamus

IHC ……Immunohistochemistry

INF ……Infundibular nucleus

IP ……...Intraperitoneal

LacZ ……..Gene encoding β-galactosidase

L-Dopa ……..L-3, 4-dihydroxyphenylalanine
LHA ……..Lateral hypothalamic area
Lep ……Leptin
LepR …….Leptin receptor
MAGE ……...Melanoma-antigen family gene
MAM……..Mammillary nucleus
MAO ……..…Monoamine oxidase
MC4R ……...Melanocortin-4 receptor
ML2/ML/Magel2 ……..Melanoma antigen family L2
MNPO ……Median preoptic nucleus
mPFC ……Medial Prefrontal cortex
MPO ……..Medial preoptic nucleus
MRI ……...Magnetic resonance imaging
MTII ……..Melanotan 2
NA …….Noradrenaline/ Norepinephrine
NAc ……...Nucleus accumbens
NME ……..Normetanephrine
NPY ……...Neuropeptide Y
Ns ……...Not significant
NTS ……Nucleus of the solitary tract
OCD ……...Obsessive-compulsive disorder
OXT ……...Oxytocin
pAKT …….Phosphorylated AKT
pCREB ……..Phosphorylated CREB
pERK …… Phosphorylated ERK
PeVN …….Periventricular nucleus
PFC ……Prefrontal cortex
PHA ……Posterior hypothalamic area
POMC ……....Pro-opiomelanocortins
pSTAT3 …….Phosphorylated STAT3
PVN ……...Paraventricular nucleus

PWS ……...Prader-Willi Syndrome

RM-493 ……Rhythm metabolic melanocortin-4-receptor agonist

SCN ……...Suprachiasmatic nucleus

Ser …….Serine

snoRNA …….

SON ……...Supraoptic nucleus

SN ……..Substantia nigra

snoRNA …….Small nucleolar RNA

SSRI ……...Selective serotonin reuptake inhibitor

STAT3 ……...Signal transducer and activator of transcription 3

SUM …….. Supramammillary nucleus

SV2 ……Synaptic vesicle protein 2

tDCS ……..Transcranial direct current brain stimulation

TH ……Tyrosine hydroxylase

TMN ……..Tuberomammillary nucleus

TPH ……...Tryptophan hydroxylase

Tyr ……Tyrosine

UPD ……...Uniparental disomy

VTA ……...Ventral tegmental area

VLPO ……Ventrolateral preoptic nucleus

VMH ……Ventromedial hypothalamus

WD ……Withdrawal

WT/W ……....Wildtype

Chapter 1: Introduction

1.1. Obesity

In recent years obesity has increased at an alarming rate to become a worldwide epidemic (Lobstein et al., 2004). The prevalence of obesity in Canada has increased drastically in the past 20 years, affecting all ages, races and sexes (Lau et al., 2007; Dubois et al., 2012). A global reduction of physical activity and a shift in feeding behaviour has led to an increase in obese individuals at greater risk of developing type 2 diabetes, cardiovascular disease, osteoarthritis, cancers and suffering a premature death (J. S. Flier, 2004; Lau et al., 2007, Dubois et al., 2012). This increase in obesity-associated morbidity and risk of premature death makes finding effective treatment interventions a public health priority.

When an individual's food intake is greater than the energy expenditure, the excess energy is stored as fat. The long-term imbalance of food intake and energy expenditure leads to obesity. An individual's body weight is determined by a combination of environmental and biological factors. Adult weight is determined by the presence of genes that enable specific responses to different environmental factors. The difference in expression of these genes makes someone more susceptible to a certain adult weight (J. S. Flier, 2004). This genetic susceptibility, paired with an environment full of energy-rich foods that demand very little physical activity to obtain, leads to obesity. The balance of environmental and genetic influence varies throughout development including stages of increased susceptibility to environmental influence (Dubois et al., 2012). There are forms of obesity that are linked to specific genetic mutations, and the study of these monogenic obesity disorders has contributed greatly to our understanding of the molecular mechanisms involved in hyperphagia and obesity (O'Rahilly & Farooqi, 2006). The disproportionate increase in obesity points to recent changes in our environment, as opposed to changes in the human genome. High-fat and high-sugar foods are more available than ever, the cost of these energy-rich foods is lower than ever, and these economical, high-energy foods require very little physical activity to obtain. Why do some people respond to this modern environment by gaining excessive amounts of weight, while other people who live in the same environment remain lean? Answering this question, and understanding the molecular action of specific "obesity genes" is key to fighting obesity in our modern fast-food environment.

1.2. Prader-Willi Syndrome

Prader-Willi Syndrome (PWS) is a genetic disease characterized by severe hyperphagia, and reduced energy expenditure leading to obesity. Early symptoms of PWS include low birth weight, infantile hypotonia, and poor sucking causing an early failure to thrive (Cassidy et al., 2012). During late infancy, 2-4 years of age, there is a transition from impaired feeding to extreme hyperphagia leading to severe childhood obesity if left untreated (Table 1.1, Cadoudal, et al., 2014; Cassidy et al., 2012). Between the ages of 5 and 7 children start to exhibit behavioural problems, they are prone to temper tantrums, are extremely dependent on routine, and often exhibit ritualistic and obsessive-compulsive behaviours (Akefeldt et al., 1998; Cassidy et al., 2012; Clarke et al., 2002). Mood swings, sleep disturbances, and psychiatric disorders are also more common in individuals with PWS, than in the general population (Clarke et al., 2002; Jin, 2011).

Individuals with PWS often present with other symptoms including, hypogonadism, infertility, scoliosis, and cognitive delay (Cassidy et al., 2012). Growth hormone treatment and strict control of the environment has greatly improved the prognosis for children with PWS (Figure 1.1). The abnormal eating observed in PWS can include eating food that has spoiled, pet food, and other foods that are not normally considered palatable. This indiscriminate eating can be attributed to an abnormal perception of what is, and is not edible. In 2000 Elisabeth M. Dykens determined that this behaviour is not from a lack of understanding of the appropriate fate of the food item but from an overall increased drive to feed despite a conscious understanding of what should be considered edible. Investigating the extreme hyperphagia observed in Prader-Willi Syndrome could be useful in understanding overeating leading to obesity in the general population.

Phases	Age	Clinical characteristics
0	Prenatal	Decreased fetal movement and lower birth weight
1a	0-6 months	Hypotonia, decreased feeding, decreased appetite
1b	9-25 months	Improved feeding and appetite and growing normally
2a	2.1-4.5 years	Weight increase without increased appetite or caloric intake
2b	4.5-8 years	Increased appetite and calories but can feel full
3	8 years- Adult	Hyperphagic, rarely feel full
4	Adulthood	Appetite is no longer insatiable

Table 1.1.The Nutritional Stages of Prader-Willi Syndrome.

Outline of the different developmental phases of PWS and the clinical characteristics that accompany each stage. Individuals with PWS undergo a failure-to-thrive state, outlined in grey, followed by a recovery and transitory rescue (purple), followed by a period of excessive feeding and weight gain, outlined in blue (Table modified from Cassidy et al., 2012- Prader-Willi Syndrome).

1.2.1. Individuals with Prader-Willi Syndrome have an abnormal motivation to eat

Individuals with PWS demonstrate abnormal functional MRI responses to images of food. After consuming a meal, people with PWS showed an increase in blood flow to the amygdala (AMY) in response to images of food (Holsen et al., 2006). This response suggests an increased drive to feed after being physiologically satiated. This increased drive to feed can also be observed in individuals with PWS and is demonstrated by the abnormal measures taken to acquire food, including stealing and hoarding food. Similarly, individuals who are obese demonstrate an exaggerated fMRI response in the amygdala to images of food in anticipation of a meal (Gearhardt, et al., 2011). Holsen et al., (2006) also demonstrated an decrease in blood flow to the prefrontal cortex (PFC) after consuming a meal in the PWS-group. The attenuated activation of the PFC following the meal suggests there is less cortical inhibitory feedback to the dopaminergic midbrain. The increase in blood flow to the AMY shows an increase in motivation for food even following a meal.

1.2.2. Individuals with Prader-Willi Syndrome have a loss of oxytocin neurons in the paraventricular nuclei

Neurons in the hypothalamus (HYP) that express oxytocin are involved in inhibiting food intake. There is an observed reduction in the number of oxytocin-expressing neurons in the paraventricular nucleus (PVN) of the HYP, and an impaired oxytocin receptor gene expression in individuals with PWS (Swaab et al., 1995; Bittel et al., 2006). These neurons send projections to the nucleus of the solitary tract (NTS) of the brainstem, the AMY and the substantia nigra (SN) to modify food intake. The anorexigenic function of these neurons comes from their involvement in gastric reflexes (Sabatier et al., 2013). The loss of this specific subset of neurons in individuals with PWS suggests a loss of gastric reflex-induced inhibition of feeding consistent with the observed phenotype. Gastric rupture has been reported in individuals with PWS and in several extreme cases this has lead to the death of the individual (Stevenson et al., 2007). The loss of oxytocin (OXT) is consistent with mouse models of PWS and mice modelling the loss of MAGE genes specifically. The loss of either *Necdin* or *Maged1*, both MAGE genes, causes abnormalities in hypothalamic OXT, and the obese phenotype. The loss of OXT in the hypothalamus causes narcolepsy, this is consistent with the observed sleep disturbances in individuals with PWS (Saper & Lowell, 2014). Oxytocin has also been shown to act in concert with serotonin (5-HT) to mediate the reward value of social interaction in the nucleus accumbens (NAc) (Dolen et al., 2013). This could help explain some of the deficits in social attribution observed in individuals with PWS, which include difficulty understanding the

salience of specific social information, using affective language, and interpreting emotion related signals (Koenig et al., 2004).

1.2.3. Individuals with Prader-Willi Syndrome have abnormal levels of neurotransmitters and their metabolites

In 1998 Åkefeldt et al. assessed the levels of monoamine metabolites in the cerebral spinal fluid of adolescents with PWS. High-Performance liquid chromatography (HPLC) analysis showed higher levels of the serotonin metabolite 5-hydroxyindoleacetic acid (5HIAA), and the dopamine metabolite homovanillic acid (HVA) in the cerebral spinal fluid (CSF) of individuals with PWS. An altered serotonin metabolism could influence locomotion, body temperature, as well as the perception of pain. These are all responses that are affected by PWS, and treatment with serotonin reuptake inhibitors is useful for the treatment of both obsessive-compulsive behaviours (skin picking) and hyperphagia in a PWS population (Åkefeldt et al., 1998).

1.3. Current treatment options for individuals living with Prader-Willi Syndrome

During the first nutritional stage of PWS, treatment is focused on ensuring that the infant receives adequate nutrients. During this stage, infants may require a feeding tube (Cassidy et al., 2012). Throughout both the failure to thrive and the hyperphagic states of PWS, a major component to treatment is to monitor food intake to ensure normal growth. During the hyperphagic stage, behavioural interventions include regulating the caloric intake as well as ensuring the child participates in regular physical activity. In adulthood, behavioural interventions often includes being place in a group home with regular supervision. Adults with PWS have an increased risk of obesity-related death demonstrating the importance of controlling the nutritional environment (Jin, 2011).

1.3.1. Growth hormone Therapy

Growth Hormone (GH) deficiency plays a role in several of the PWS symptoms, and an early diagnosis is important to maximize the benefit of GH intervention (Jin, 2011). Individuals with PWS exhibit short stature, increased fat mass, and endocrine dysfunction that can be ameliorated with GH therapy throughout development (Cadoudal, et al., 2014; Cassidy et al., 2012). Growth hormone therapy has been successful at treating some of physiological symptoms of PWS. Long-term treatment causes amelioration in the body composition of patients including an increase in adult height, reduced fat mass and an increase in lean mass. Growth Hormone therapy administered in early childhood also reduces the

severity of the neurological symptoms observed in PWS (Figure 1.1. Jin, 2011; Cadoudal et al., 2014; Cassidy et al., 2012).

1.3.2. Interventions to treat the individual symptoms of Prader-Willi Syndrome

There is no cure for Prader-Willi Syndrome. Treatments for PWS focus on managing the individual symptoms that present. The incidence of scoliosis in PWS is high (45-86 %) with 15-20 % of cases requiring surgical intervention (Greggi et al., 2010). Bracing and surgery can be used to correct spinal deformities in PWS. Individuals with PWS often present with sleep abnormalities including sleep apneas and other sleep-related breathing disorders, excessive daytime sleepiness, increased nocturnal sleep, and narcolepsy (DeMarcantonio et al., 2010; Cassidy et al., 1990; Helbing-Zwanenburg et al., 1992). Treatment options for sleep abnormalities in individuals with PWS are similar to treatments for the general population. Along with behavioural treatments, other interventions include light therapy, melatonin, use of a CPAP, and in severe cases, surgery (Didden & Sigafoos, 2001; DeMarcantonio et al., 2010). There are several behavioural disturbances that occur with PWS including compulsive behaviour, self-injurious behaviour, and disordered affect (Ho & Dimitropoulos, 2010; Cassidy et al., 2012; Clarke et al., 2002; Symons et al., 1999). Treatment for these behaviours includes antipsychotics, antidepressants, and mood stabilizers. The psychiatric medications prescribed most commonly to individuals with PWS include the antipsychotics, risperidone, haloperidol, and the selective serotonin reuptake inhibitors (SSRIs) fluoxetine, citalopram, and sertraline. The side effects of these medications often include sedation and weight gain that can be particularly problematic in a PWS population (Soni et al., 2007).

1.3.3. Clinical trials for Prader-Willi Syndrome

There are several potential pharmacological interventions that are currently being trialed for use in a PWS population. RM-493 is a melanocortin-4 receptor agonist. RM-493 is currently in a phase-2 clinical trial (F. Fiedorek et al., Rhythm Metabolic). Short-term treatment with RM-493 has proven useful in increasing the resting energy expenditure in both non-human primates and in obese individuals (Chen et al., 2015). Another MC4R agonist, MTII, has been used on our mouse model of PWS. Our PWS mouse model, the *Magel2*-null mouse, has demonstrated an exaggerated anorexigenic response to the administration of MTII (Mercer et al., 2013). The success of MTII in our rodent model of PWS, and RM-493's success in both human and primate models make this a promising potential therapy for PWS.

Another potential therapy for PWS is the use of intranasal oxytocin. Phase 1 trials for oxytocin therapy are currently being conducted in a PWS population (J. L. Miller, University of Florida). This

double-blind placebo controlled study will not only assess oxytocin as a treatment for hyperphagia, but also analyze the effect that intranasal oxytocin has on the social deficits observed in children with PWS. Oxytocin has a wide variety of functions, playing a role in childbirth and lactation, maternal behaviour, the formation of social bonds, and trust and cooperation (H. Shen, 2015). Oxytocin therapy is also being considered for treatment of obsessive-compulsive disorder OCD, autism spectrum disorder, and schizophrenia. Impaired OXT signaling through either receptor deficiency, or through the loss of oxytocin-producing cells, has been linked to the development of obesity in several rodent models (Deblon et al., 2011; Takayanagi et al., 2008; Maejima et al., 2011). A normal weight is rescued in diet-induced obese rats with OXT treatment (Deblon et al., 2011). Oxytocin treatment causes a decreased reward-driven food intake in human males (Ott et al., 2013). The reduced hyperphagia-induced obesity in several rodent models being treated with oxytocin makes oxytocin therapy a potential solution to the hyperphagia-induced weight gain observed in children with PWS. The oxytocin analog, Barusiban (FE 200 440), is also undergoing clinical trials for the potential use in a PWS population (Miller et al., 2015).

Beloranib is another potential treatment for PWS currently in phase 3 clinical trials. Beloranib, originally investigated for its anti-angiogenesis properties, is now in clinical trials for the treatment of obesity in both a hypothalamic injury-associated obese (HIAO) population and in a PWS population (R. H. Howland, 2015; Shoemaker et al., 2015; Miller et al., 2015).

Other potential therapies for PWS include Exanatide, Diazoxide, and AZP-531. Exanatide, is a GLP-1 receptor agonist aimed at suppressing weight gain, currently in phase 2 clinical trials (Miller et al., 2015). Diazoxide is a potassium channel agonist aimed at aiding in hyperpolarizing hypothalamic neurons that have lost responsiveness to the effects of the hormone leptin. Diazoxide is currently in phase 2 clinical trials. AZP-531, a ghrelin analog, is another potential therapy for PWS. Clinical trials for AZP-531 in a PWS population are not yet underway (Miller et al., 2015). There is also the potential for brain stimulation as a therapy for individuals with PWS. Clinical trials for the use of transcranial direct current brain stimulation (tDCS) to reduce hyperphagia are currently underway in a PWS population (M. G. Butler, University of Kansas Medical Centre Research Institute).

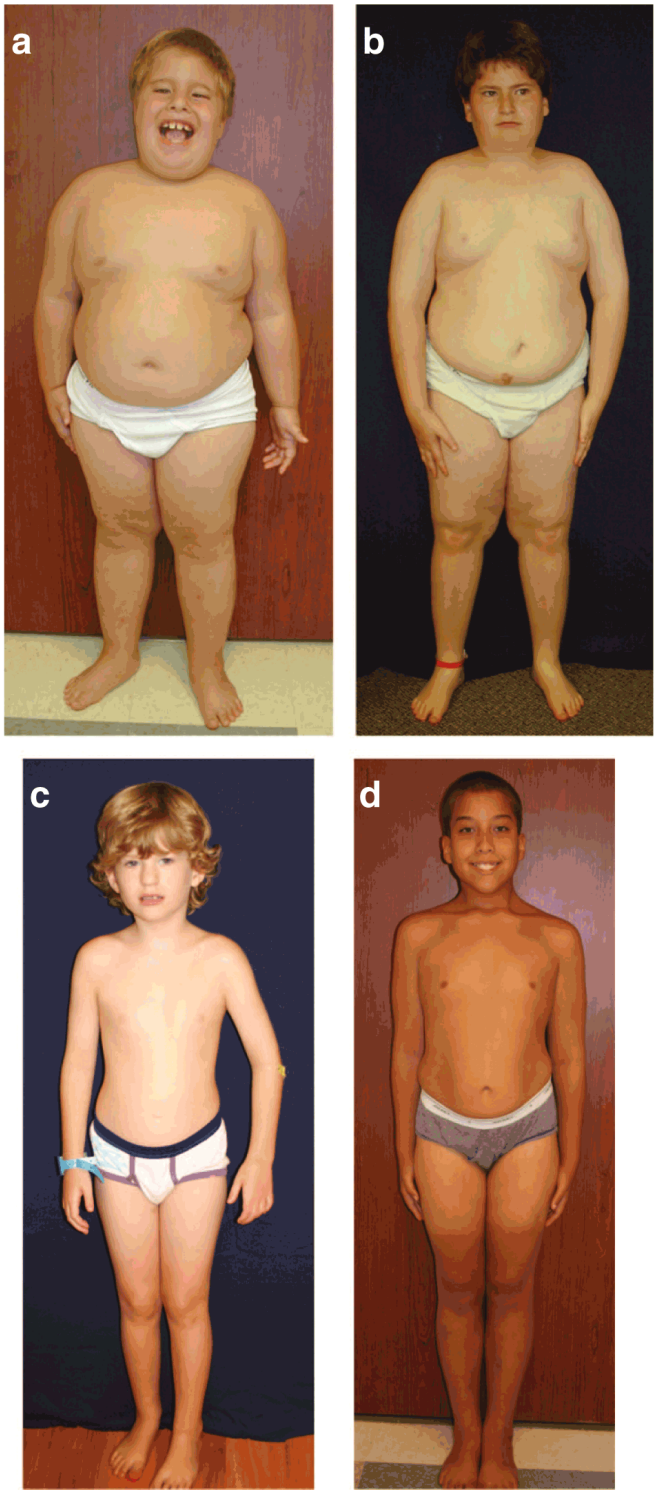

Figure 1.1. The Prader-Willi Syndrome phenotype with growth hormone therapy

The PWS phenotype without growth hormone therapy (a & b), and with GH treatment (c & d). The body composition of the children treated with GH is less severe than children that are not undergoing GH therapy (Figure adapted from Cassidy et al. 2012: Prader-Willi Syndrome).

1.4. Causes of Prader-Willi syndrome

Prader-Willi syndrome results from the loss of expression of a group of paternally expressed genes on chromosome 15q11.2-q13 (Figure 1.2). This group of genes is maternally silenced and the loss of the paternal copy leads to the complete loss of expression and the development of PWS (Cassidy et al., 2012). The majority of PWS cases result from a 5-6 Mb deletion on the long-arm of the paternal chromosome 15. Other cases can arise from a maternal uniparental disomy (UPD) or from an imprinting defect (Cassidy et al., 2012). The genetic subtype influences the physiological phenotype and the behavioural phenotype of the individual. For example, individuals with a paternal deletion demonstrate higher rates of hypopigmentation (Gillessen-Kaesbach et al., 1995). The paternal deletion is also associated with a higher level of self-injurious behaviour, whereas individuals with maternal disomy tend to have a more severe disordered affect phenotype, including a poorer response to psychiatric medication, and greater reoccurrence of psychiatric symptoms (Symons et al., 1999; Soni et al., 2007). The PWS region consists of five imprinted protein-coding genes and several snoRNA genes (Schaaf, et al., 2013). Among the affected protein-coding genes is *MAGEL2*, which is the focus of this research project. The loss of *MAGEL2* alone has been shown to be sufficient to produce a PWS-like phenotype (Schaaf, et al. 2013). Several mouse models have been used to study the loss of individual genes within the PWS region including modelling the loss of the protein coding genes MKRN3, NDN, SNURF-SNRPN, and MAGEL2 (Schaaf, et al., 2013). The loss of the snoRNA SNORD116 also produces a PWS-like phenotype and has been used as a model to study this disease. The candidate gene that is the primary focus of the Wevrick laboratory is MAGEL2. The modelled loss of *MAGEL2* in mice has provided a greater understanding of the hormonal and hypothalamic impairment involved in PWS and will continue to provide insight into this disorder.

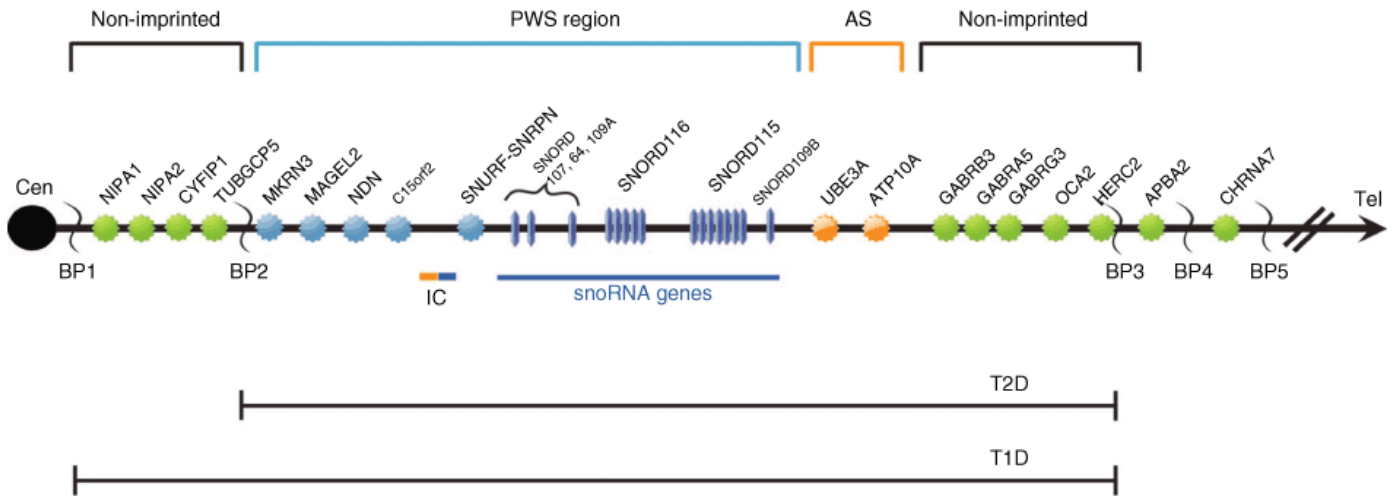

Figure 1.2. Map of the 15q11-q13 chromosome region involved in Prader-Willi Syndrome

Prader-Willi Syndrome is caused by the loss of expression of a group of paternally expressed gene labelled in blue (PWS region). MAGEL2 is one of the protein coding genes in the PWS region of maternally imprinted genes. Due to the imprinting nature of this region, the maternal copy is not expressed and the loss of the paternal copy leads to total loss of expression (Adapted from Cassidy et al., 2012: Prader-Willi Syndrome).

1.5. MAGEL2

MAGEL2 is a type II MAGE protein, a member of the greater melanoma antigen (MAGE) family, encoding for the protein *MAGEL2*. MAGE proteins all contain a conserved MAGE homology domain (MHD) and are involved in a range of cellular functions including cell differentiation and apoptosis (Doyle et al., 2010; Mercer et al., 2009). The exact function of the MAGE protein MAGEL2 has yet to be determined, however this protein does interact with E3 ubiquitin ligases (Doyle et al., 2010). This suggests a potential role for *MAGEL2* in intracellular protein fate determination. *MAGEL2* could influences the fate of specific proteins and the loss of MAGEL2 could influence how proteins are targeted within the cell. This could have a wide range of effects within the various groups of cells that express *MAGEL2*.

In mice, the homologous *Magel2* protein shares a 77 % overall similarity to the human protein (Boccaccio et al., 1999). In mice, *Magel2* is most prominently expressed in the hypothalamus with the highest level of expression being in the arcuate nucleus and the suprachiasmatic nucleus (Lee et al., 2003). These nuclei are involved in the homeostatic maintenance of feeding and the circadian clock.

The primary focus of the Wevrick lab is to identify the molecular function of *MAGEL2*. Our laboratory focuses on understanding what this protein does on a cellular level, how the loss of this protein affects various organ systems, and how this translates into a physiological and behavioural phenotype. There are several ongoing projects in the Wevrick lab aimed at determining the cellular function of *Magel2*, how the loss of *Magel2* could lead to the observed *Magel2*-null phenotype in mice, and how this loss of function could contribute to the observed phenotype in individuals with PWS.

1.6. *Magel2*-null mouse model

To study the biological function of *Magel2*, our lab uses a knock-in mouse model where *Magel2* is no longer expressed (Magel2-null, ML2 (C57BL/6-Magel2^{tm1Stw}). In 2007 Kozlov et al. designed the *Magel2*-null mouse model used by our lab (Figure 1.3). This was done by inserting a *LacZ* reporter gene into the open reading frame in place of the *Magel2* gene, creating a mouse that expresses **β**-galactosidase in place of *Magel2* (Figure 1.3, Bischof et al., 2007; Kozlov et al., 2007). The continued characterization of this mouse model has demonstrated its usefulness in studying Prader-Willi Syndrome. The PWS phenotype of this mouse model is particularly useful in studying the reward pathway. Many of the cardinal features of PWS are recapitulated in this model. *Magel2*-null mice demonstrate both of the nutritional states of PWS. *Magel2*-null mice exhibit an initial failure-to-thrive period indicated by neonatal growth retardation and decreased body weight up until weaning. This failure-to-thrive is followed by a period of increased weight

gain (Bischof et al., 2007). *Magel2*-null mice also present with several other physiological, neuroanatomical, and behavioural symptoms that form a good representation of PWS. Along with an increased fat mass and reduced lean mass, *Magel2*-null mice have an altered activity pattern, including a significant decrease in voluntary activity during waking hours (Bischof et al., 2007). *Magel2*-null mice have reduced fertility and abnormal responses to both novel objects and novel environments (Mercer et al., 2009). The *Magel2*-null mice have also demonstrated hypothalamic impairments, including a loss of response to the anorexigenic signaling molecule leptin (Mercer et al., 2013). This LacZ-insertion model has also allowed us to identify the tissues expressing *LacZ* in place of Magel2. Understanding where Magel2 is expressed is a primary step in determining the biological function of this protein. Along with peripheral fibroblast expression, *Magel2* is expressed in several areas of the brain including the hindbrain, the NAc, the temporo-parietal cortex, the olfactory bulb, the NTS, and most notably in the suprachiasmatic nucleus (SCN) and the arcuate nucleus (ARC) of the hypothalamus (Mercer et al., 2009, Lee et al., 2000).

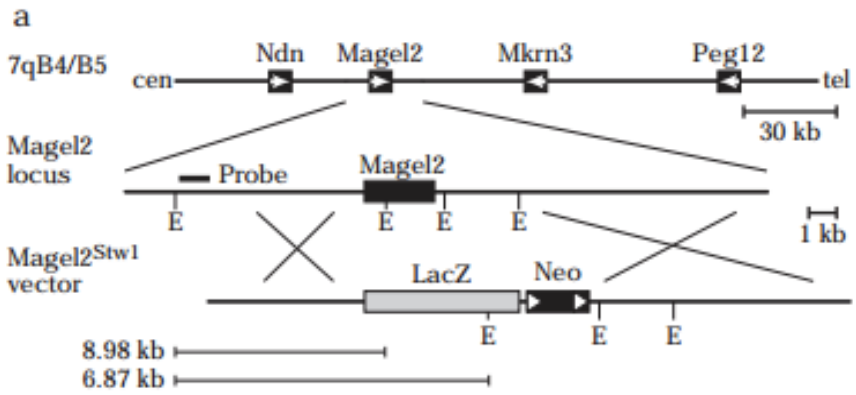

Figure 1.3. Magel2-null mouse design

Schematic design of the genetic insertion of the *LacZ* gene into the *Magel2* locus. This in-frame *LacZ* insertion into the open reading frame of the *Magel2* gene and under the control of the *Magel2* promoter produces a mouse that expresses β -galactosidase in place of *Magel2*. This insertion causes the loss of expression of *Magel2* altogether. (Kozlov et al., 2007: The imprinted gene *Magel2* regulates normal circadian output.)

1.6.1. *Magel2*-null mice have deficits in the dopamine reward pathway

Quantitative-MRI demonstrated a decrease in brain volume in the *Magel2*-null mice. This included reduced volume of the hippocampus, the parieto-temporal lobe, the cortex, the AMY, and in the NAc (Mercer et al., 2009). *Magel2*-null mice show reduced concentrations of metabolites of both the catecholamine and the indolamine pathways in the hypothalamus. This result is observed in adult mice but not in embryonic mice indicating that hypothalamic dopamine signaling becomes impaired at some point during development (E18.5) (Mercer et al., 2009). Bischof et al. (2007), have shown altered activity patterns corresponding to an abnormal circadian rhythm. *Magel2*-null mice showed increased feeding in anticipation of the dark cycle, as well as a reduced feeding toward the end of the dark cycle. This behaviour is indicative of an altered motivation to feed. This eagerness to feed, like the abnormal post-meal activation of the amygdala in PWS, suggests an exaggerated neuroanatomical food-seeking response (Holsen et al., 2006). Hunger, or the experienced force motivating us to feed, can be salient enough to alter activity patterns, including the sleep-wake cycle, suggesting that an insatiable appetite could be influencing the activity patterns of the *Magel2*-null mice (Ribeiro et al., 2007).

1.6.1.1. *Magel2*-null mice have an attenuated response to changes in diet and to both chemical and natural rewards

Magel2-null mice have an abnormal response to both natural rewards and chemical rewards. Our lab has previously performed several feeding experiments on the *Magel2*-null mice and observed an attenuated weight change in response to altered diets. In response to a chronic high-fat diet (HF), *Magel2*-null mice demonstrated an attenuated weight gain (Bischof et al., 2007). Another feeding experiment performed on our *Magel2*-null mouse model was a fasting/re-feeding experiment where food was removed and returned after 48 hours. *Magel2*-null mice also had a reduced weight loss during the fast, and similarly, they showed a reduced weight gain in response to the return of food following the withdrawal. During the re-feeding, the *Magel2*-null mice ate significantly less than they did before the removal of the diet (Mercer et al., 2013). This loss of compensatory re-feeding could suggest the loss of a withdrawal response. Along with the blunted physiological response to the exposure of different diets, *Magel2*-null mice have a blunted behavioural response to the chemical reward of cocaine. Cocaine acts directly on the dopaminergic synapse mediating the effect of dopamine by blocking pre-synaptic DA reuptake. *Magel2*-null mice have an attenuated locomotive response to cocaine (Figure 1.4) which is consistent with the locomotive response to

cocaine observed in animal models of obesity (Fulton et al., 2006). When given an intraperitoneal (IP) injection of cocaine, *Magel2*-null mice are slower to respond and don't reach the same level of locomotive activity as their WT littermates (Figure 1.4, Luck et al., in press). This experiment gives us information on the dopamine-mediated locomotive response and not directly the dopamine-mediated reward response. It is suggestive of an impaired dopamine response in general and is used to assess dopamine signaling in general as measuring euphoria, or experienced reward, in a mouse model is more complicated.

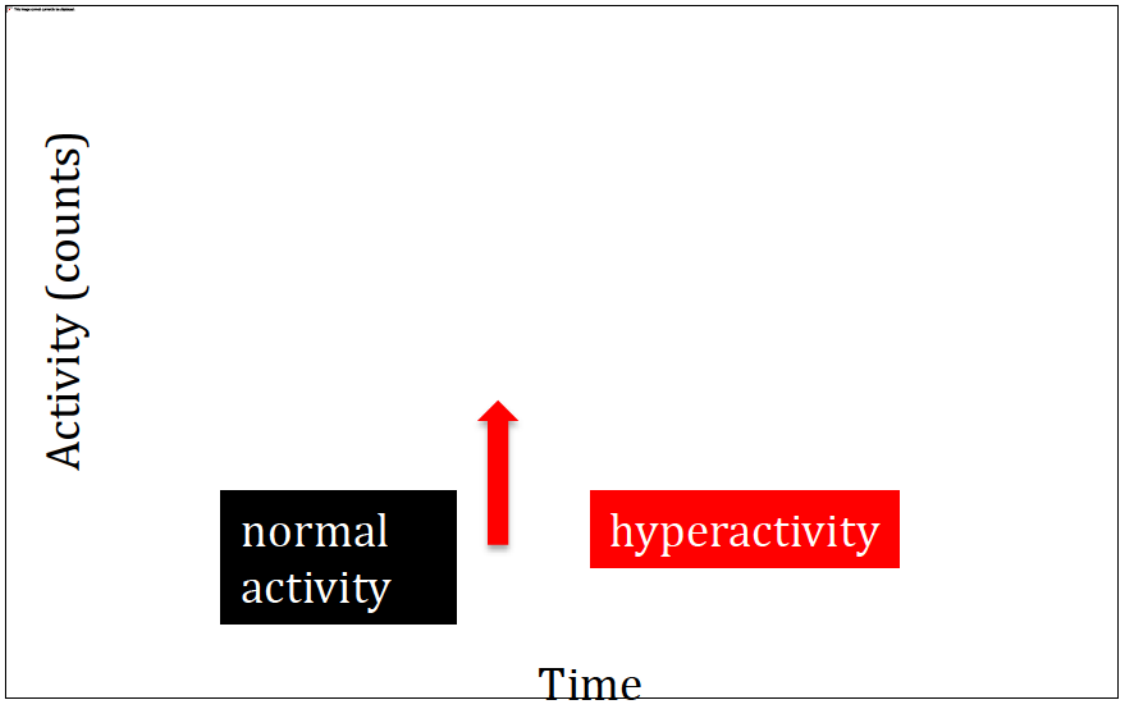

Figure 1.4 . Locomotive response to intraperitoneal cocaine injection

Magel2-null mice have reduced hyperlocomotion in response to a cocaine injection when compared to their wildtype littermates. Magel2-null mice and Wildtype mice have an increase in locomotor activity following the intrperitoneal injection of cocaine followed by a return to baseline activity. The *Magel2*-null mice fail to reach the same level of locomotor activity, and the have a quicker return to baseline activity suggesting a blunted response to the cocaine (Luck et al., in press).

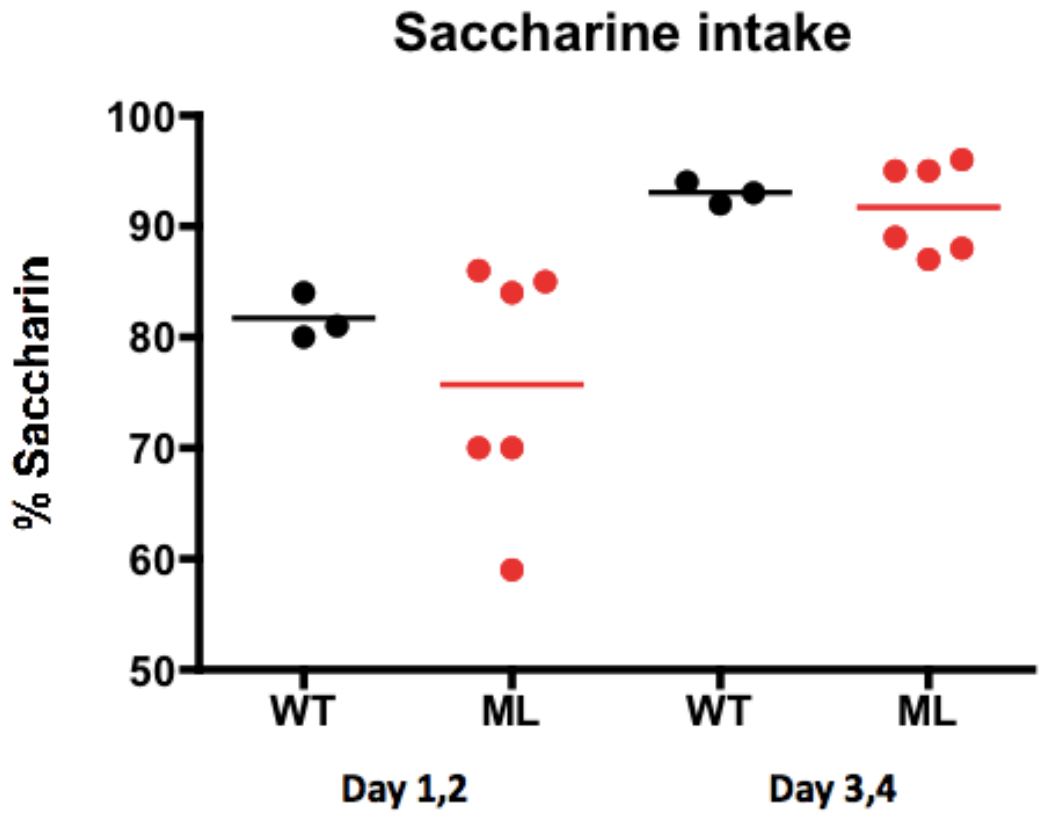

Figure 1.5. Anhedonia in Magel2-null mice

The saccharin preference test was performed to measure anhedonia. The *Magel2*-null mice demonstrated an initial hesitation to consume the novel drink. This initial hesitation is overcome in days 3 and 4 when *Magel2*-null mice consumed a comparable quantity of saccharin indicating an intact anhedonic response despite an initial hesitation to consume the novel saccharin (Luck et al., in press).

1.6.1.2. *Magel2*-null mice have an attenuated response to novelty

Magel2-null mice consume significantly less standard chow when it is given as a powder (Bischof et al., 2007). This suggests that the *Magel2*-null mice may have an aversion to the novelty of the food item and not the food item itself. This is consistent with the need for routine and adverse response to change observed in children with PWS. This hesitation to feed on novel food items could complicate any experiments involving a novel diet and must be accounted for when analyzing feeding results. In a saccharin preference test for anhedonia, *Magel2*-null mice showed an initial lack of preference for the saccharine. After a few days of exposure, they did develop the same preference for the saccharine as their WT littermates (Figure 1.5, Luck et al., in press). *Magel2*-null mice demonstrate an increase in anxiety indicated by an increased freezing response to a novel environment (Mercer et al., 2009). This suggests that *Magel2*-null mice, like individuals with PWS, have an exaggerated response to unfamiliarity. *Magel2*-null phenotype observed in our mouse model makes it a good model for PWS.

1.6.2. *Magel2*-null mice have defects in satiety signalling pathways.

Magel2-null mice have defects in homeostatic satiety signalling pathways. This includes a reduction in the signaling activity of orexins, and leptin. Leptin is a satiety signal important for relaying the body's energy status to the central nervous system. In collaboration with the Colmers' lab (University of Alberta, Dept. of Pharmacology), our lab has previously demonstrated that *Magel2*-null mice have a central insensitivity to leptin (Mercer et al., 2013). This insensitivity is due to the loss of neurons in the ARC expressing pro-opiomelanocortins (POMC) and the loss of response to leptin in the remaining POMC-expressing cells. The loss of POMC+ neurons and their insensitivity to leptin limits the release of the anorexigenic metabolite **α**-melanocortin-stimulating hormone (**α**-MSH). MTII is a **α**-MSH agonist that causes an exaggerated anorexigenic response in *Magel2*-null mice (Mercer et al., 2013). The use of this synthetic POMC+ metabolite allows us to bypass the leptin insensitivity observed in *Magel2*-null mice, making this a promising potential treatment for leptin insensitive obesity. There are several other nuclei that contain leptin receptors, these include the midbrain and the amygdala. We have not yet investigated the effect the loss of Magel2 has on leptin signalling in these nuclei.

Orexin, a neuropeptide that helps regulate appetite, is also disrupted in the hypothalamus of our *Magel2*-null mice (Kozlov et al., 2007; Mercer et al., 2013). Orexin-A and Orexin-B are produced in the lateral hypothalamic area (LHA) and have axons projecting throughout the central nervous system including the cortex, the olfactory bulb, the hippocampus, the AMY, the striatum, the midbrain, the

brainstem, and throughout the hypothalamus (Willie et al., 2001). Several of these targets include nuclei involved in the arousal, feeding, and reward integration. These targets include both anorexigenic (POMC+) and orexigenic (NPY+) cell populations (Figure 1.8, Mercer et al., 2013). Orexin projections from the LHA activate neuropeptide-Y (NPY) neurons and inhibit the activity of POMC neurons (Figure 1.8). The loss of these neurons causes an impaired feeding response to both fasting and re-feeding similar to the response in the *Magel2*-null mice (Yamanaka et al., 2003). Narcolepsy is a symptom of PWS and is caused by specific loss of orexin in the LHA leading to the abnormal initiation of sleep during waking hours (Saper & Lowell, 2014). Along with mediating the states of arousal, orexin signaling also plays a role in reward-seeking behaviour. Orexin signaling has not been investigated outside of the hypothalamus of *Magel2*-null mice.

1.7. Neural Feeding Pathways

There are two neural pathways that regulate food intake and energy expenditure; the homeostatic circuit and the hedonic feeding circuit. These circuits work both discretely and in concert to regulate food intake and energy expenditure. The homeostatic feeding pathway is often disrupted in people with obesity. The homeostatic feeding system has previously been addressed in the *Magel2*-null mouse model, and the primary focus of my research project was to address the hedonic feeding system in a mouse lacking *Magel2*.

1.7.1. Homeostatic Feeding

The hypothalamus is the primary nucleus involved in mediating physiological or homeostatic feeding. This system is responsible for long-term maintenance of a person's weight (Figure 1.6). The hypothalamus is the control centre for several autonomic processes including immune and endocrine responses, mediating arousal and sleep states, thermoregulation, cardiovascular regulation, hormone balance, metabolism, and appetite (Baroncini et al., 2012; Saper & Lowell, 2014). The hypothalamus is divided into several small nuclei that work together to receive information from the periphery and integrate these energy-status signals into a behavioural output (Figure 1.7). The rostral most hypothalamus is composed of the preoptic nuclei, the SCN, and the infundibulum. This section of the hypothalamus is mainly responsible for circadian rhythm, maintaining body temperature, and regulating sexual behaviour. The infundibulum is responsible for regulating hormone release by enabling communication between the rest of the hypothalamus and the posterior pituitary gland. The caudal hypothalamus is composed of mammillary bodies and the posterior hypothalamic nucleus. The main output for these nuclei is the hippocampus where they mediate arousal. The medial hypothalamus is the area responsible for mediating

feeding. The central section of the hypothalamus includes the ARC, the PVN, the periventricular nucleus (PeVN, A14), the ventromedial hypothalamus (VMH), the dorsomedial hypothalamus (DMH), and the LHA. Together these nuclei are involved in feeding, sexual behaviour, and the endocrine response (Saper & Lowell, 2014).

The ARC is the primary nucleus involved in energy regulation. There are two neuronal populations in the ARC involved in the regulation of food intake and energy expenditure. The first subset of cells is a group of neurons expressing orexigenic molecules including agouti-related peptide (AgRP), neuropeptide-Y (NPY), and the inhibitory neurotransmitter GABA, these cells will be referred to as NPY+ cells (Saber & Lowell, 2014). The second subset of neurons includes anorexigenic neurons expressing pro-opiomelanocortins (POMC) and cocaine- and amphetamine-regulated transcript (CART). These cells will be referred to as POMC+ neurons. Pro-opiomelanocortins can be broken down into smaller anorexigenic peptides like **α**-MSH and Beta-endorphin (Mercer et al., 2013). Both POMC+ and NPY+ neurons contain leptin receptors. POMC neurons respond to leptin by secreting **α**-MSH, a small molecule that acts on melanocortin-4 receptors (MC4R) of PVN neurons to produce an anorexigenic response. AgRP is a MC4R inverse agonist inhibiting the downstream anorexigenic effects of the melanocortin receptor (Saper & Lowell, 2014; Sabatier, 2013). Leptin is a cytokine that inhibits the release of AgRP, reducing the inhibition of the MC4R receptor, driving an anorexigenic response. Hypothalamic AgRP cells also respond to ghrelin, an orexigenic molecule produced in the stomach (Figure 1.6, Wren et al., 2000). Ghrelin induces the stimulation of AgRP inhibiting the downstream anorexigenic activity of the MC4R receptor in the PVN. Although POMC and NPY neurons respond to the same ligand and act on the same postsynaptic MC4R receptor in the PVN, the action of leptin on POMC is a much slower process (Saper & Lowell, 2014). These orexigenic and anorexigenic molecules play an important role in the development and maintenance of an obese state.

The primary hypothalamic satiety signal is the hormone leptin, a cytokine produced in adipocytes. Leptin receptors in the brain, specifically the hypothalamus, respond to circulating levels of leptin to suppress appetite (Figure 1.7, J. S. Flier, 2004). Nuclei throughout the brain including the hypothalamus, the midbrain, and hippocampus, and the cortex all contain leptin receptors, however it is the ARC of the hypothalamus that is primarily responsible for its anorexigenic activity (Funahashi et al., 2003). Leptin protects against obesity by signaling to the central nervous system when there is an increase in adiposity. In humans, with the development of obesity, there is a chronic increase in the levels of circulating leptin. This can lead to leptin insensitivity, and a dulled anti-obesity response from the hypothalamus (J. S. Flier,

2004). This insensitivity not only accelerates weight gain but also makes it extremely hard to return to the original weight.

Oxytocin is a hormone involved in several physiological events, namely labour and social bonding. Oxytocin deficiency has also been implicated in the development of obesity (Camerino, 2009). Oxytocin-producing parvocellular neurons in the PVN containing MC4Rs respond to **α**- MSH to modify food intake (Kim et al., 2000; Sabatier et al., 2013). The Oxytocin-producing neurons of the PVN project to the NTS to modulate the gastric reflex in response to a meal. The OXT+ neurons in the PVN also project to the VTA where they influence dopamine (DA) release (Figure 1.8, Succu et al., 2008). The function of OXT+ PVN neurons in limiting food intake is partially due to the suppression of the reward pathway. The loss of OXT+ neurons in the PVN observed in individuals with PWS suggests that there could be downstream effects on hedonic feeding, leading to the loss of inhibition. The loss of OXT in the PVN causes an increase in consumption of sugar-water but not the consumption of HF-chow (Sabatier, 2013). For addressing my research questions, I have used a HF-diet to investigate the loss of *Magel2* on the reward pathway, this will minimize any confounding effect of the possible PVN OXT cell loss.

Magel2-null mice do have abnormalities within the homeostatic feeding pathway. These include a hypersensitivity to the α-MSH-like compounds MTII, an impaired hypothalamic leptin signalling, and an elevated level of serum leptin. *Magel2*-null mice also have other hypothalamic abnormalities including an abnormal circadian rhythm (Pravdivyi et al., 2015; Mercer et al., 2013; Bischof et al., 2007). These homeostatic abnormalities along with the PWS –like body composition of *Magel2*-null mice, and the high-level of *Magel2* expression in the hypothalamus do tell us there is a distinct disruption in homeostatic feeding.

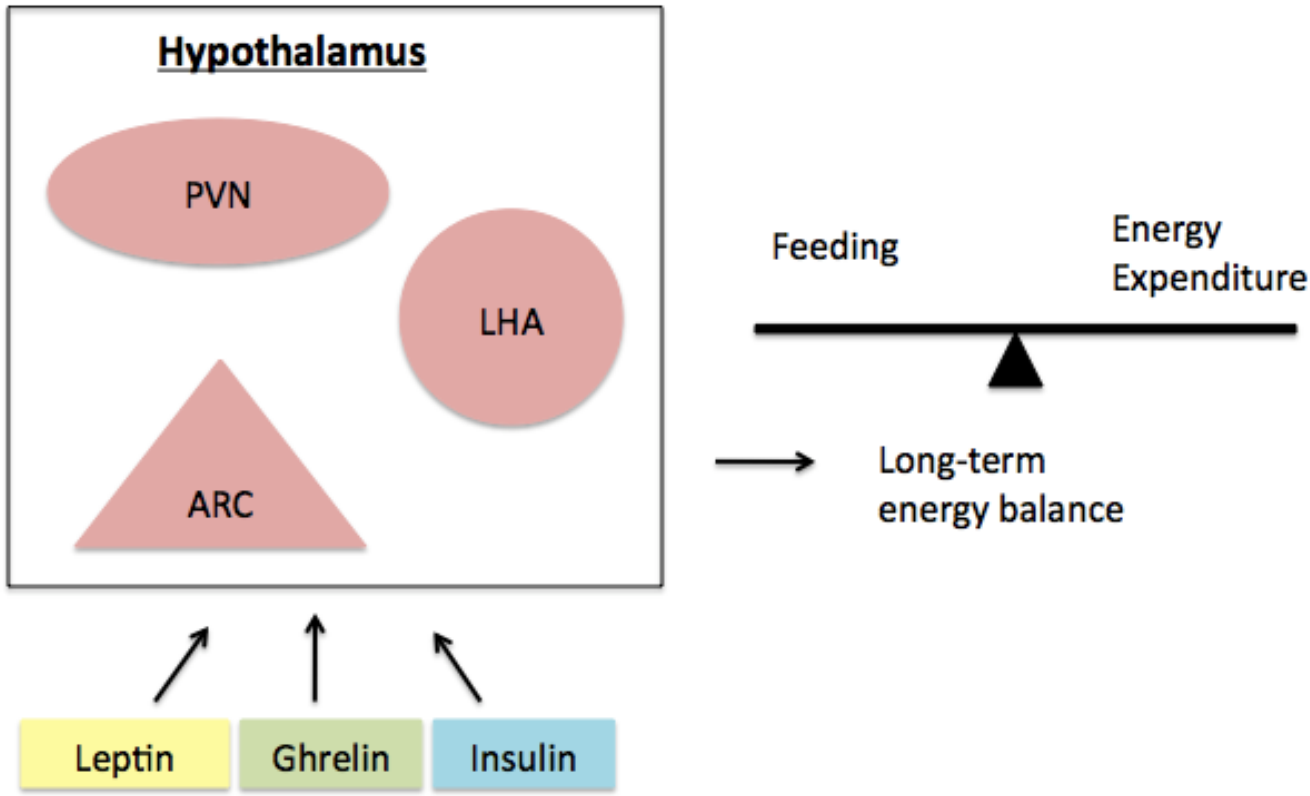

Figure 1.6. Homeostatic Feeding

Schematic of the homeostatic feeding nuclei within the hypothalamus (pink). Hormonal signals are received from the periphery and the hypothalamic nuclei work in concert to maintain long-term energy balance by adjusted feeding and energy expenditure according to physiological demand. Among the peripheral signals are leptin and insulin, both anorexigenic molecules mediating the satiety response, and the orexigenic molecule ghrelin.

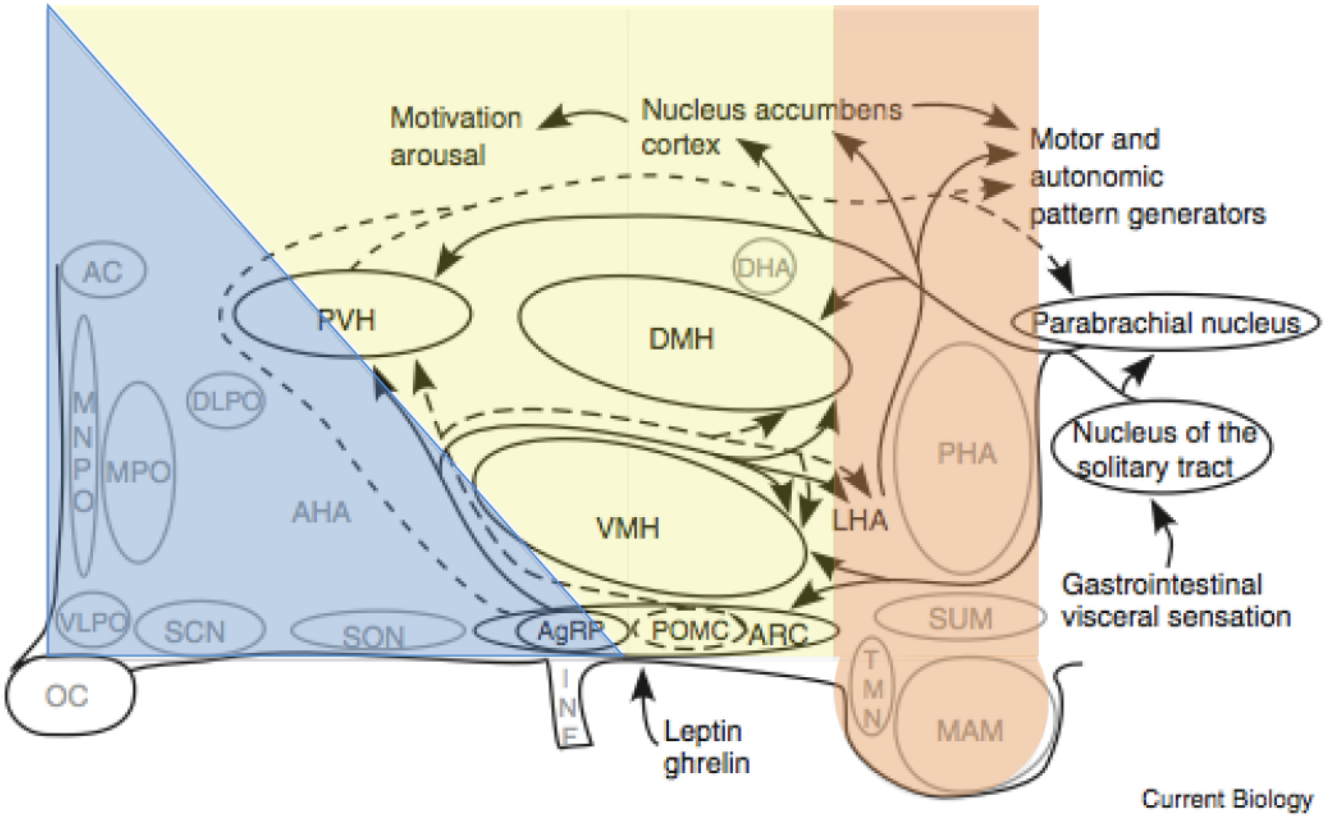

Figure 1.7. Hypothalamic nuclei

The rostral hypothalamus (blue) consists of the preoptic nuclei including the median preoptic nucleus (MNPO), the ventrolateral preoptic nucleus (VLPO), the medial preoptic area (MPO), the dorsolateral preoptic nucleus (DLPO), and the suprachiasmatic nucleus (SCN). The rostral part of the hypothalamus is responsible for circadian function. The caudal nucleus (orange) consists of the mammillary bodies including the mammillary nucleus (MAM), the supramammillary nucleus (SUM), the tuberomammillary nucleus (TMN), and the posterior hypothalamic area (PHA). This portion of the hypothalamus is involved in several processes involved in the arousal state of the animal. The median hypothalamus (yellow) consists of the arcuate nucleus (ARC), the ventromedial hypothalamic nucleus (VMH), the dorsomedial hypothalamic nucleus (DMH), the infundibular nucleus (INF), the lateral hypothalamic nucleus (LHA), and the paraventricular nucleus (PVH, PVN). (Modified from Saper & Lowell, 2014: The Hypothalamus).

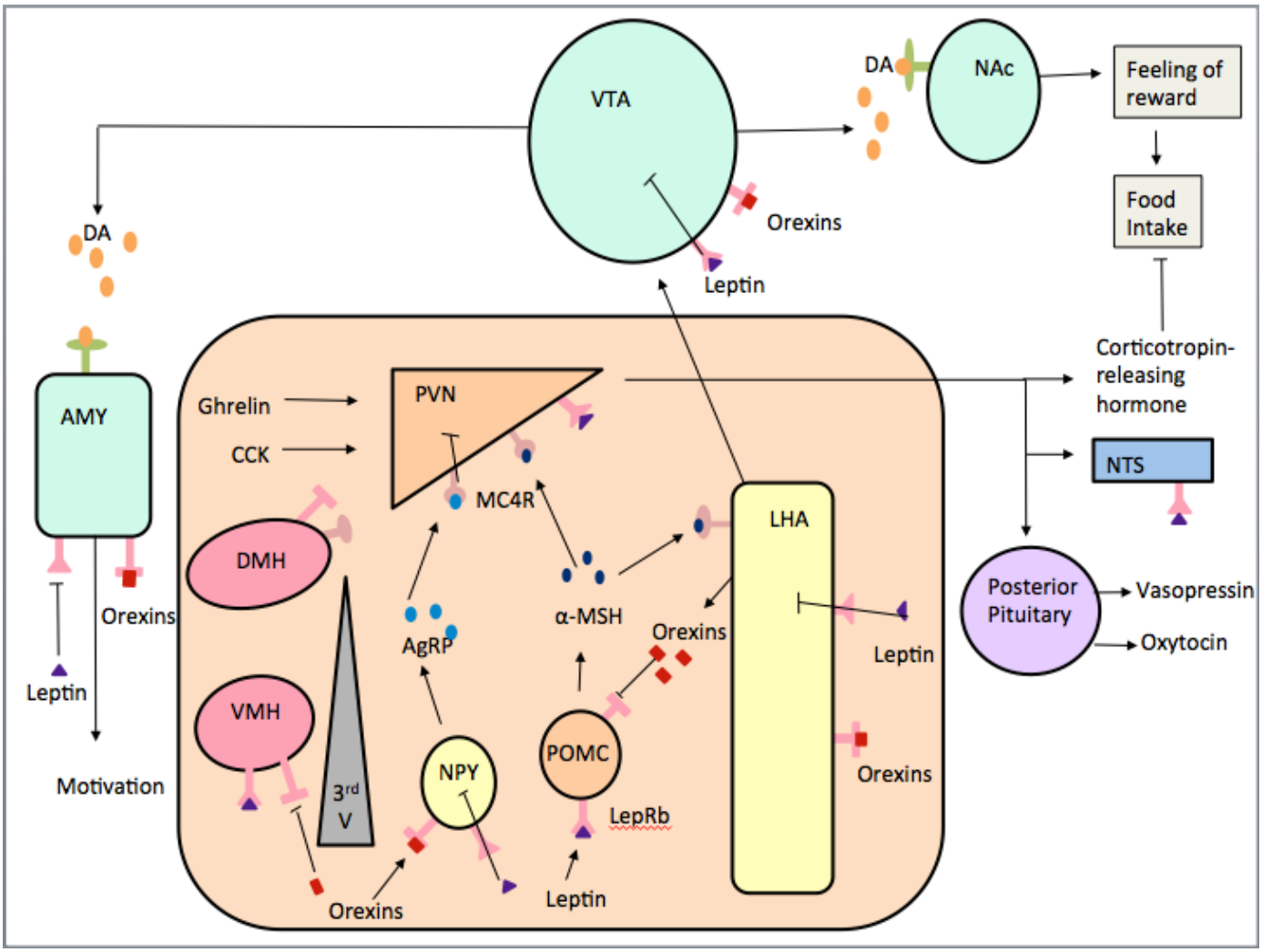

Figure 1.8. The molecular neurocircuitry that mediates feeding behaviour

Feeding behaviour is controlled by a complex circuit of brain nuclei. The arcuate nucleus of the hypothalamus (ARC) responds to circulating leptin produced in adipocytes and the orexin produced in the lateral hypothalamic area (LHA). In response to these energy-status cues NPY+ and POMC+ neurons in the ARC produce AgRP and alpha-MSH, respectively. Both alpha-MSH and AgRP act on the melanocortin-4 receptor (MC4R) in the PVN to modify feeding behaviour.

1.7.2. Hedonic Feeding

Food intake and energy expenditure can also be regulated by the rewarding properties of the food items. This is the hedonic, or reward-driven feeding pathway, controlled by the nuclei of the mesolimbic reward pathway. Hedonic feeding is driven by the inherent reward of the food item itself and not necessarily any nutritional gain. This feeding pathway functions based on the release of dopamine causing a feeling of euphoria paired with the consumption of a palatable food item (Small et al., 2003). This rewarding experience allows for the consumption of palatable food items even in the absence of a physiological need. In 1999 Neel developed the theory of a "thrifty phenotype". This theory states that "thrifty genes" allow us to take advantage of a high-energy food source and that this behaviour would be adaptive in an environment where there is uncertainty about the availability of a subsequent meal (Neel, 1999). Hedonic feeding not only allows us to store energy for times of scarcity, but has also evolved to allow us to take advantage of high-energy food when it is available, even in the absence of physiological need. This short-term weight maintenance pathway allows the availability of an energy-rich food source to override physiological demand. This hedonic feeding system functions on the basis that every food item carries a specific reward value. Changes in dopamine synthesis and transmission have been observed in changes in diet including the binge feeding response to palatable foods (Avena & Bocarsly, 2012).

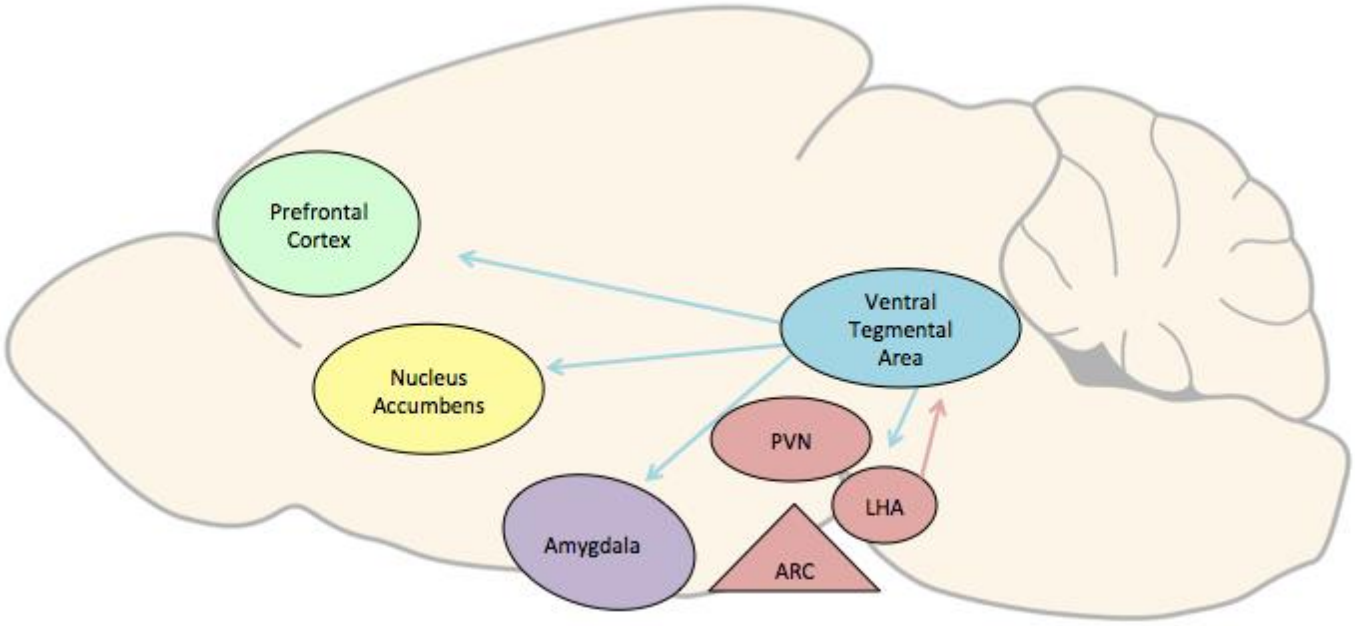

Figure 1.9. The mesolimbic reward nuclei

The mesolimbic reward pathway consists of dopamine-producing neurons in the ventral tegmental area (VTA) of the midbrain (blue). The VTA then sends dopaminergic projections to other nuclei including the prefrontal cortex, the nucleus accumbens, the amygdala, and the hypothalamus (shown in pink) and together these nuclei are responsible for reward-related behaviour.

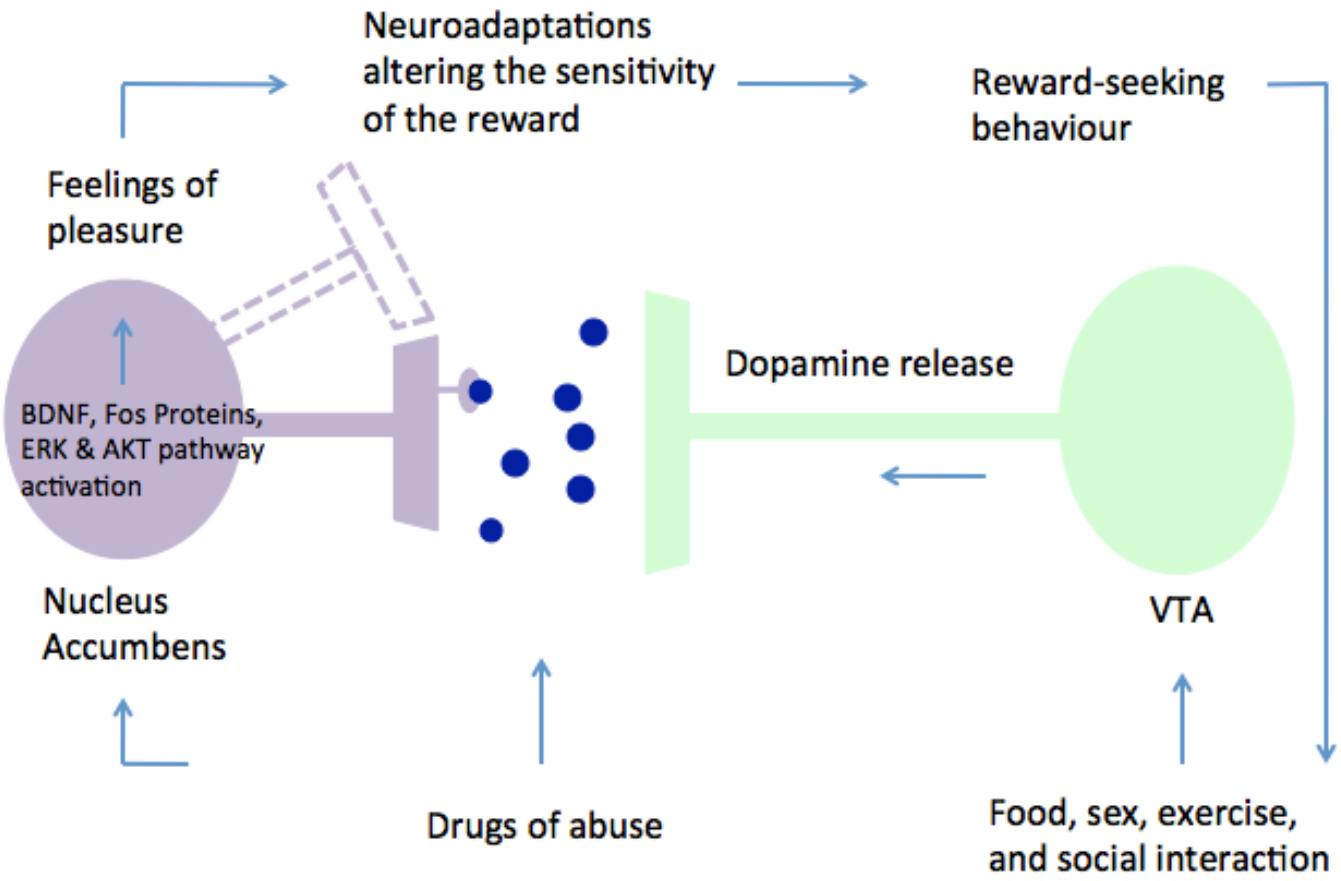

Figure 1.10. Neuroadaptative response to hedonia

The mesolimbic response involves an initial hedonia. This hedonia is produced in the nucleus accumbens in response to dopamine released from dopaminergic neurons in the midbrain. This acute response causes the feelings of reward associated with a specific behaviour or drug. The exposure to reward items also causes a neuroadaptive response. These neuroadaptations include morphological changes and changes in gene expression leading to an altered sensitivity to any subsequent exposure. The transcription factors CREB and Δ FosB are responsible for the acute and chronic effects of an exposure.

1.7.3. Overlap of the homeostatic and the hedonic feeding pathways

The homeostatic and hedonic feeding pathways work together to maintain body weight. There is feedback between the midbrain and the hypothalamus to integrate both energy-status information, as well as information on the reward value of the food item. The LHA communicates directly with the VTA to modulate dopamine activity based on the physiological level of satiety (Figure 1.8). Leptin receptor positive (LepR+) neurons in the LHA respond to leptin to modify the incentive value of a food item (Figure 1.7, Lenninger et al., 2009). Along with the LHA projecting to the midbrain, the VTA and the SN also express leptin receptors, further modifying reward-driven feeding (Figlewicz et al., 2003). Furthermore, it is the same subset of neurons in the VTA that are both dopaminergic and express leptin receptors suggesting that leptin has a direct influence on DA transmission from the midbrain. These midbrain neurons respond to leptin by reducing the dopamine transmission (Nogueiras & Seeley, 2012). The overlap of the hedonic and homeostatic feeding pathways, suggests that despite being able to override homeostasis in the presence of high-reward food, there is still a homeostatic pressure to stop feeding once satiated. This feedback explains why the apparent reward of an item is dependent on the energy status of an animal. Both human and animal models show a similar interaction between energy-status and the reward value of food. Typically, food-restricted animal models show a sensitized reward response, whereas rodent models of hyperphagia and obesity typically demonstrate a desensitized dopamine response (Frank et al., 2012). The reward is modified based on the energy requirements of the individual. For example, in times of low circulating energy the reward value of food increases. So how hungry your body is actually modifies the reward received from different foods. When obese humans are given a palatable food item a similar response is observed. Using fMRI, Gearhardt, et al. (2011), demonstrated exaggerated activity in the amygdala in anticipation of the reward followed by a reduced activation of the striatum to the actual consumption of the reward. The same increased anticipation and reduced striatal activity is observed in individuals with substance dependence (Gearhardt et al., 2011).

1.8. The Dopamine Reward Pathway

1.8.1. Dopamine Circuit

Dopamine is a monoamine that functions in the central nervous system as a neurotransmitter. Dopamine is synthesized from the amino acid tyrosine. Tyrosine hydroylase (TH) is the rate-limiting

enzyme in the conversion of tyrosine into dopamine, and TH is commonly used as a proxy measure for the level of dopamine being produced. In the central nervous system, dopamine acts as a neurotransmitter involved in several neural circuits including the mesolimbic system responsible for hedonic feeding (Figure 1.8; Figure 1.9; Figure 1.10). Dopamine also plays a role in several other behaviours including motor function, sexual behaviour, and drug use (Nestler & Carlezon, 2006). The mesolimbic dopamine pathway consists of dopamine-producing neurons in the ventral tegmental area (VTA) that project to the striatum to produce the feeling of euphoria associated with a reward. The VTA also sends projections to the PFC, the AMY, and the hypothalamus (Figure 1.8). The mesolimbic system is involved in not only the feeling of euphoria but is also involved in the process of learning the reward value of a specific behaviour or consumable, remembering this value, motivating the reward-seeking behaviour, and involved in predicting and planning for obtaining the reward (DiLeone et al., 2012). This learning is facilitated by neuroadaptations morphologically modifying the synapse to alter a subsequent exposure (Figure 1.10). Dopamine dysfunction is involved in several disorders including Parkinson's disease, a neurodegenerative disease where the loss of DA in the substantia nigra causes an initial motor impairment, followed by psychiatric involvement. Dopamine has also been implicated in the development of schizophrenia and most notably in drug dependence. Most antipsychotic medications target dopamine signaling.

The initial exposure to a reward causes a cascade of dopamine-mediated effects. In response to a reward, dopaminergic neurons in the VTA send dopamine projections to the amygdala. Dopamine receptors in the amygdala respond to the level of dopamine in the synapse. The amount of dopamine release and the time spent in the synapse, before reuptake, along with the post-synaptic receptor density, mediate the strength of the response. The amygdala is responsible for learning the value of the reward, learning the context that the reward came with, and forming emotional ties to the context and the specific reward (Fried et al., 2001). The dopaminergic neurons in the midbrain also send projections to the PFC. The prefrontal cortex responds to the synaptic dopamine by planning and predicting a subsequent exposure to the reward. It is the PFC that is responsible for the goal-directed behaviour required to obtain the reward (D'Ardenne et al., 2012). The VTA also sends projections to the striatum. The striatum responds to the dopamine in the synapse and converts this signal into the feeling of euphoria. The NAc, the reward centre of the striatum, mediates the level of euphoria experienced, based on the level of dopamine released into the synapse (Volkow et al., 2011). Dopamine also functions in the periphery to regulate several physiological functions including the sympathetic response, cardiac function, hormonal responses, and olfaction (Beaulieu & Gainetdinov, 2011). In the central nervous system there are several DA-mediated

circuits including the mesocortical pathway, the tuberinfundibular pathway, the nigrostriatal pathway, and the mesolimbic dopamine pathway responsible for hedonic feeding (Beaulieu & Gainetdinov, 2011).

1.8.2. Serotonin Pathway

Serotonin (5-HT) is a neurotransmitter that plays a role in the regulation of sleep, mood, and feeding behaviour. Central serotonin secretion is mediated by the pineal gland via melatonin. In 1990 Chamberlain & Herman suggested that melatonin is linked to several autistic phenotypes and that this is supported by findings of altered levels in individuals with autism. There are several overlapping characteristics of both autism and PWS, including at times the diagnosis. These symptoms include an increased pain tolerance and the loss of interest in social activities (Chamberlain & Herman, 1990). There is a hyposecretion of melatonin in a subset of children with autism contributing to the phenotype. This pineal hyposecretion can lead to the potential deregulation of hypothalamic POMC and 5-HT, both molecules that have been demonstrated to be disrupted in our mouse model (Chamberlain & Herman, 1990; Mercer et al., 2012; Mercer et al., 2013).

1.8.3. Dopamine and serotonin synthesis pathways

In the pre-synaptic cell, dopamine is produced from the amino acid tyrosine. The conversion of tyrosine into L-dopa is both the first step and the rate-limiting step in dopamine production (Figure 1.11). This reaction is catalyzed by the enzyme tyrosine hydroxylase (TH). Once TH is converted into L-dopa, this can then be converted into active dopamine. This reaction is catalyzed by the enzyme aromatic amino acid decarboxylase (AADC) (Elsworth & Roth, 1997). At this point, functional dopamine is released into the synapse and both post-synaptic dopamine receptors, and pre-synaptic autoreceptors, respond in a nuclei-specific manner. Dopamine is removed from the synapse through several different mechanisms. First, the presynaptic cell can recycle the dopamine in the synapse limiting the post-synaptic affect. This removal of synaptic dopamine is facilitated by the DAT reuptake transporter. The DAT transporter is mechanically blocked by cocaine, increasing the time active dopamine is in the synapse and the subsequent post-synaptic response to the DA release. Another mechanism for DA removal is the breakdown of dopamine to homovanillic acid (HVA) either via dopac or 3MT intermediates (Figure 1.11, Elsworth & Roth, 1997). This breakdown is catalyzed by MAO and COMT enzymes. Dopamine is also a precursor to noradrenaline; a neurotransmitter whose primary function is to mediate states of arousal. Dopamine is converted into noradrenaline by the enzyme dopamine B-hydroxylase (DBH).

Serotonin is synthesized by the hydroxylation of tryptophan. Tryptophan hydroxylase (TPH) is the rate-limiting enzyme catalyzing this reaction. Serotonin (5-HT) is then oxidized by monoamine oxidase (MAO) converting it to 5HIAA (Figure 1.12, Squires et al., 2006). Individuals with PWS have demonstrated abnormal concentrations of both serotonin and dopamine metabolites in assays of their cerebral spinal fluid (Åkefeldt et al., 1998).

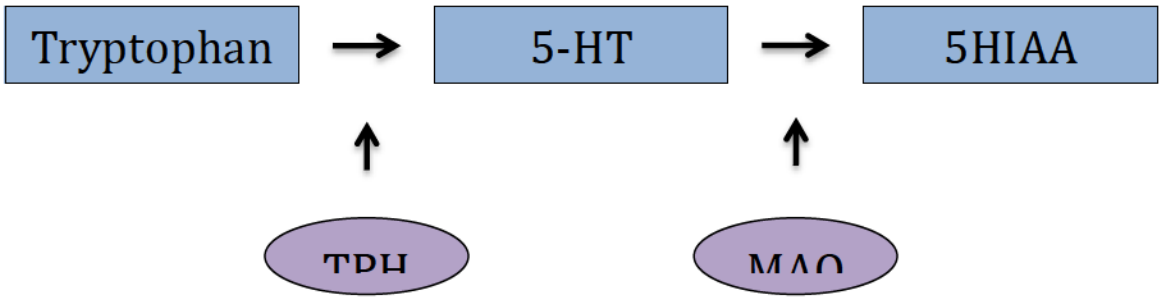

Figure 1.11. Serotonin synthesis pathway and breakdown pathway

Serotonin is synthesized by the hydroxylation of tryptophan. This reaction is catalyzed by the rate-limiting enzyme tryptophan hydroxylase (TPH). Serotonin (5-HT) is then converted to 5HIAA. This oxidation reaction is catalyzed by the enzyme monoamine oxidase (MAO).

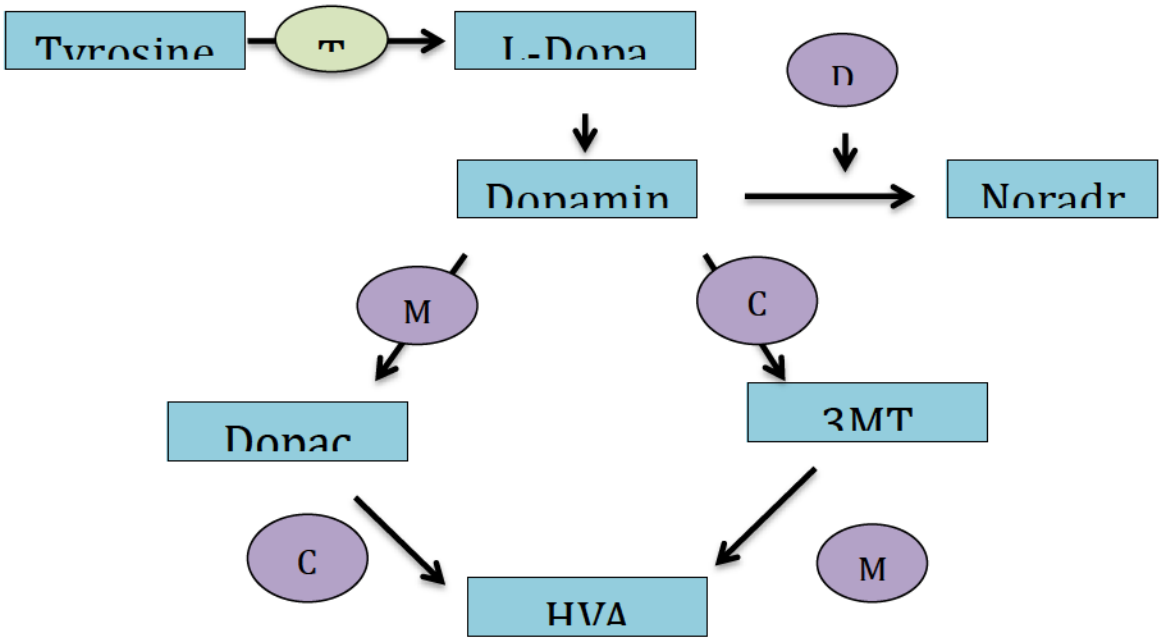

Figure 1.12. Dopamine synthesis and breakdown pathway

The synthesis of dopamine involves the conversion of the amino acid tyrosine into L-Dopa. This reaction is catalyzed by tyrosine hydroxylase (TH). This is the rate-limiting step in dopamine synthesis. L-Dopa is then converted into dopamine, which is then broken down into either 3,4-Dihydroxyphenylacetic acid (Dopac) or 3-Methoxytyramine (3-MT). Dopamine is methylated and converted to 3-MT by the enzyme catechol-O-methyl transferase (COMT). Alternatively, dopamine can be broken down into dopac by the enzyme monoamine oxidase (MAO). Both dopac and 3-MT are further metabolized to homovanillic acid (HVA) via COMT and MAO respectively.

1.8.4. Dopamine projections and receptors

The dopaminergic influence on feeding behaviour is not only determined by the level of presynaptic dopamine being release, but is also dependent on the post-synaptic reception of the dopamine. This post-synaptic influence includes the morphology of the dendritic cell, the signal transduction downstream, of the receptor, and the specific receptor density. There are five dopamine receptors, D1, D2, D3, D4, and D5. These receptors can be divided into 2 types; D1-class receptors (D1 and D5) that activate adenylyl cyclase activity and D2-class receptors (D2, D3, D4) that inhibit adenylyl cyclase activity (Beaulieu & Gainetdinov, 2011). Depending on the post-synaptic DA receptor-type composition, the downstream effects of dopamine differ. Striatal receptor density has been implicated in various psychiatric disorders as well as in binge feeding disorder (Davis et al., 2008).

1.9. Binge eating disorders

Binge eating disorder (BED) is characterized by episodes where individuals consume excessive amounts of food. These bingeing episodes consist of a loss of control, a lack of experienced satiation, and an exaggerated striatal dopamine release (Wang et al., 2011). Bingeing is also observed in individuals with PWS, suggesting that an understanding of the neural mechanisms behind the abnormal motivation to feed in a PWS model could be applicable to a number of feeding-related obesity disorders. An exaggerated striatal signal is observed in BED in response to the exposure of a palatable food (Wang et al., 2011). Individuals with BED are characterized by their impulsivity and their compulsive behaviours surrounding food, much like individuals with PWS. They also share this compulsive drive with drug users who demonstrate a similar lack of control surrounding their drug of choice. In both substance abuse, and binge feeding, the absence of the reward enhances the value of a subsequent exposure making relapse a common occurrence with dieting and drug detoxing (Wang et al., 2011).

1.10. Drug use: Hedonic feeding gone awry?

Abnormal DA signaling is involved in several psychiatric disorders including schizophrenia, Parkinson's disease, and the pathological reinforcement of maladaptive behaviours, commonly referred to as addiction. Abnormal DA signaling is also observed in human binge eating disorder (BED). The dopaminergic reinforcement of adaptive behaviours is important for motivating feeding behaviour and other adaptive behaviours including social interactions and sexual behaviour. Dopamine is released to reinforce these adaptive behaviours by producing the feeling of euphoria, and learning this euphoric value. This learned-euphoria drives the repeated participation in this behaviour and over time these

behaviours become routine. This pattern formation is the result of changes in synaptic morphology and gene expression. These changes in synaptic morphology lead to individual preference and habit formation, based on the nutritional and situational context. This dopamine-mediated habit formation is important for reinforcing behaviours that are adaptive in a given environmental context. This reinforcement can become pathological in nature leading to the addiction of naturally adaptive things like food, sex, exercise, and social interaction (Figure 1.9). This dopamine-reward system can also mediate a euphoric response to other non-natural behaviours in a given environment. For example, behaviours that are inherently risky can become addictive through a dopamine-mediated reward. This includes behaviours like gambling, and extreme sports where there is a risk of severe loss. Addiction can also occur in response to chemical drugs that act directly on the dopamine reward pathway. Drugs are often considered to be "hijacking" the reward pathway to lead to the dependence (DiLeone et al., 2012). In many ways the molecular mechanisms behind compulsive drug-use and compulsive feeding overlap.

The state of addiction involves long-lasting changes in the brain that lead to the compulsive and pathological consumption of a reward. These changes in synaptic morphology and gene expression drive reward-seeking behaviour and are responsible for the withdrawal phenotype in the absence of the reward. Some of the molecular changes can persist long after the discontinued exposure making quitting the behaviour a long-term challenge. The changes in gene expression and in synaptic morphology are not only responsible for addiction and withdrawal phenotypes but are also responsible for the increased risk of relapse months to years after the cessation of use (E. J. Nestler, 2004). The neuro-molecular responses to exposure and withdrawal can be quantified to assess any abnormalities in the reward pathway influencing hedonic behaviour.

One of the initial molecular changes that occur in response to exposure, is the increased phosphorylation of cAMP response element binding protein (CREB) in the NAc. CREB is a transcription factor that once phosphorylated (Ser133) binds to CRE (cAMP response element). Once bound, pCREB regulates gene expression of several proteins involved in the sensitivity of a response, including dynorphin (E. J. Nestler, 2004). In the NAc the phosphorylation of CREB is responsible for decreasing an animal's response to a specific reward creating a molecular tolerance. CREB activity in the NAc not only desensitizes an animal to the exposure but also desensitizes the animal to the effects of other rewards (Baladi et al., 2015; Barrot et al., 2002). An increased activity of pCREB is observed in response to the exposure of opioids and natural rewards like palatable food. The activity of CREB in the NAc is also increased with the exposure to stress to modify the amount of a reward required to produce a response

(Barrot et al., 2002). This tolerance drives an increase in required dosage to receive the original reward (E. J. Nestler, 2004). In the absence of the reward the CREB-induced tolerance is responsible for the initial anhedonic response to withdrawal. The phosphorylation of CREB in other reward nuclei also influences an animal's tolerance to a drug. This includes the AMY, the hypothalamus, and the midbrain (Jentsch et al., 2002; Olson et al., 2005; Georgescu et al., 2003).

Chronic exposure to drugs of abuse also leads to changes in gene expression and morphological changes to the synapse. In response to chronic exposure of both drugs of abuse and palatable food there is also an accumulation of ΔFosB in the striatum (E. J. Nestler, 2004). DeltaFosB is involved in the sensitizing an animal to both the specific rewards, driving repeated exposure after long-term use. In the NAc, ΔFosB forms a heterodimer with Jun proteins to form activator protein-1 (AP-1) complexes. These transcription factor complexes are responsible for regulating gene expression. Among the genes induced by ΔFosB are GluR2, a glutamate receptor, Cdk5 involved in neuronal growth, and NF-KB. These ΔFosB-mediated changes in gene expression are involved in the synaptic plasticity that leads to an increase in spine density sensitizing the animal to subsequent exposure (E. J. Nestler, 2004). DeltaFosB and the phosphorylation of CREB can both be used as molecular markers for an animal's addiction response.

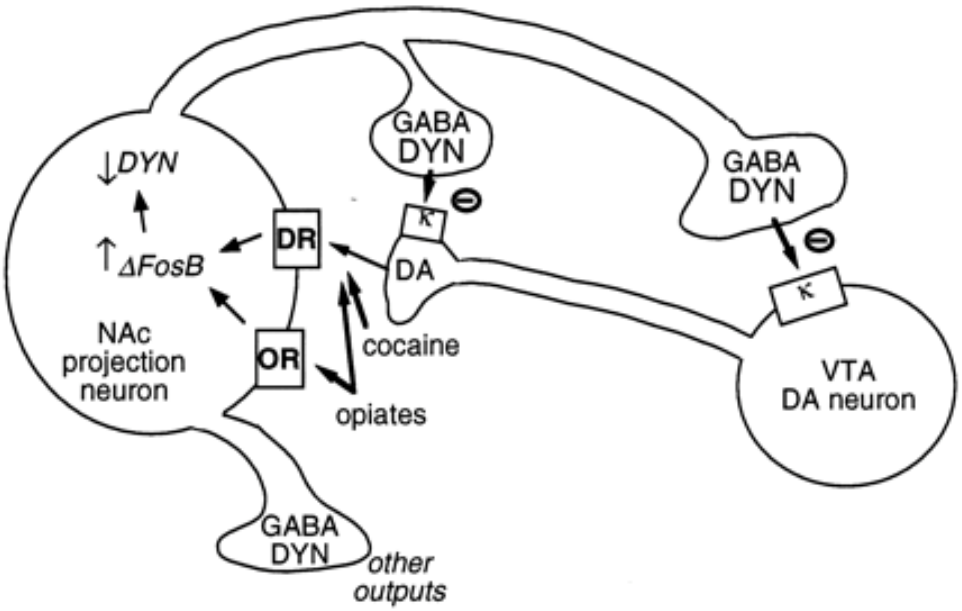

Figure 1.13. Molecular feedback in response to exposure within the mesolimbic dopamine pathway

In response to the long term exposure of a drug of abuse, or the chronic exposure of a natural dopamine release-inducing reward, there is the induction of the Fos protein Δ FosB. The accumulation of this protein in the post-synaptic striatal cell alters the expression of post-synaptic dynorphin causing a morphological change that feeds back to the pre-synaptic cell facilitating the sensitization to a subsequent exposure. (Adapted from Nestler et al., 2004: Molecular mechanisms of drug addiction.)

1.11. Hypothesis and Aims

Dopamine-related behavioural abnormalities have been observed in PWS. These include mood swings, abnormal fMRI responses to food, and abnormal concentrations of dopamine metabolites (Clarke et al., 2002; Holsen et al., 2006). These abnormalities suggest that an impairment in the dopamine reward system is contributing to the PWS phenotype. The aim of this research project is to characterize the dopamine reward pathway in our mouse model of PWS. Understanding how reward-driven feeding has gone awry in this mouse model could influence how childhood obesities including PWS are addressed. This research project aims to pinpoint how the loss of *Magel2* is influencing reward-driven feeding in the hedonic feeding pathway.

First, the pre-synaptic dopamine nuclei, the post-synaptic nuclei, and the projections within the reward pathway were assessed for any dopamine-related abnormalities. The characterization of the dopamine-reward pathway is an important first step in understanding how the loss of *Magel2* throughout development has influenced the dopamine-related neuro-functionality of the system. The second aim was to evaluate how the loss of *Magel2* influences both the behavioural and neuromolecular responses to changes in diet. This included the limited exposure of a HFD, the chronic exposure to a HFD, and the withdrawal of a chronic HFD.

In combination with determining the specific cellular function of MAGEL2, the results of these experiments could influence how binge-feeding in Prader-Willi Syndrome is addressed. I hypothesize that a loss of dopamine signaling to the striatum from the VTA is influencing the PWS-like phenotype observed in our Magel2-null mouse model, and that a same loss of dopamine response is also influencing the compulsive feeding phenotype observed in individuals with PWS.

Chapter 2: Materials and Methods

2.1. Mouse Model

All of the experiments performed were done on brain tissue from mice that were bred from *Magel2*-null mice acquired from the Jackson Laboratory (Stock #009062, C57BL/-Magel2$^{tm1Stw/J}$). This mouse strain was previously developed by inserting a *LacZ* reporter cassette into the ORF of the *Magel2* gene leaving a mouse that expresses *LacZ* in place of *Magel2* (Figure 1.3, Bischof et al., 2007; Kozlov et al., 2007). *Magel2*-carrier males were bred with wildtype females. Magel2 is maternally silenced with only the paternal copied leading to the expression of the protein. This cross produces *Magel2*-null offspring, heterozygous for *Magel2* and the *LacZ* insertion, and homozygous control littermates expressing endogenous *Magel2*. For all the experiments both male and female adult mice (8-12 weeks) were used. Mice were housed in groups of 2-6 mice per cage. All the mice were maintained on standard chow (4 % Calories from fat), unless otherwise stated. Breeders were fed a diet with 9 % of the total Calories being from fat. Mice were housed in the University of Alberta Health Science Laboratory Animal Services HSLAS facilities under standard conditions (12 hr light/dark cycle, lights on from 6am – 6pm, temperature maintained at 21 °C). Mice were bred in pairs. The mice were euthanized by administering a lethal dose of euthanyl into the peritoneum. This was either followed by a cardiac perfusion once mice reached surgical plane, or dissection following death. The University of Alberta Animal Care and Use Committee approved all procedures involving animals in accordance with the guidelines of the Canadian Council on Animal Care.

2.2. Antibodies

Most of the experiments performed relied heavily on the use of antibodies for either detecting or quantifying the differences within the reward pathway of the *Magel2*-null mice. The antibodies used for IHC include rabbit polyclonal anti-tyrosine hydroxylase (Chemicon), at a concentration of 1/2000, and rabbit polyclonal phospho-STAT3 (Tyr705) (Cell Signaling) used at a concentration of 1/1000 (Table 2.1). The secondary antibodies used for the IHC experiments include fluorescently-tagged goat anti-rabbit Alexa-Fluor 488 and goat anti-rabbit Alexa-Fluor 594. To assess the molecular response to different feeding conditions the following antibodies were used: rabbit monoclonal anti-phospho-CREB (Ser133) (Cell Signaling), rabbit monoclonal anti-CREB (Cell Signaling), anti-phospho-p44/p42 map kinase (phospho-ERK1/2)(Cell Signaling), rabbit polyclonal anti-ERK (1/2) (Santa Cruz), rabbit polyclonal anti-tyrosine hydroxylase (Chemicon), polyclonal rabbit anti-AKT (Cell Signaling), rabbit monoclonal anti-

phospho-AKT (T308) (Cell Signaling), and rabbit polyclonal anti-ΔFos (Santa Cruz) (Table 2.1). To assess the response to leptin injection the following antibodies were used: rabbit polyclonal anti-phospho-STAT3 (Tyr705)(Cell Signaling), and rabbit monoclonal anti-STAT3 (Cell Signaling). Immunoblotting with the following antibodies was used to detect glial fibrillary acidic protein (rabbit polyclonal anti-GFAP (H50) (Santa Cruz)), synaptic vesicle glycoprotein-2 (mouse monoclonal anti-SV2 (DSHB), and neurofilament (mouse monoclonal anti-2H3 (DSHB)). The phophorylated proteins were quantified using the total protein levels as a control. The remaining immunoblots were normalized using either mouse monoclonal anti-γ-tubulin (Sigma) or mouse monoclonal anti-β-actin (Sigma) (Table 2.1). The secondary antibodies used for immunoblotting include enhanced chemiluminescence (ECL) anti-rabbit IgG horseradish peroxidase-linked (HRP-linked) whole antibody from donkey (GE Healthcare), and ECL anti-mouse IgG HRP-linked whole antibody from sheep (GE Healthcare). A complete listing of the antibodies that were used and the concentrations used is outlined in Table 2.1.

2.3. Tissue Histology

In order to collect tissue for immunohistochemistry and thionine histology the mice underwent a cardiac perfusion. The mice were injected with 100 µL of euthanyl, and once they reached surgical plane, determined by the lack of toe-pinch response, we proceeded to open the chest cavity. The heart was exposed by making one cut up the midline through the ribcage and another incision laterally below the left side of the rib cage. The left half of the diaphragm was carefully cut following the lateral incision exposing the heart. A 25 G butterfly needle was then inserted into the left ventricle of the heart. The liver was immediately cut allowing the blood to exit the system and 20 ml of saline was perfused through the animal followed by 20 mL of 4% ice-cold paraformaldehyde (PFA). Once perfused, the brain was removed and post-fixed in 4% PFA for 4 hours at 4 °C. The whole brain was then placed in a sucrose gradient. The brain was dropped in 15 % sucrose and once the brain had sunk to the bottom of the sucrose, this was repeated with 30 % sucrose. The brain was then frozen in a block of optimal cutting temperature compound (OCT) in liquid nitrogen (LN2) and stored at -80 °C.

2.4. Cryosectioning

For immunohistochemistry, coronal and sagittal sections of the brain were used. After being perfused, whole brains were sectioned on the cryostat with a chamber temperature of -20 °C and a mount temperature of -16 °C. To investigate the individual nuclei within the reward pathway 30 µm coronal sections were used. Sections were carefully mounted onto glass slides by thawing the frozen section using

a gloved finger. To locate the appropriate brain region, thionine staining was performed on every 4th section. This protocol was adapted from the thionine staining protocol from Dr. Greer's laboratory (University of Alberta, Dept. of Physiology). Thionine was used to stain Nissl substance in neuronal cells, this provided us with a visual of the ultrastructure of the section. Thionine was prepared by combining 10 mL of solution A (1 g Thionine/100 mL Milli-Q (MQ) water) with 60 mL of solution B (6 mL glacial acetic acid/ L MQ water), and 40 mL of solution C (13.6 g sodium acetate/L MQ water). The three solutions were combined on low heat for 1 hour with constant stirring. Slides were brought to RT before staining. Slides were then placed in 50 % ethanol (EtOH) for 2 minutes then washed in MQ water for 2 minutes. Slides were then placed in the thionine stain for 30 seconds followed by three 2-minute washes in MQ water. Slides then underwent a differentiation step to remove some of the background. This differentiation step included an EtOH gradient with 2-minute washes in each dilution (50, 75, 95, 100 %). Slides were then placed in Xylene for 3 minutes, and again for 4 minutes before being mounted with VectaMount (Vector Laboratories). The Mouse Brain in Stereotaxic Coordinates, compact, Third Edition: The coronal plates and diagrams (Franklin & Paxinos) was used as a reference atlas to identify the thionine-stained sections containing the nuclei of interest, and the adjacent section was used for immunostaining. Coronal sections from the SN and the VTA were collected from the midbrain, the ARC and PVN from the hypothalamus. Sections were stored at -20 °C until immunostained. Thionine staining was also used to compare the general structures of the hypothalamic nuclei of *Magel2*-null and wildtype mice.

2.5. Immunohistochemistry

Immunohistochemistry (IHC) was used to quantify the number of dopamine producing neurons within the nuclei of the reward pathway, and to measure the area of the dopaminergic nuclei. Immunohistochemistry was also used to address the levels of TH reaching the target nuclei in sagittal sections. Frozen sections were thawed and brought to room temperature (RT) for 15 minutes before beginning the staining protocol. The appropriate sections were outlined with a PAP pen and rinsed in PBS-T (PBS/0.1 % Tween-20). The slides were then incubated with blocking buffer (3 % normal goat serum, 0.3 % Triton X-100 in PBS) for 1 hour at RT. The blocking buffer was then poured off the slide and the sections were incubated in primary antibody (1/200-2000, 1 % normal goat serum) overnight at RT in a humidified slide box (See Table 2.1 for antibody dilutions). The slides were then washed in PBS-T three times for 10 minutes in a coplin jar with gentle rocking. The secondary antibody (2°Ab) was then incubated at RT for 2 hours in the humidified slide box and then was again washed for 10 minutes three

times in PBS-T at RT. After the final wash slides were then washed again for 10 minutes in 1:250 Hoechst stain (Thermo Scientific): PBST in order to counterstain the nuclei of the cells. Slides were washed once more for 10 minutes in PBS-T, then using 50 µl of 1:3 glycerol: PBS as mounting media, the cover slips were mounted. Alternatively ProLong gold anti-fade reagent with DAPI (Molecular Probes) was used to stain the nuclei and as a mounting media. Slides were sealed with clear nail polish, left to dry, and stored at -20 °C until imaged.

2.6. Imaging

In order to quantify the number of dopamine producing cells, immunostained sections were imaged using the LEICA TCS SP5 Laser Scanning Confocal microscope in the University of Alberta core facility. Images were taken at 10 X magnification. Z-stacks of 15 images were taken, compressed and exported to ImageJ where TH+ cells were counted. Three adjacent sections were counted from the nuclei of at least three different animals of each genotype. These images were then used to quantify the TH+ area of each nuclei, outlined by TH+ cells. The LEICA TCS SP5 confocal microscope was also used to image the target nuclei in the sagittal sections. Two-dimensional images were taken at 63 X magnification. The number of TH+ cells was determined by counting the number of cells containing signal in the cytoplasm, and a linescan profile was used to compare the level of staining in the target nuclei. ImageJ was also used to measure the area of the individual nuclei, determined by the borders of the TH+ cells. For experiments using fresh tissue of various brain regions slices were imaged on the Olympus SZX16 stereomicroscope system. This was done to maintain consistency between tissue punches. The thionine stained sections were also imaged on this system. Tyrosine hydroxylase-stained sagittal sections were analyzed for the thickness of the axon bundles. These sections were imaged on the Eclipse TE2000-4 microscope (Nikon) using NIS-Elements BR 4.00.03 imaging software. The sagittal images were taken at 100 X magnification, exported, and analyzed on ImageJ software.

2.7. Feeding experiments

2.7.1. Exposure and withdrawal of a high-fat diet

The exposure to a palatable food source can cause biochemical responses that contribute to an addictive phenotype. In order to determine the involvement of *Magel2* in this response, we subjected *Magel2*-null mice and their wildtype littermate to a high-fat (HF) diet. Mice were divided into three different feeding groups. The first group was fed a standard diet for 28 days. The second, the exposure group, was fed a HF-diet (DIO Rodent Purified Diet with 60 % Energy from fat, TestDiet) for 28 days. The

third feeding group, the withdrawal group, was fed a HF-diet for 28 days followed by a 24-hour return to standard chow. At the end of the feeding period the mice were euthanized with 200 µL of euthanyl and fresh tissue was collected for HPLC and immunoblot analysis. During the feeding trial the weight of each individual animal was recorded every other day to ensure they were physiologically exposed to the high-fat diet. Animals were housed in groups of 2-4 animals/cage. The food intake of the cage was recorded for 2 days before the trial and every other day throughout the trial. Tissue was collected from both hemispheres of the brain. Tissue from one hemisphere was used for immunoblotting, and the other hemisphere was collected for HPLC analysis. Tissue included samples from the hypothalamus, the amygdala, the prefrontal cortex, the hippocampus, the hindbrain, the striatum, and the VTA. The remaining hindbrain was collected and used to check the genotype by staining for the presence of *LacZ*. This experiment was repeated to increase the number of animals in each feeding group. (n=5-8/feeding group).

2.7.2. Binge-feeding paradigm

Limited access to a desirable food source induces binge-feeding behaviour in mice. Exposing the mice to a palatable food source for a limited time allowed us to assess this bingeing response in *Magel2*-null mice. Adult mice were individually housed for 2 weeks leading up to the binge-feeding trial. Mice were given access to high-fat food (60 % energy from fat, TestDiet) daily for one hour at noon. The mice had access to standard chow at all times. The amount of HF food consumed within the hour of access was recorded over 10 days of limited exposure. This protocol was developed by Halpern et al. (2013).

2.8. Tissue punch collection

Using a rodent brain slicer (Zivic), 1 mm and 2 mm coronal slices were collected from fresh brains. Whole brains were removed from the mice and put in ice-cold PBS for 1 minute before being placed in the brain matrix and sliced with 0.009 inch blades. Slices were removed from the brain matrix and placed on glass slides. Slides were put on dry ice to harden tissue, and punches were collected using various sized tissue punchers (0.5- 2.0 mm, Harris, Uni-core). Tissue punches were snap frozen in liquid nitrogen and stored at -80 °C. Samples were then processed for either protein quantification through immunoblot analysis, or for quantification of biogenic amines through HPLC analysis.

2.9. Immunoblotting

Tissue punches collected from the reward nuclei were used to analyze the protein levels between *Magel2*-null mice and their wildtype littermates. Sodium dodecyl sulfate denatured polyacrylamide gel electrophoresis (SDS-PAGE) followed by immunoblotting was used to compare total protein levels, as well

as the phosphorylation state of certain proteins in both standard fed animals and those exposed to, and withdrawn from a HF-diet (Protocols modified form: Weber & Osborn, 1973, and Towbin et al., 1979). Samples were prepared by sonicating the tissue in 2X modified sample buffer (20 % glycerol, 4 % SDS, 1.53M Tris) with complete Mini EDTA-free protease inhibitor tablets (Roche) and phosphoSTOP phosphatase inhibitor tablets (Roche), and centrifuged at 14,000 rpm at RT. Samples were then heated to 65 °C for 10 minutes. Total protein levels were then quantified using the BCA protein assay kit (Thermo Scientific). Once quantified, 2 % of saturated bromophenol blue and 1 % of β-mercaptoethanol was added to each sample. Samples were boiled for 5 minutes. Depending on the size of the protein of interest, samples were loaded onto 7.5 %, 10 % or 12.5 % SDS-PAGE acrylamide gels. Aiming for a total protein concentration of 20 µg per well, proteins were electrophoresed along with Precision Plus Dual color standard (BIO-RAD) at 80 milliamps for roughly 45 minutes, or until the ladder had separately appropriately. Once separated on the gel, proteins were transferred onto Immobilon-P transfer membranes (Millipore) either overnight at 30 volts, or for 90 minutes at 100 volts. Depending on the protein of interest, the membranes were blocked in either TBSTM (TBST/5 % Milk) or TBST containing 5 % BSA. When probing for phosphorylated proteins, TBST-BSA was used instead of TBSTM. The membranes were incubated at various times and temperatures depending on the antibody. After the primary incubation, membranes underwent three 10-minute washes in TBST. The blot was incubated with the secondary HRP-linked antibody at RT for 1 hour, followed by three 10-minute washes in TBST. Membranes were then incubated in Immobilon Western Chemiluminescent HRP Substrate kit (Millipore) for 5 minutes before being imaged on the Kodak Imager. The phosphorylated proteins were normalized by stripping blots with Restore western blot stripping buffer (Thermo Scientific) for 30 minutes at RT, and reprobing with a primary antibody for the total protein. The non-phospho-proteins blots were stripped and reprobed for either β-actin or γ -tubulin. The blots were quantified using ImageJ software.

2.10. High-performance liquid chromatography

High-performance liquid chromatography was performed in Dr. Glen Baker's laboratory in the Department of Psychiatry at the University of Alberta, under the supervision of Gail Rauw. The protocol used for the detection of these metabolites was developed in Dr. Glen Baker's laboratory (Parent et al., 2001).

Tissue samples from each of the described feeding groups were analyzed for their levels of serotonergic and dopaminergic metabolites. The 2 mm diameter tissue punches were homogenized over ice in 20 X

volume of 0.1 N perchloric acid containing EDTA and ascorbic acid. Homogenized samples were centrifuged at 10,000 rpm for 5 minutes at room temperature. Standards containing known concentrations of each metabolite were prepared fresh for each run, containing DA, NA, Dopac, 5HIAA, HVA, 5HT, NME, 3MT or tryptophan. The standards ranged from a blank to 100 ng of each amine dissolved in 0.1 N perchloric acid. The samples were run through a Waters Atlantis dC18 column for roughly 50 minutes, and detected on a Waters 2465 Electrochemical detector with an applied potential of 0.6 volts. Samples included tissue from the amygdala, the prefrontal cortex, the striatum, the hypothalamus, the hindbrain, and the ventral tegmental area.

2.11. *LacZ* staining – genotyping

To determine the genotype of each mouse, our laboratory technician Jocelyn Bischof performed PCR analysis on DNA from ear notches from all the animals using a modified protocol from the Jackson laboratory (https://www.jax.org/strain/009062). *LacZ* staining was used on fresh tissue to test for the presence of β-galactosidase activity, to confirm previously performed PCR genotyping. Immediately after euthanizing the animal, hindbrain tissue was collected into a microfuge tube and 100 µL of *LacZ* stain with X-gal (5-bromo-4-chloro-3-indolyl-β-D-galactopyranoside), prepared fresh, was added. The hindbrain was incubated with the *LacZ* stain at 37 °C for 30 minutes. The hindbrain was used due to the high expression of *Magel2* and because it was not needed for several of the experiments. The genotype was determined by the presence or absence of the β-galactosidase insertion indicated by the tissue turning blue in Magel2-null mice carrying the *LacZ* reporter cassette.

2.12. Statistical analysis

Statistical analysis was done to determine significance of all results. For the experiments making a direct comparison between wildtype and *Magel2*-null mice, a Student two-tailed t-test was performed with a statistical significance being set at a p-value of less than 0.05. Several of the experiments analysed the effect that two independent variables had on the result. For these experiments a 2-way ANOVA was used to identify any significant interaction between the two variables. These experiments include the effect that both diet and genotype have on the amount of protein and biogenic amines present. An interaction was considered significant with a p-value of less than 0.05. This test measures the effect that genotype has across a group of metabolites, allowing us to determine how the genotype influences an entire metabolic pathway. Similarly, this test allows us to determine how a variable like genotype affects an outcome across a group of brain regions. In cases where the 2-way ANOVA detected a significant effect of genotype, post-

hoc analysis was performed to identify the specific compounds that contribute to the difference between genotypes. The statistical analyses were performed using GraphPad Prism software (San Diego, CA), this program was used to produce graphs that display the means of each measurement with error bars demonstrating the standard error of the mean (SEM). The SEM was used to report variability unless otherwise stated.

Summary of Antibodies				
Primary Antibodies	Host	Supplier	WB Concentration	IHC Concentration
Tyrosine hydroxylase (TH)	Rabbit Polyclonal	Chemicon	1:1000	1:2000
Phospho-STAT3 (Tyr705)	Rabbit Polyclonal	Cell Signaling	1:1000	1:1000
Phospho-CREB (Ser133)	Rabbit Polyclonal	Cell Signaling	1:1000	
CREB	Rabbit Monoclonal	Cell Signaling	1:1000	
Phospho-ERK1/2 (p42/p44)	Rabbit Polyclonal	Cell Signaling	1:1000	
ΔFos	Rabbit Polyclonal	Santa Cruz	1:500	
AKT	Rabbit Polyclonal	Cell Signaling	1:1000	
pAKT (T308)	Rabbit Monoclonal	Cell Signaling	1:1000	
ERK1/2	Rabbit Polyclonal	Santa Cruz	1:1000	
STAT3	Rabbit Monoclonal	Cell Signaling	1:1000	1:1000
GFAP (H50)	Rabbit Polyclonal	Santa Cruz	1:500	
SV2 (Synaptic Vesicle Protein-2)	Mouse Monoclonal	DSHB	1:500	
2H3 (Neurofilament)	Mouse Monoclonal	DSHB	1:200	
Y-Tubulin	Mouse Monoclonal	Sigma	1:5000	
B-Actin	Mouse Monoclonal	Sigma	1:50000	

Table 2.1. Summary of antibodies

Summary of the antibodies used throughout the included experiments. Antibodies are listed next to the dilutions used for both immunoblot (WB) and immunohistochemistry (IHC) experiments.

Chapter 3: Results

3.1. Baseline comparison of *Magel2*-null mice to their wildtype littermates

3.1.1. *Magel2*-null mice have fewer dopamine-producing cells in the periventricular hypothalamic nuclei

Tyrosine hydroxylase (TH) is the rate-limiting enzyme in the pre-synaptic production of dopamine (Figure 1.11). Using TH immunohistochemistry, the number of neurons that produce dopamine were counted. In 2009 Mercer et al. found reduced levels of dopamine in the hypothalamus of *Magel2*-null (ML2) mice compared to wildtype (WT). We expected to find fewer dopamine-producing cells in one or more of the hypothalamic nuclei to account for the observed loss of dopamine. We would also expect fewer dopamine-producing neurons in the VTA, which would help explain the loss of response to cocaine, and the reduced dopamine observed in whole brain lysates (Mercer et al., 2009; Luck et al., in press, Figure 1.4).

There was no detectable difference in the number of TH+ neurons in either of the midbrain nuclei measured. This included the VTA and the SN (Figure 3.2, VTA WT n=17, ML2 n=12; SN, WT n=12, ML2 n=9). In the hypothalamus, TH+ cells were counted in the paraventricular nucleus (PVN), the arcuate nucleus (ARC) and the periventricular nucleus (PeVN). The periventricular neurons were distinguished from the paraventricular neurons using the third ventricle as a reference (Figure 3.1). There was no observable difference in the number of TH+ cells in the ARC (Figure 3.3, ARC, WT n=20, ML2 n=8). The A13 (PVN) originally showed a significant increase in TH+ cell number in the *Magel2*-null mice (Figure 3.3, PVN, 1.17-fold increase, WT n=8, ML2 n=5, p=0.04). This experiment was repeated to verify the significance of this result. The second data set showed no significant difference between genotypes (A13, WT n=3, ML2 n=3). The PeVN was subdivided into rostral and caudal areas. Despite being a continuous nucleus, these dopaminergic cells can be separated into the A14 and A15 cell groups, with A15 cells being situated more rostrally and the A14 group located more caudally (Gayrard et al., 1995; Vulpen et al., 1999). There were significantly fewer TH+ cells in the caudal A14 region and a similar trend in the rostral A15 region of *Magel2*-null mice (Figure 3.4, Caudal A14, WT n=7, ML2 n=6, p=0.05; Rostral A15, WT n=6, ML2 n=6 p=0.08). A 2-way ANOVA of both the rostral and caudal regions of the PeVN also showed a significant effect of genotype (p=0.01). Both the A15 and A14 regions of periventricular hypothalamus send projections to the supraoptic nucleus (SON) of the hypothalamus where the release of specific hormones, namely oxytocin and vasopressin, is regulated (Vulpen et al., 1999).

Along with abnormal numbers of OXT+ neurons, the paraventricular nuclei of individuals with PWS have also been shown to be smaller in size, and to have fewer total cells, indicated through thionine staining (Swaab et al., 2013). No obvious difference was observed between the *Magel2*-null mice and their wildtype littermates by thionine staining (Figure 3.5 & Figure 3.6). Tyrosine hydroxylase staining was used to measure the area of the hypothalamic and midbrain dopaminergic nuclei. There was no observable difference in the area of either hypothalamic nucleus, or either of the midbrain nuclei (Figure 3.7, PVN, n=6, ns; ARC, n=3, ns; SN, n=3, ns; VTA, n=3, ns).

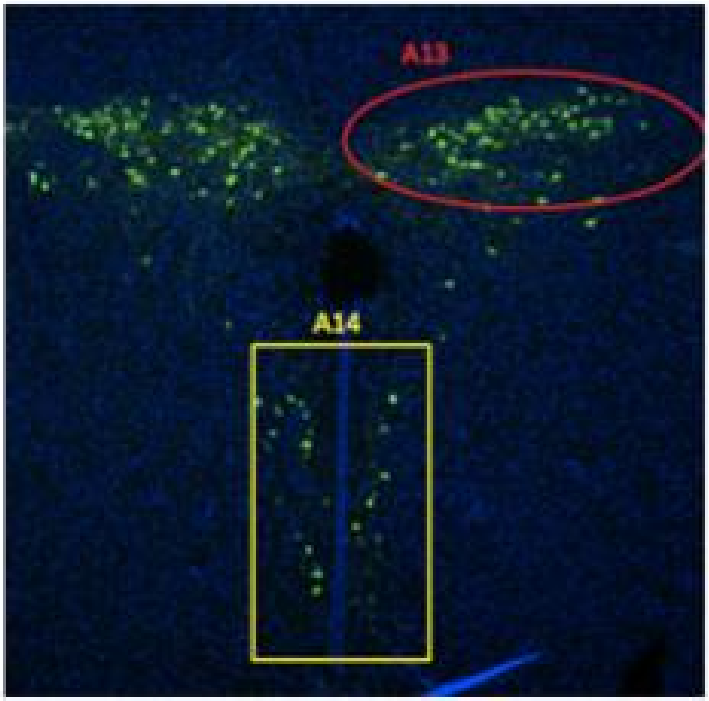

Figure 3.1. Identifying the dopaminergic cell groups within the hypothalamus

Tyrosine hydroxylase (TH) immunohistochemistry was used to demonstrate the different dopamine-producing cell groups within the hypothalamus. This was done using TH immunohistochemistry on coronal sections of hypothalamic tissue. TH is in green (AlexaFluor 488), and cell nuclei are counter-stained in blue (DAPI). The paraventricular nucleus (PVN, A13) is outlined in red and is situated above the third ventricle. The caudal region of the periventricular nucleus (PeVN, A14) is outlined in yellow and is situated on either side of the third ventricle, and ventral to the A13 nucleus.

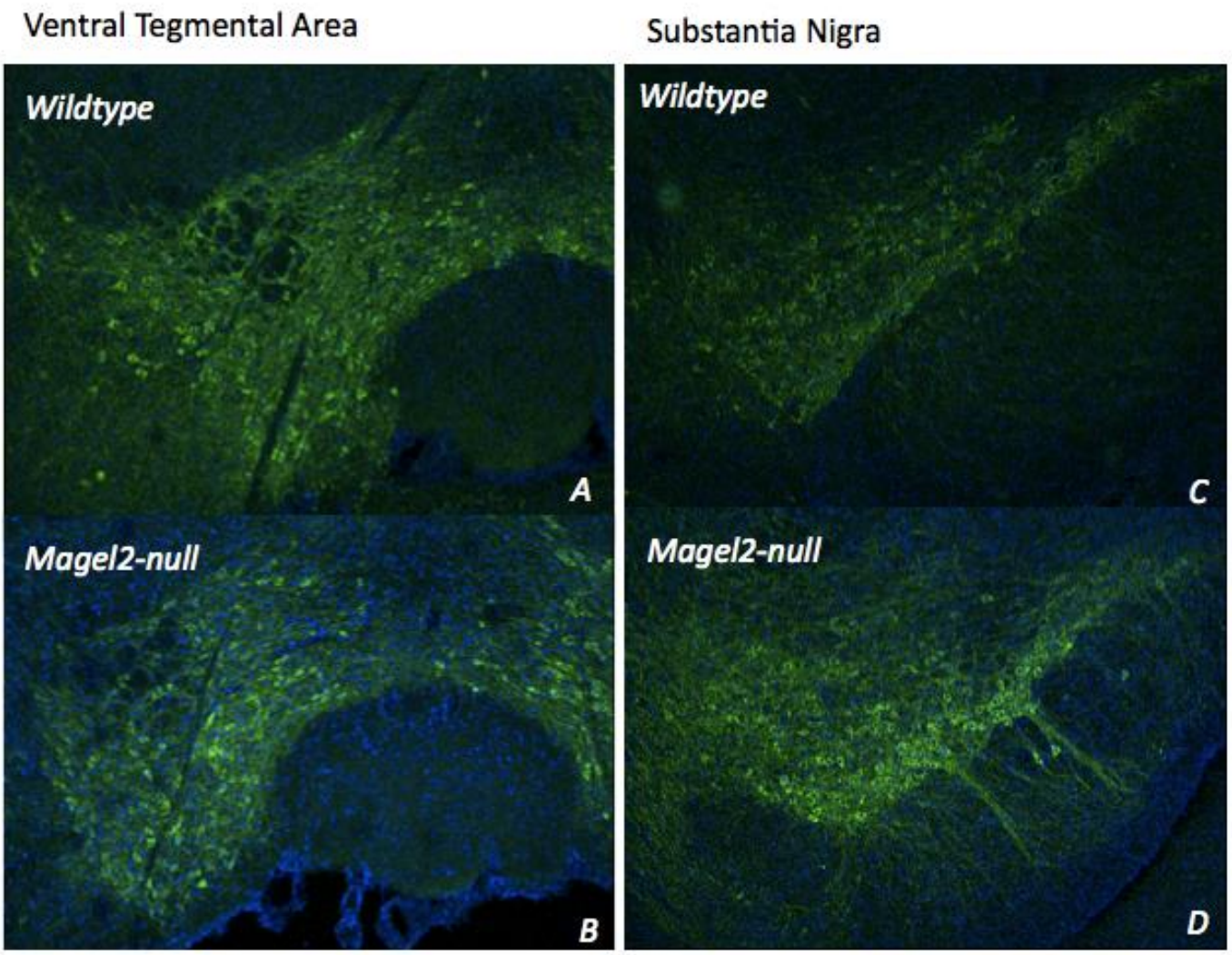

Figure 3.2. Cell count of dopaminergic cells within the midbrain

Tyrosine hydroxylase IHC of the substantia nigra (SN) and the ventral tegmental area (VTA) in *Magel2*-null and wildtype mice. Midbrain coronal sections were imaged on the LEICA TCS SP5 confocal microscope at 10X magnification. TH is in green (AlexaFluor 488) and cell nuclei are counter-stained in blue (DAPI). (A and B: VTA WT n=17, ML2 n=12, ns; C and D: SN, WT n=12, ML2 n=9, ns; E & F TH+ cell quantification). There was no difference between genotypes in the number of TH+ cells in the VTA or SN.

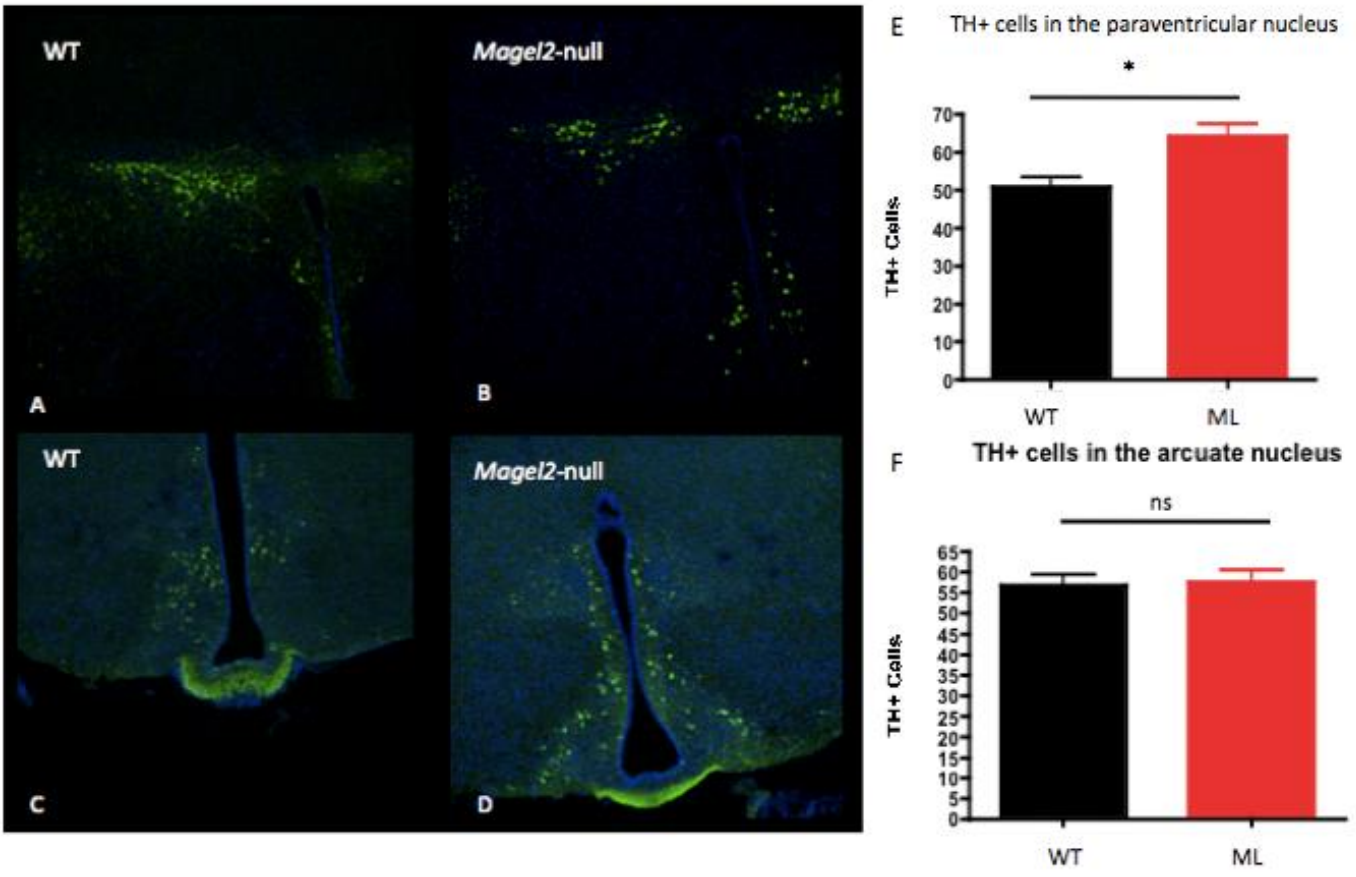

Figure 3.3. Cell count of dopaminergic cells within the hypothalamus

Tyrosine hydroxylase-immunostained hypothalamic nuclei. Coronal hypothalamic sections were imaged on the LEICA TCS SP5 confocal microscope at 10X magnification. TH is in green (AlexaFluor 488), and cell nuclei are counter-stained in blue (DAPI) (A & B: PVN, 1.17 fold increase, WT n=8, ML2 n=5, p=0.04; C & D: ARC, WT n=20, ML2 n=8, ns; E & F quantification of the cell counts). Note that the difference in E was not reproducible in a second trial.

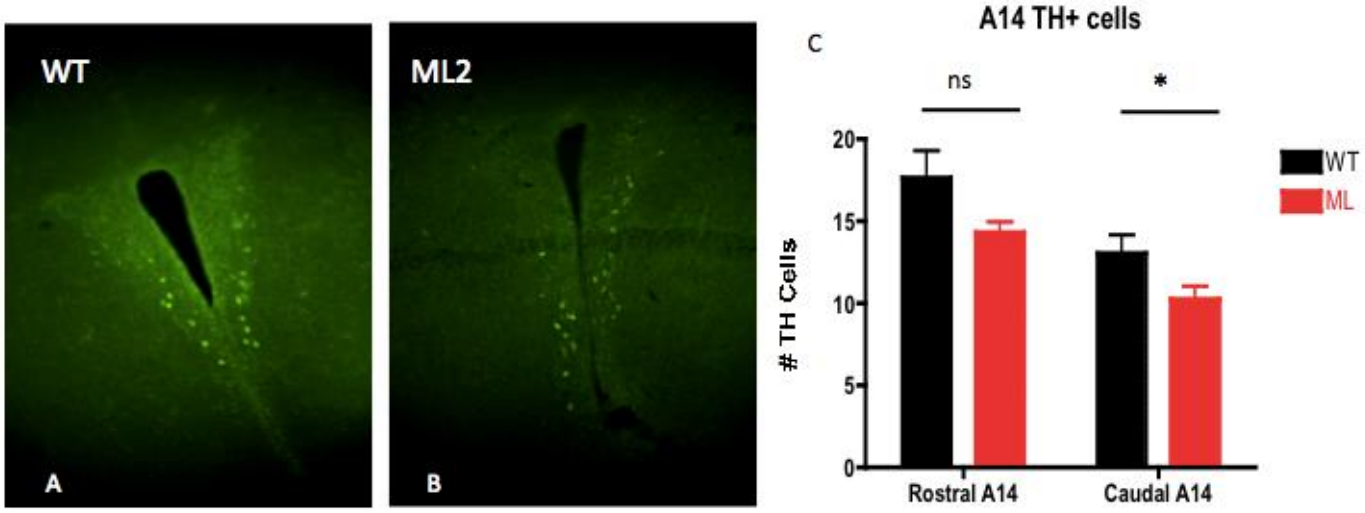

Figure 3.4. Cell count of dopaminergic cells in the periventricular nucleus

Coronal sections of the periventricular nucleus imaged on the TE2000-4 microscope (Nikon) at 20X magnification. *Magel2*-null mice have a 1.3-fold decrease in the number of TH+ cells in the caudal A14 when compared to wildtype littermates and a similar trend in the rostral A14 dopaminergic cell group (Caudal A14, WT n=7, ML2 n=6, p=0.05; Rostral A14 (A and B), TH+ cells, WT n=6, ML2 n=6 p=0.08).

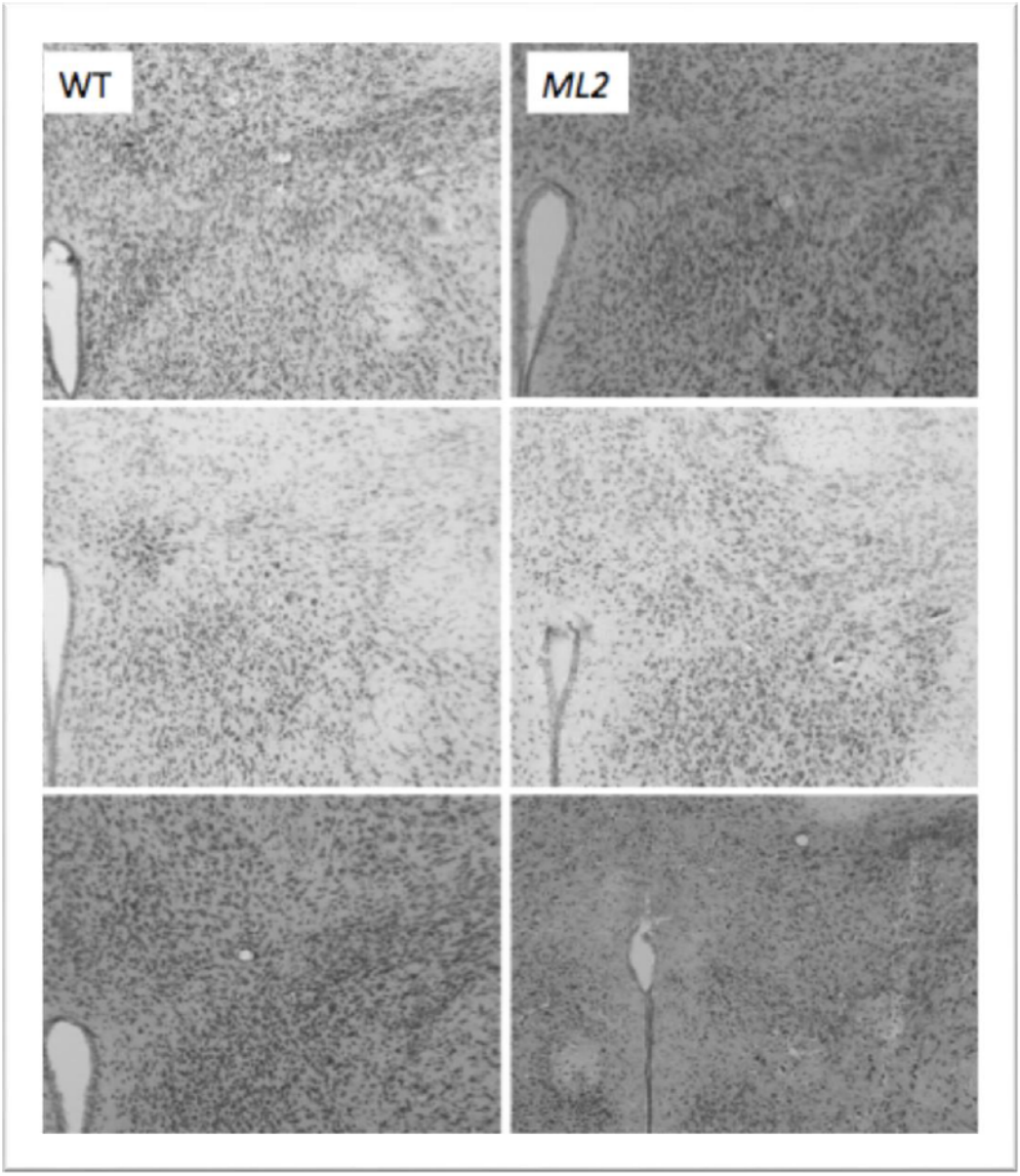

Figure 3.5. Structure of the paraventricular nucleus

Thionine staining of 30 µm coronal sections of the PVN in adult *Magel2*-null and wildtype mice were imaged on the Olympus SZX16 stereomicroscope system light microscope at 10X magnification. There was no observed difference in the ultrastructure of the paraventricular hypothalamus between genotypes (WT n=8, ML2 n=5).

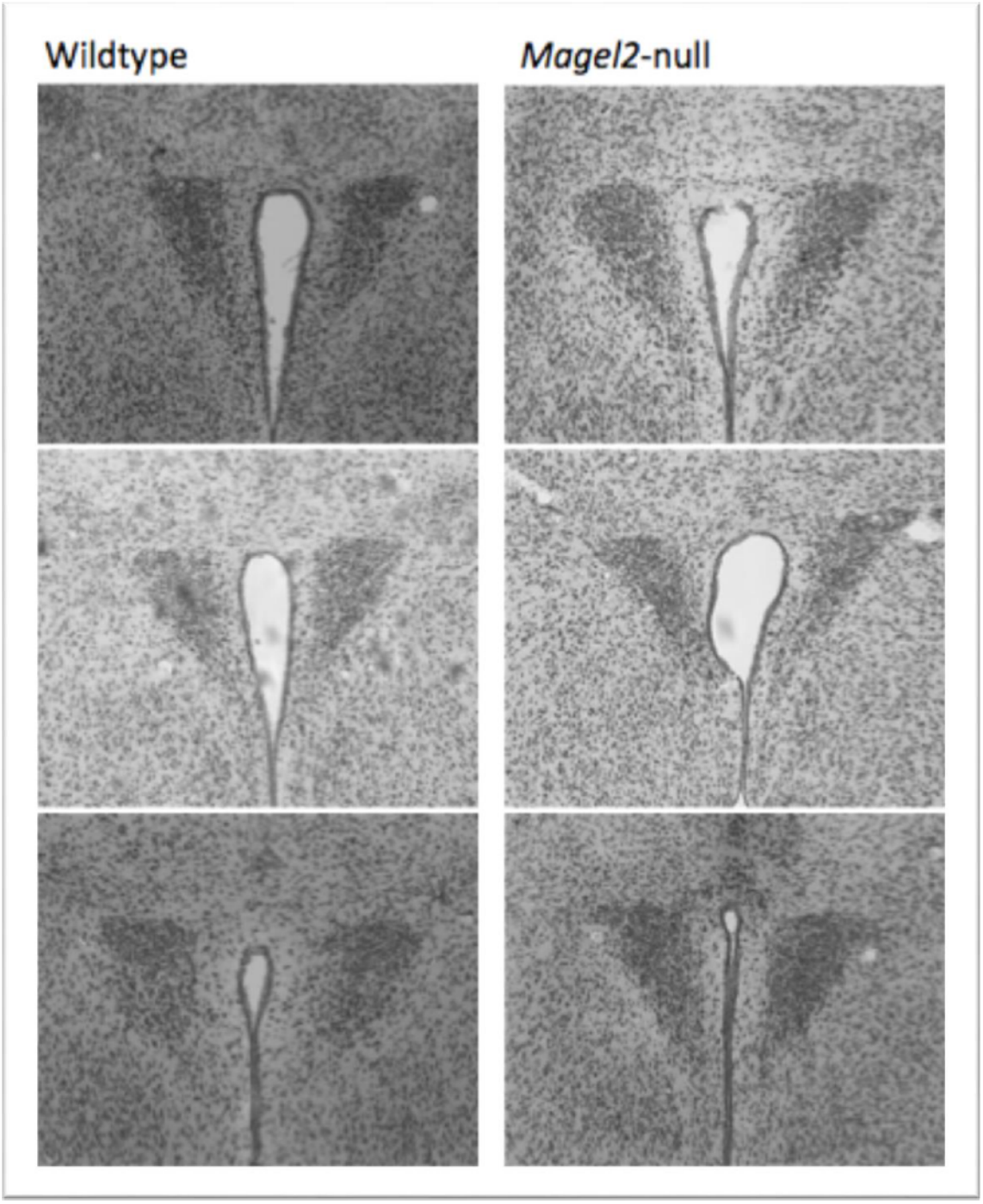

Figure 3.6. Structure of the periventricular nucleus

Thionine stained 30 µm coronal sections of the periventricular nucleus in *Magel2*-null and wildtype mice were imaged on the Olympus SZX16 stereomicroscope system light microscope at 10X magnification. There was no observed difference in the periventricular ultrastructure between genotypes (WT n=8, ML2 n=5).

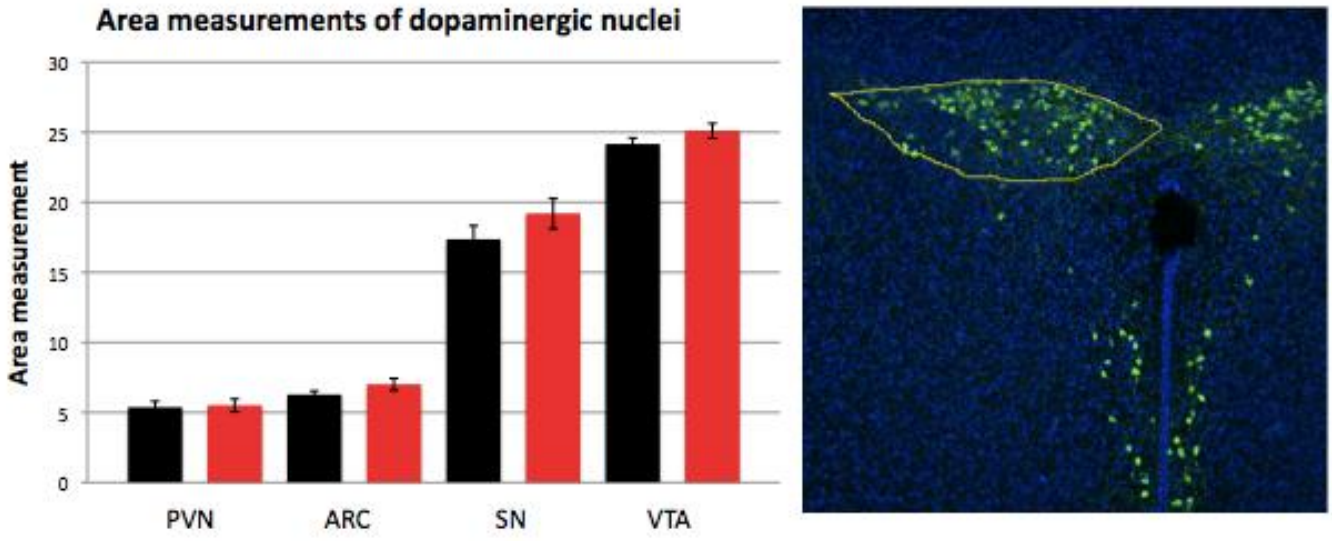

Figure 3.7. Area count of the dopaminergic nuclei

Tyrosine hydroxylase-immunostained hypothalamic and midbrain nuclei were imaged on the LEICA TCS SP5 confocal microscope at 10X magnification. Quantification demonstrates no significant difference between genotypes for any of the measured nuclei. TH+ cells in green (AlexaFluor 488), and nuclei counter stained in DAPI (Blue) (PVN, n=6 ns; ARC, n=3 ns; SN, n=3 ns; VTA, n=3, ns).

3.1.2. *Magel2*-null mice have an increase in the level of tyrosine hydroxylase in the amygdala

Immunoblotting was used to quantify tyrosine hydroxylase levels in the midbrain nuclei and the downstream targets of these neurons. This was used as a measure of baseline dopamine content. Previous experiments from our laboratory have shown a reduced level of dopamine and its metabolites in the hypothalamus and in whole brain lysates (Mercer et al., 2009). We expected to see a similar result for TH levels in the hypothalamus. We would also expect to see less TH in other reward nuclei to account for the global reduction of dopamine previously observed, in particular in the VTA, where tyrosine hydroxylase has been shown to be reduced in obese animal models (Fulton et al., 2006). In quantifying the level of tyrosine hydroxylase in specific nuclei within the reward pathway, we aim to pinpoint which dopaminergic nuclei are affected by the loss of *Magel2*.

There was no significant difference observed in TH protein levels in tissue punches collected from the caudate putamen (CPu), the VTA, the hippocampus, or the PFC (Figure 3.8, PFC n=6, p=0.06; CPu n=6, ns; VTA, n=8, ns; HYP, n=4, ns). In the amygdala a 3.6-fold increase in the level of tyrosine hydroxylase was observed in the *Magel2*-null mice (Figure 3.8, p=0.04).

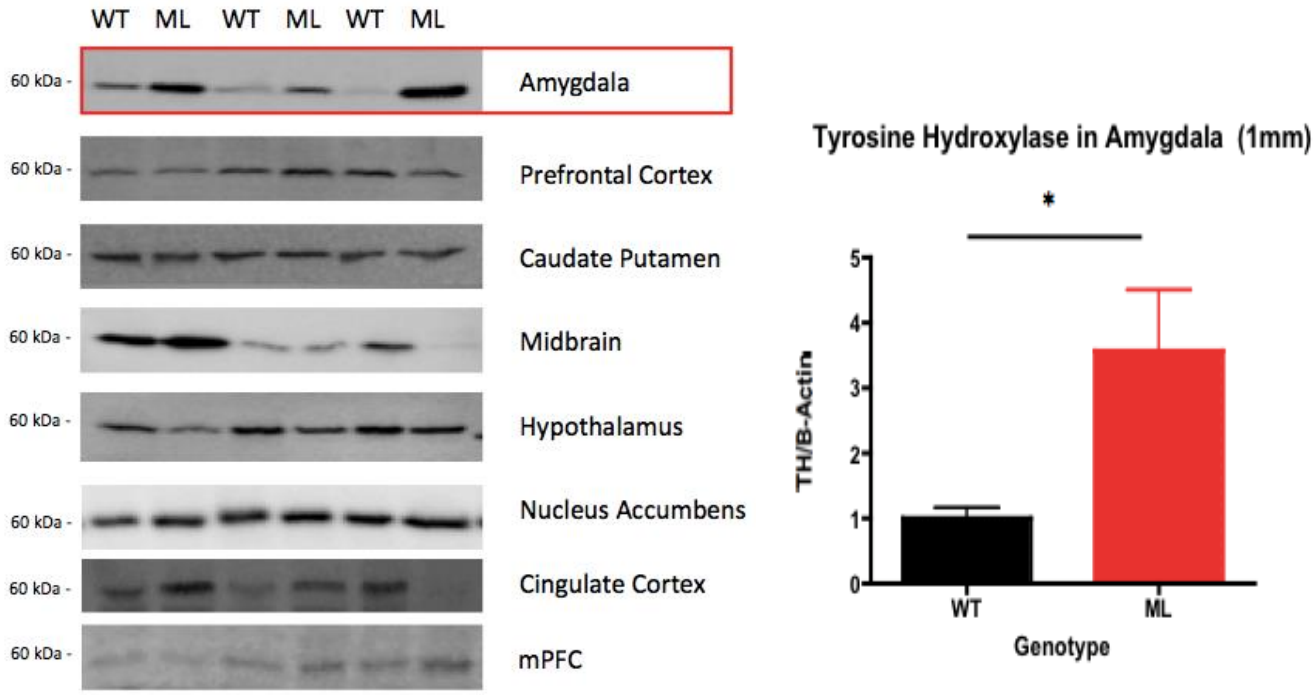

Figure 3.8. Immunoblot quantification of tyrosine Hydroxylase throughout the reward pathway

Immunoblot analysis for tyrosine hydroxylase was performed on tissue from the mesolimbic pathway including the medial prefrontal cortex (mPFC), the prefrontal cortex, the caudate putamen, the midbrain (VTA), the cingulate cortex (Cing), the nucleus accumbens, the hypothalamus, and the amygdala. One mm tissue punches from the mPFC, Cing, CPu, AMY, and the NAc were used. Two mm tissue punches were collected from the midbrain and the PFC. There was a significant increase in the TH levels of the amygdala from *Magel2*-null mice. (PFC n=6, ns; mPFC n=3, ns; Cing n=3, ns; CPu n=6, ns; NAc n=3, ns; VTA, n=8, ns; HYP, n=4, ns; AMY, 3.1-fold increase in *Magel2*-null (ML2) mice p=0.04). Thicker tissue punches (2 mm) from the amygdala were also assessed with no significant difference between genotypes (data not shown).

3.1.3. *Magel2*-null mice have an abnormal distribution of neural cell types

Our results suggest there are a comparable number of dopamine-producing cells in the midbrain of *Magel2*-null mice. This suggests that the mechanism driving the abnormal phenotype in *Magel2*-null mice could be downstream of the VTA in the post-synaptic reception of the dopamine signal. Alterations in synaptic morphology are responsible for sensitizing or habituating an animal to a particular behaviour. In order to assess the post-synaptic effects that the loss of dopamine signalling could produce, cell-type specific protein levels were assessed in the post-synaptic nuclei. Glial, neuronal, and synaptic protein markers were quantified. The glia cell marker Glial Fibrillary Acidic Protein (GFAP), and the neuronal cell protein neurofilament detected by the monoclonal antibody, 2H3 were assessed by immunoblot analysis. This analysis allowed us to infer the ratio of these two cell types. Neurofilament proteins are involved in both axonal transport and neuronal morphology, and are upregulated in the reward pathway in response to the exposure to drugs of abuse, mediating the effects of a subsequent exposure (Beitner-Johnson, et al., 1992). *Magel2*-null mice have an attenuated response to rewards implicating either the axonal transmission of dopamine or the post-synaptic reception of the neurotransmission. We expected that if *Magel2*-null mice have abnormal dopamine signaling to the hypothalamus, that they might also have an abnormal post-synaptic cellular profile indicated by an imbalance of neuronal/glial cell markers.

In the hypothalamus, *Magel2*-null mice showed a 1.5-fold decrease in GFAP and a 1.7-fold increase in neurofilament protein detected by 2H3 antibody (Figure 3.9, GFAP, n=11, p=0.03; 2H3, n=14, p=0.02). Levels of neurofilament were measured in the other nuclei of the dopamine reward pathway including the amygdala, the caudate putamen, the hippocampus, and the prefrontal cortex. There was no significant differences detected between genotypes (Figure 3.10, n=3).

Along with the neuronal/glial profile, the synaptic density was also assessed. The synaptic density was investigated by measuring the levels of synaptic vesicle protein-2 (SV2). Immunoblot analysis of SV2 demonstrated no significant difference within the hypothalamus (Figure 3.9, HYP SV2 n=12). Western blot analysis of SV2 showed no significant difference in the VTA, the SN, or the amygdala (data not shown, n=4). Synaptic transmission was further analyzed by measuring the axonal thickness of dopaminergic projections between the midbrain and the target nuclei (Figure 3.11). *Magel2*-null mice demonstrated a 1.5-fold decrease in the thickness of axon bundles projecting from the midbrain to the frontal cortex (Figure 3.12, WT n=9, ML2 n=7, p=0.03). Axon bundle thickness was measured in tyrosine hydroxylase immunostained sagittal sections. The thickness of the axon bundles projecting from the

midbrain to the striatum demonstrated a similar trend, but this difference was not significant (Figure 3.12, WT n=14, ML2 n=11).

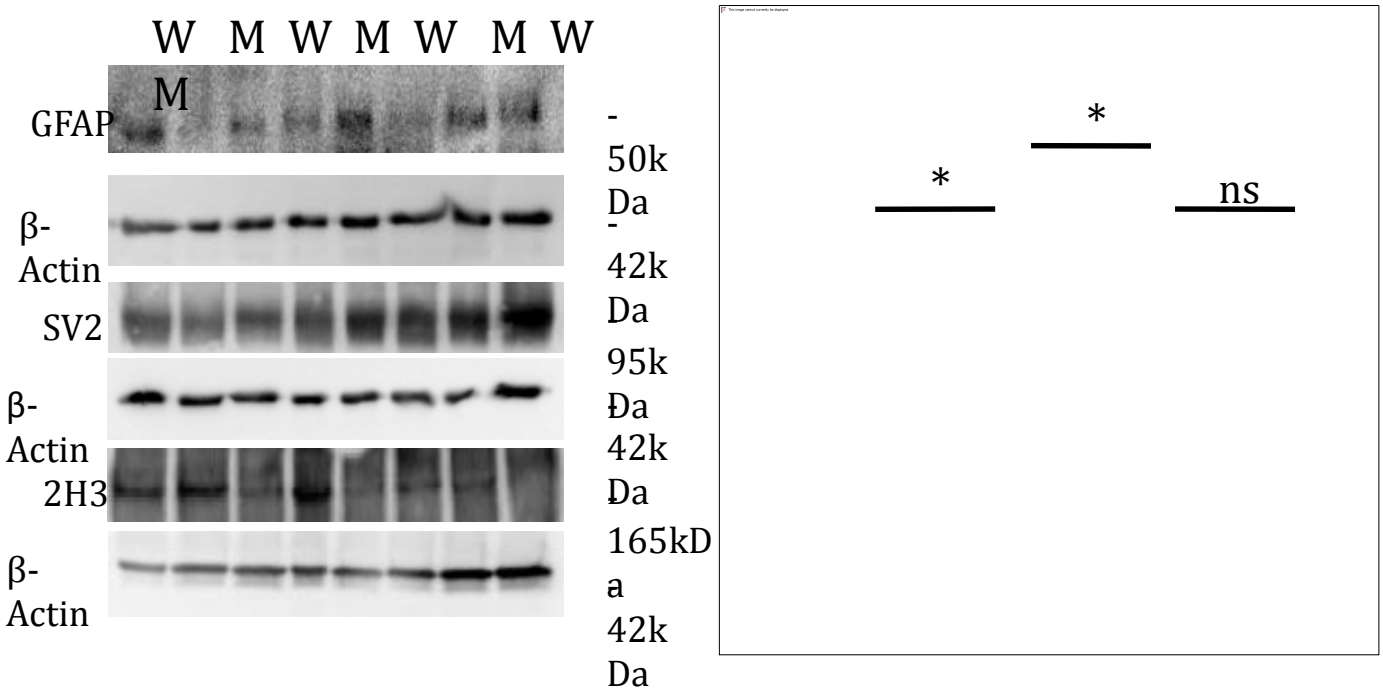

Figure 3.9. Immunoblot analysis of cell type specific proteins

The hypothalamic nuclei from wildtype (WT) and *Magel2*-null (ML) mice were analyzed for synaptic vesicle protein and specific cell type protein markers by immunoblot analysis. The protein markers included the glial marker, GFAP, the neuronal neurofilament protein marker, 2H3, and the synaptic vesicle protein marker, SV2. Protein quantification was done by normalizing protein levels to β-Actin. There was significantly more 2H3, and significantly less GFAP in the *Magel2*-null mice when compared to wildtype littermates (GFAP, n=11, p=0.03; 2H3, n=14, p=0.02; SV2 n=12, ns).

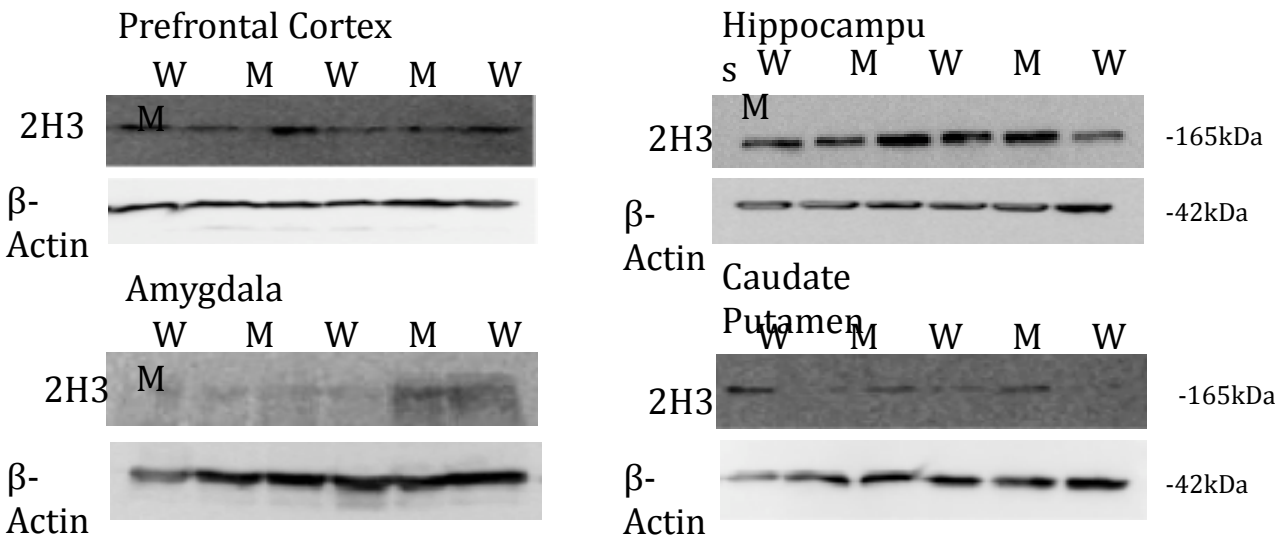

Figure 3.10. Immunoblot analysis of the neurofilament marker protein, 2H3

Immunoblot analysis of neurofilament (2H3) in the PFC, the hippocampus, the CPu, or the AMY of wildtype (W) and *Magel2*-null mice (M). Protein levels were normalized to β-Actin. There was no significant difference between genotypes in any of the quantified nuclei (WT n=3, ML2 n=3, ns).

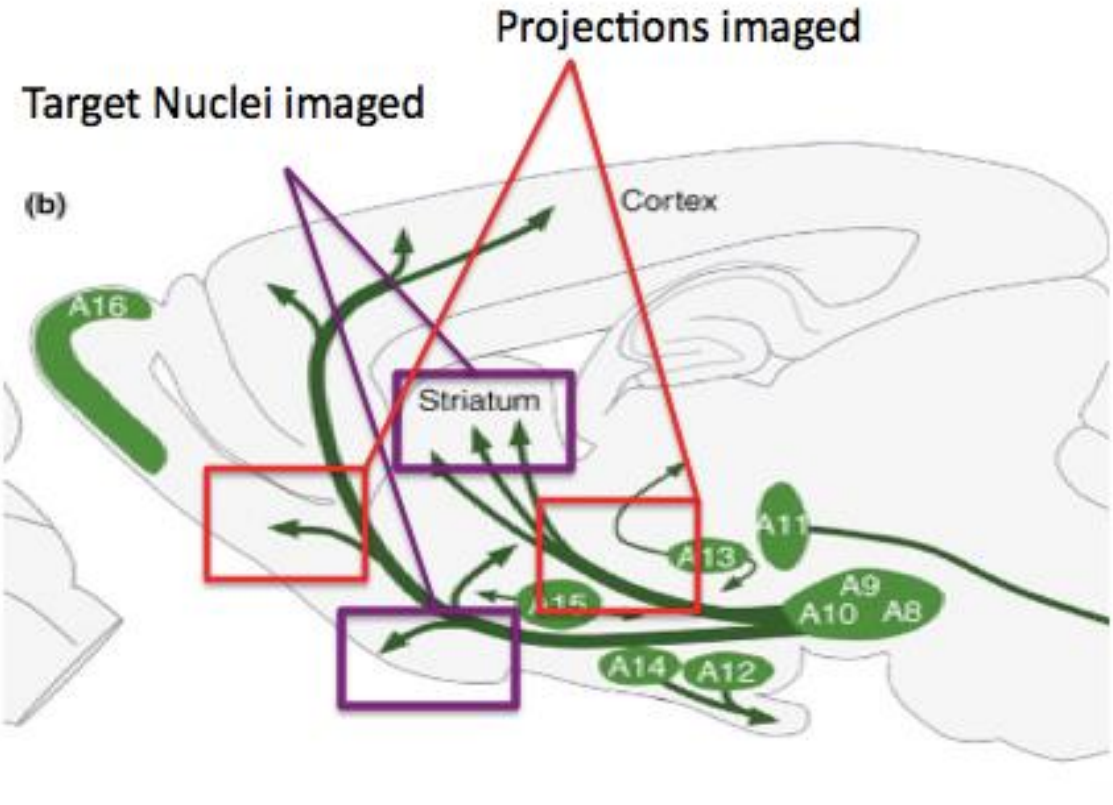

Figure 3.11. Schematic of the areas used for the analysis of dopaminergic axonal projections and the downstream target nuclei

The sagittal images used for the analysis of axon bundle thickness include midbrain projections to both the prefrontal cortex and to the striatum (red). The target nuclei of these midbrain projections include the amygdala and the striatum (purple). (Figure modified from Bjorklund & Dunnett 2007: Dopamine neuron systems in the brain: an update)

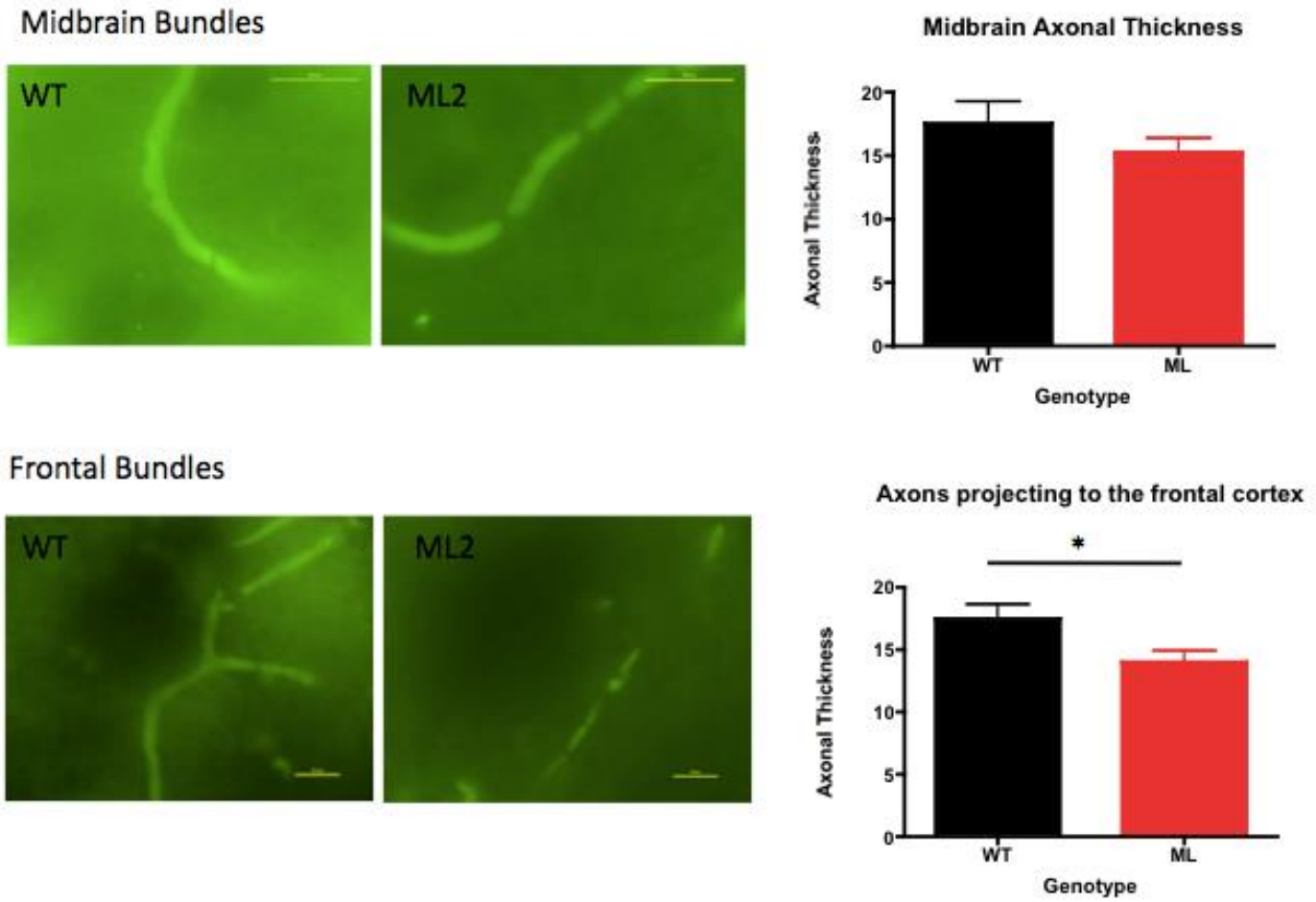

Figure 3.12. Dopaminergic axon calibre

Tyrosine hydroxylase IHC of axon bundles projecting to the striatum (top) and the prefrontal cortex (bottom) from the midbrain in wildtype (WT), and *Magel2*-null (ML) mice. Images were taken on the TE2000-4 microscope (Nikon), at 100X magnification and the calibre was measured using ImageJ software. The axon bundle calibre was significantly reduced in the *Magel2*-null sections when compared to wildtype littermates (Midbrain; WT n=14, ML2 n=11, ns, Frontal projections; WT n=9, ML2 n=7, p=0.03).

3.1.4. Immunohistochemical analysis of tyrosine hydroxylase reaching the post-synaptic dopamine target nuclei

Tyrosine hydroxylase immunostaining of the striatum and the amygdala was done to determine if the level of dopamine reaching the target nuclei is altered in the *Magel2*-null mice. For this experiment, images were taken from the amygdala and the ventral striatum (NAc), (Figure 3.11). To account for the global loss of dopamine in the *Magel2*-null mice, we expected less dopamine reaching the target nuclei. A linescan was done and the mean pixel intensity was measured. We did not detect a difference in the pixel intensity of TH-immunostained axon terminals in the either of the target nuclei (Figure 3.13. Amygdala; WT n=7, ML2 n=4, Striatum; n=3).

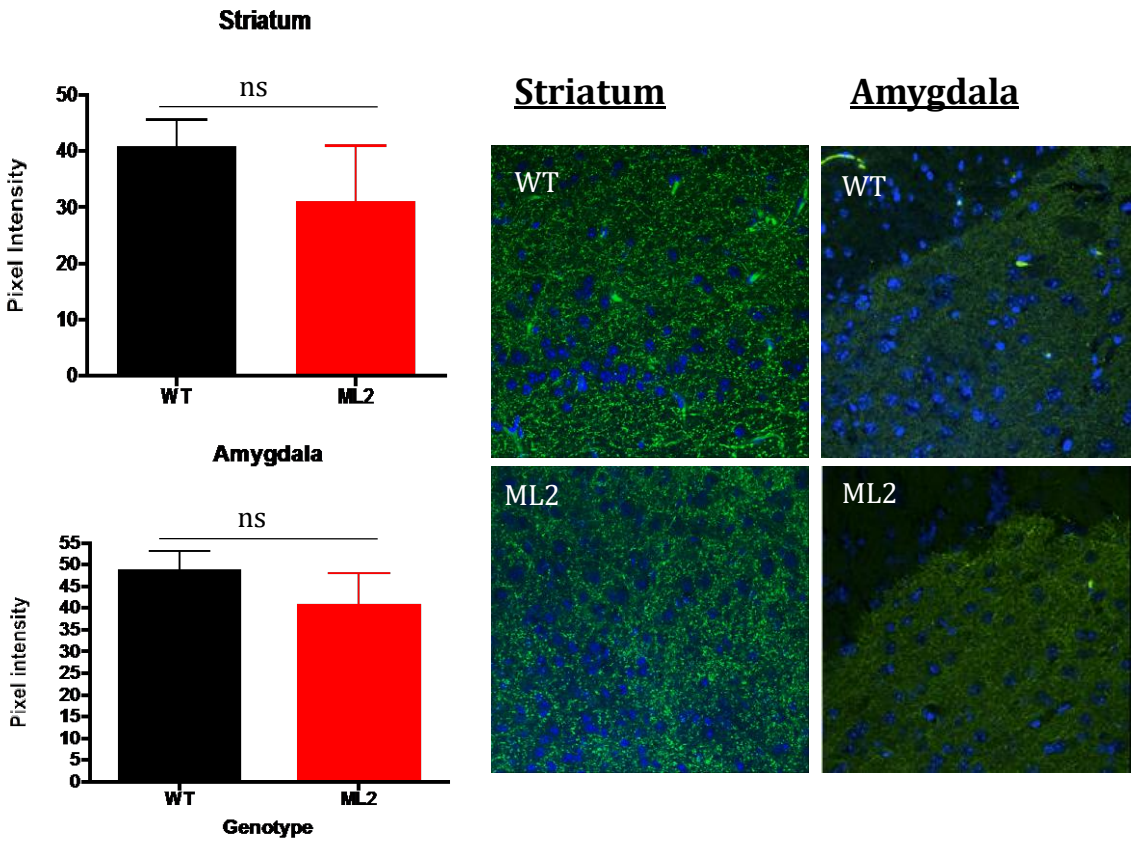

Figure 3.13. Tyrosine hydroxylase in the dorsal and ventral striatum

Pixel intensity was used to determine the level of TH downstream of the VTA. Sagittal sections treated with tyrosine hydroxylase immunohistochemistry were imaged on the LEICA TCS SP5 confocal microscope at 63X magnification. There was no observed difference between genotypes (Amygdala; WT n=7, ML2 n=4, ns Striatum; n=3, ns).

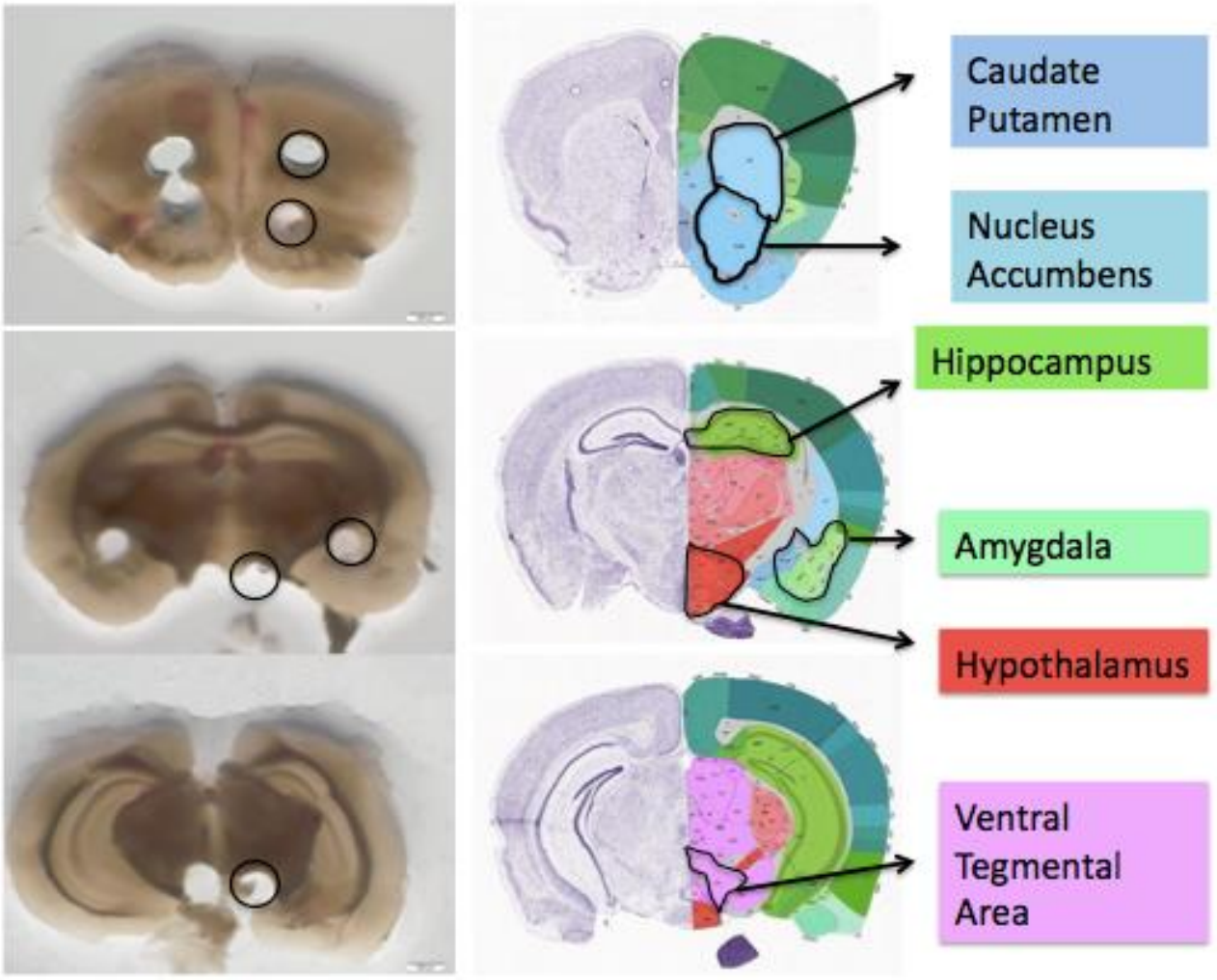

Figure 3.14. Tissue punches used for protein and biogenic amine analysis

Images of brain slices after the tissue punches were collected for immunoblot and HPLC analysis (left), and the corresponding anatomical structures (right). Images were taken to ensure consistency between dissections (Figure created using images from the Allen Mouse Brain Atlas.)

3.1.5. *Magel2*-null mice show a global reduction in dopamine and serotonin metabolites within the nuclei of the reward pathway

The catecholamine and indolamine pathways were investigated in the *Magel2*-null mice using HPLC analysis of biogenic metabolites involved in the synthesis and breakdown of dopamine and serotonin. Previous work from the Wevrick laboratory demonstrated abnormal levels of catecholamines and indolamines in crudely dissected samples of the cerebral cortex and the hypothalamus of adult *Magel2*-null mice (Mercer et al., 2009). Using a more precise dissection method, and including several previously uncharacterized nuclei, I repeated the HPLC analysis (Figure 3.14). We expect a similar loss of dopamine and serotonin metabolites in the hypothalamus, and possibly the compensation for this loss elsewhere in the reward pathway. We expected to see a reduction in the level of dopamine in the VTA and the NAc, as this has been observed in obese animals (Fulton et al., 2006). We also expect a shift in the synthesis pathway to compensate for the abnormal levels of dopamine metabolites observed in both our *Magel2*-null mice and in individuals with PWS.

There are neuroanatomical differences in the size of the brain regions, observed through high-resolution MRI of *Magel2*-null mice. Several of the nuclei within the reward pathway are smaller in *Magel2*-null mice, including the hippocampus, the cortex, the amygdala and the striatum (Mercer et al., 2009). The absolute weight of the sample is used to determine the concentration of the biogenic amines, suggesting that if a specific nucleus were to differ in density or size, this could influence the metabolite concentration. The weight of the tissue punches did not differ between the *Magel2*-null mice and the wildtype mice, minimizing the effect of any structural differences.

3.1.5.1. Serotonin metabolites

In the indolamine pathway, three serotonin metabolites were quantified. These included serotonin (5-Hydroxytryptamine, 5-HT), 5-Hydroxyindoleacetic acid (5HIAA), and tryptophan, the amino acid precursor to serotonin (Figure 3.15). The 2-way ANOVA analysis for the effect of genotype on the pathway as a whole demonstrated a significant interaction in several reward nuclei including the midbrain, the striatum, the hindbrain, and most notably the hypothalamus (Table 3.1, Figure 3.16; HYP, n=13, p=0.0004; Striatum p=0.003, WT n=19, ML2, n=18; Hindbrain, WT n=15, ML2 n=13, p=0.05; MID, WT n=16, ML2 n=13, p=0.0014). There was no significant interaction between genotype and the serotonergic pathway in the prefrontal cortex or the amygdala (AMY, n=18; PFC, WT n=22, ML2 n=19). Further analysis of the specific metabolites demonstrated a significant decrease in the levels of 5HIAA, the primary

metabolite from the breakdown of serotonin, in several reward nuclei. These included the hypothalamus, the striatum, the prefrontal cortex and the midbrain of the *Magel2*-null mice (Figure 3.17; HYP, 1.4-fold decrease, n=13, p=0.0007; Striatum, 1.1-fold decrease, WT n=19, ML2 n=18, p=0.05; PFC, 1.3 fold decrease, WT n=23, ML2 n=20, p=0.03; Midbrain 1.2-fold decrease, WT n=16, ML2 n=13, p=0.003). A similar trend was observed in the amygdala and the hindbrain, but was not statistically significant. There was no difference in the levels of 5-HT in any of the nuclei assessed. There was a global trend towards increased tryptophan in the *Magel2*-null mice. This included the hypothalamus, hindbrain, striatum, amygdala, prefrontal cortex, and the midbrain, however none of these increases reached statistical significance in post-hoc analyses (Figure 3.18). The pathway-wide reduction of 5HIAA, and trend towards increased tryptophan suggest there is a disruption in the conversion of tryptophan to 5-HT throughout the central nervous system in the *Magel2*-null mice. By comparing the relative amounts of metabolites we can determine the turnover rates, this gives us an idea of where in the metabolic pathway the loss of Magel2 has the greatest effect, and what metabolic enzymes may be involved. In the serotonergic pathway, tryptophan hydroxylase (TPH) and monoamine oxidase (MAO) activity were assessed. In the hypothalamus, we observed a 1.4-fold decrease in TPH activity (n=11, p=0.05). TPH is the rate-limiting enzyme involved in the synthesis of serotonin from tryptophan, and MAO is responsible for the oxidative deamination of serotonin into 5HIAA (Lam et al., 2010). The relative levels of serotonin and the amino acid precursor, tryptophan, suggest that there could potentially be a reduction in TPH activity in the hypothalamus of *Magel2*-null mice.

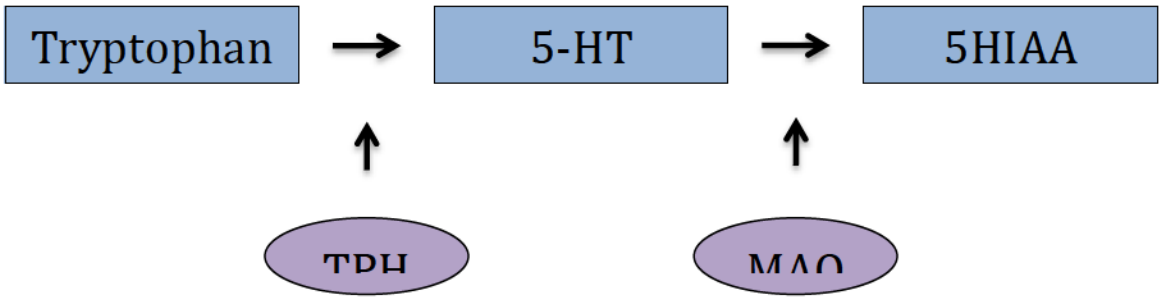

Figure 3.15. Serotonin synthesis pathway

Serotonin is synthesized by the hydroxylation of tryptophan. This reaction is catalyzed by the rate-limiting enzyme tryptophan hydroxylase (TPH). Serotonin (5-HT) is then converted to 5HIAA. This oxidation reaction is catalyzed by the enzyme monoamine oxidase (MAO).

HPLC Analysis of Serotonergic Metabolites						
	Serotonergic Amines			Metabolite Turnover		
	5HIAA	5HT	Tryptophan	MAO (5HIAA/5HT)	TPH (5HT/Tryp)	Pathway
Amygdala						
WT	314±58	433±117	5.0±1.4	0.7±0.3	87±30	**Not**
ML	276±52	440±153	4.6±1.2	0.6±0.3	96±44	**Significant**
Hypothalamus						
WT	412±78	407±79	4.7±1.4	1.0±0.3	86.6±24	**Significant**
ML	307±57	322±135	5.0±1.4	1.0±0.5	64.4±28	***
	p=0.0007				**p=0.05**	**p=0.0004**
Striatum						
WT	286±43	521±826	8.6±20	0.5±0.6	60.6±30.3	**Not**
ML	253±56	232±63	6.0±7.0	1.1±0.6	38.7±66.0	**Significant**
	p=0.05					
PFC						
WT	367±142	407±174	5.7±0.5	0.9±1.5	71.4±51	**Not**
ML	283±103	384±170	6.3±3.8	0.7±0.4	61.0±67	**Significant**
	p=0.03					
Midbrain						
WT	877±141	563±161	4.0±1.0	1.6±0.5	142±73	**Significant**
ML	704±139	476±140	4.4±1.1	1.5±0.5	108±53	**
	p=0.003					**p=0.001**
Hindbrain						
WT	734.67±246	341±156	4.4±1.6	2.2±0.9	78±40	**Significant**
ML	578.08±241	279±142	4.7±1.9	2.1±1.2	59±35	*
						p=0.05
Concentrations of biogenic amines in ng/g of tissue (Tryptophan µg/g). Enzyme activity is inferred based on the relative concentrations of metabolites within the pathway.						

Table 3.1. HPLC analysis of the serotonin metabolic pathway

Results of HPLC analysis including the concentrations of tryptophan, serotonin, and 5HIAA +/- the standard deviations of each group of samples. The concentrations of 5HIAA and serotonin are in ng/g, and tryptophan is displayed in µg/g tissue. Using a 2-way ANOVA analysis of the entire pathway, the genotype had a significant effect in the hypothalamus, the midbrain (MID) and the hindbrain. (n=13-23/ metabolite). In post-hoc analysis, there was less 5HIAA in the HYP, PFC, midbrain and the striatum of *Magel2*-null mice (HYP, 74 %, n=13, p=0.0007; Striatum, 88 %, WT n=19, ML n=18, p=0.05; PFC, 77 %, WT n=23, ML n=20, p=0.03, MID, 80 %, WT=16, ML n=13 p=0.003). There was also a significant decrease in the turnover rate of 5-HT/tryptophan (tryptophan hydroxylase (TPH)) in the hypothalamus of *Magel2*-null (ML) mice (HYP, 73 % n=12, p=0.05).

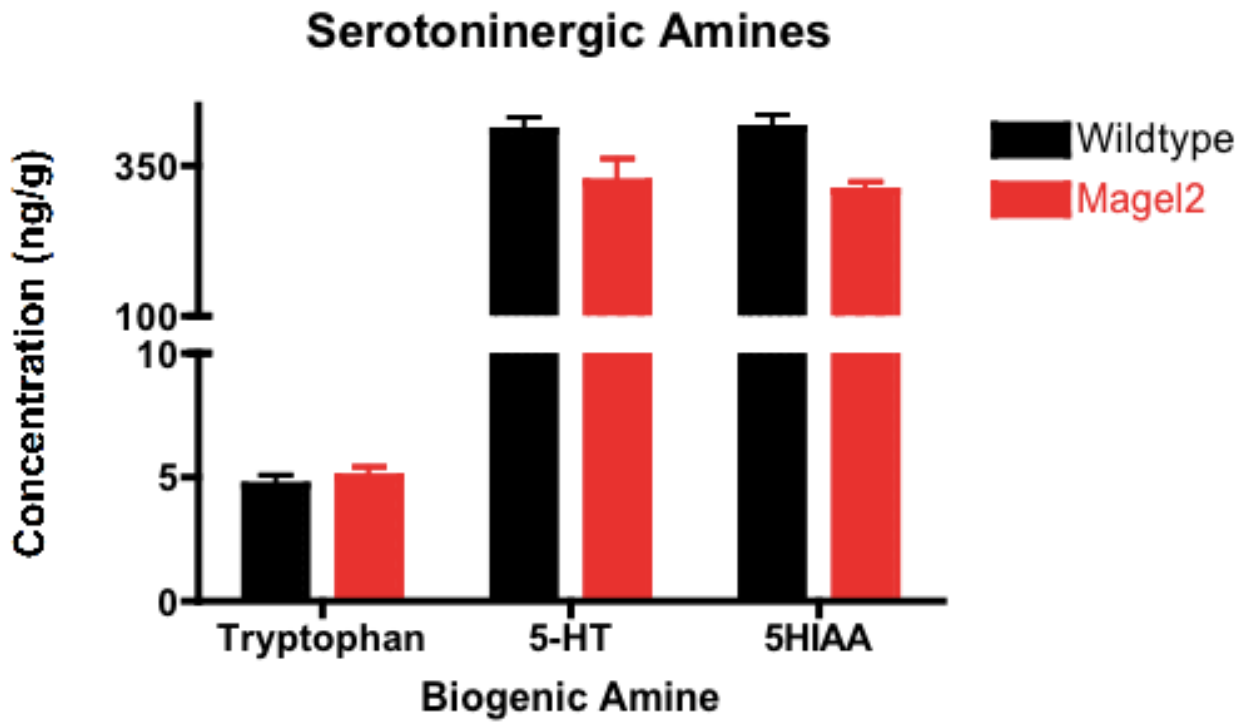

Figure 3.16. Serotonin metabolites in the hypothalamus

HPLC analysis of tissue punches taken from the hypothalamus. There is significantly less 5HIAA in the hypothalamus of *Magel2*-null mice compared to WT littermates. (5HIAA n=13 p=0.0007, pathway analysis p=0.0004).

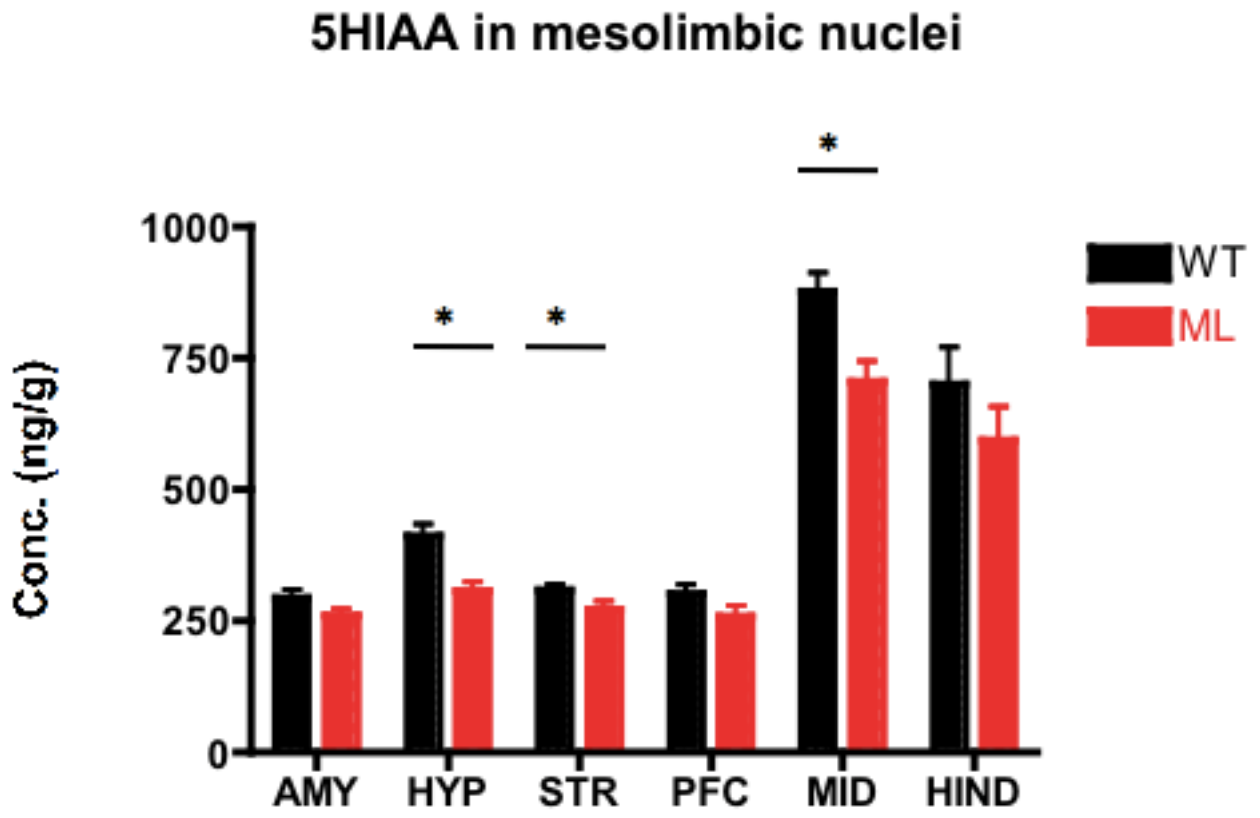

Figure 3.17. 5-Hydroxyindoleacetic acid concentrations in the mesolimbic reward nuclei

HPLC analysis of 5HIAA throughout the reward pathway. There is significantly less 5HIAA in the hypothalamus, the striatum, and the midbrain of *Magel2*-null (ML) mice, compared to wildtype (WT) littermates (HYP, 74 %, n=13, p=0.0007; Striatum, 88 %, WT n=19, ML n=18, p=0.05; PFC, 77 %, WT n=23, ML n=20, p=0.03, MID, 80 %, WT=16, ML n=13 p=0.003).

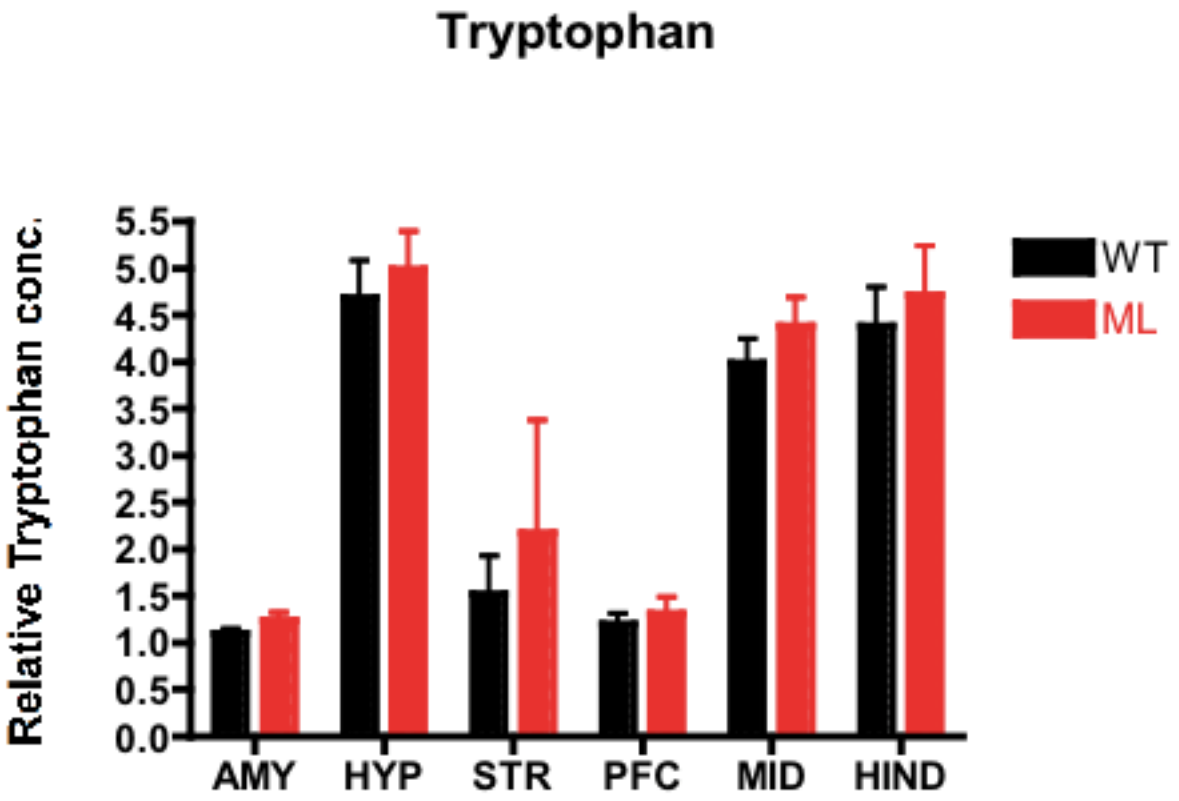

Figure 3.18. Tryptophan concentrations in nuclei of the reward pathway

HPLC analysis of tryptophan throughout the nuclei of the reward pathway. There was a global trend towards increased tryptophan in the *Magel2*-null mice, but there was no significant difference in the level of tryptophan between wildtype (WT) and *Magel2*-null (ML) mice in specific brain regions in post-hoc analyses.

3.1.5.2. Dopaminergic metabolites

The catecholamines analyzed by HPLC included dopamine (DA), noradrenaline (NA), 3,4-Dihydroxyphenylacetic acid (Dopac), 3-Methoxytyramine (3-MT), normetanephrine (NME), and homovanillic Acid (HVA) (Figure 3.19). The 2-way ANOVA analysis of this pathway as a whole demonstrated a significant effect of genotype in the hypothalamus, the prefrontal cortex, the midbrain and the hindbrain (Table 3.2; HYP, n=11-14, p=0.0004; PFC, n=14-23, p=0.05; MID, n=12-16 p=0.007; Hindbrain, n=11-15 p=0.04). A significant interaction was not observed in the striatum or the amygdala. A lower level of metabolites in the entire catecholamine synthesis pathway was observed in the hypothalamus of *Magel2*-null mice, and 2-way ANOVA showed a significant interaction between the dopamine metabolites and the genotype (Figure 3.20 p=0.0004). This included a 2-fold decrease in dopamine levels and reduced levels of NA, Dopac, and HVA (NA 1.3-fold decrease, n=13, p=0.004; Dopac 1.4-fold decrease, WT n=14, ML2 n=12, p=0.01; DA 2-fold decrease, WT n=14, ML n=12, p=0.003; HVA 1.2-fold decrease, WT n=14, ML2 n=13, p=0.0007). Normetanephrine (NME) levels showed a similar trend but did not reach statistical significance. The HPLC analysis also showed lower levels of dopamine metabolites in other brain areas, most notably the hindbrain. In the hindbrain of *Magel2*-null mice, all the dopamine metabolites trended towards lower concentrations in the mutants. Dopamine and NME levels were significantly lower in the hindbrain of *Magel2*-null mice (Figure 3.21; NME 2.1-fold decrease, WT n=12, ML2 n=11, p=0.003; DA 1.6-fold decrease, WT n=15, ML2 n=12, p=0.02). The midbrain showed the same trend throughout the catecholamine pathway, with HVA being significantly lower in the *Magel2*-null mice (Figure 3.22; HVA 1.1-fold decrease, WT n=15, ML2 n=13 p=0.05).

Using the relative concentrations of the dopaminergic metabolites, the enzymatic activity was also inferred. In the hindbrain, there was 1.8-fold higher inferred activity of MAO/COMT enzymes in the *Magel2*-null mice (WT n=13, ML2 n=12, p=0.003). HPLC analysis of the hypothalamus showed a 1.5-fold increase in DBH activity (WT n=15, ML2 n=11, p=0.02). The inferred increased activity suggests that dopamine is being broken down at an increased rate in the hypothalamus and the hindbrain of *Magel2*-null mice.

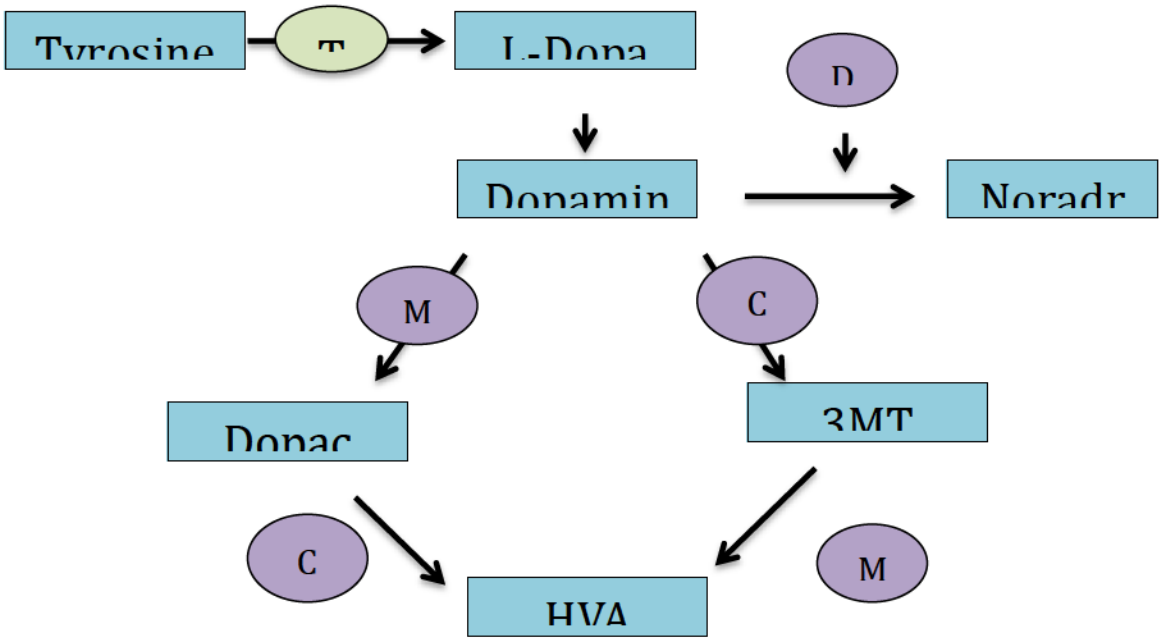

Figure 3.19. The dopamine synthesis pathway

The synthesis of dopamine involves the conversion of the amino acid tyrosine into L-Dopa. This reaction is catalyzed by tyrosine hydroxylase (TH). This is the rate-limiting step in dopamine synthesis. L-Dopa is then converted into dopamine, which is then broken down into either 3,4-Dihydroxyphenylacetic acid (Dopac) or 3-Methoxytyramine (3-MT). Dopamine is methylated and converted to 3-MT by the enzyme catechol-O-methyl transferase (COMT). Alternatively, dopamine can be broken down into Dopac by the enzyme monoamine oxidase (MAO). Both Dopac and 3-MT are further metabolized to homovanillic acid (HVA) via COMT and MAO respectively.

HPLC analysis of dopaminergic metabolites									
	Dopaminergic Amines						Metabolite turnover		
	NA	DOPAC	NME	DA	HVA	3MT	DBH	MAO/COMT	Pathway
Amygdala									
WT	285±55	832±336	65±13	1050±750	314±114	152±39	0.27±0.1	0.29±0.1	**Not**
ML	296±42	728±167	60±14	1187±651	288±134	139±46	0.25±0.2	0.24±0.1	**Significant**
									p=0.25
Hypothalamus									
WT	1396±334	124±44	66±26	302±153	252±7		4.6±1.6	0.8±0.5	**Significant**
ML	1050±165	88±18	51±20	151±47	213±5		7.0±2.9	1.4±0.8	***
	p=0.004	**p=0.01**		**p=0.003**	**p=0.0007**		**p=0.02**		**p=0.0004**
Striatum									
WT	153±201	1751±700	1110±675	7462±3188	989±266	786±235	0.02±0.03	0.1±0.05	**Not**
ML	142±155	1852±850	2199±2081	8082±5960	948±296	621±127	0.02±0.03	0.1±0.1	**Significant**
						p=0.03			
PFC									
WT	341±122	660±161	71±53	129±49	195±56		3.6±2.7	1.5±0.9	**Significant**
ML	344±114	613±327	50±38	95±49	178±73		3.6±2.6	1.9±0.8	*
									p=0.05
Midbrain									
WT	497.43±73	523.65±206	53.37±21	616.95±119	334.33±39		0.55±0.05	0.53±0.07	**Significant**
ML	466.43±78	438.08±94	41.23±15	544.86±126	294.80±57		0.84±0.11	0.55±0.1	**
					p=0.05				**p=0.007**
Hindbrain									
WT	864±194	378±108	32±14	271±123	73±48		3.2±1.6	0.3±0.1	**Significant**
ML	824±205	333±92	15±9	170±84	65±40		4.8±3.1	0.4±0.1	*
			p=0.003	**p=0.0186**				**p=0.003**	**p=0.04**
Concentrations of biogenic amines in ng/g of tissue. Enzyme activity is inferred based on the relative concentrations of metabolites within the pathway.									

Table 3.2. HPLC analysis of dopamine metabolites

HPLC analysis of dopamine metabolites including noradrenaline, dopac, NME, dopamine, HVA, 3MT in wildtype (WT), and *Magel2*-null mice (ML). Concentrations are all presented in ng/g +/- the standard deviation. 2-way ANOVA analysis showed an effect of genotype on the whole catecholamine pathway in the hypothalamus, the PFC, the midbrain and the hindbrain. (n=13-23 samples/metabolite). There is significantly less of each of the catecholamines in the hypothalamus of *Magel2*-null mice. (NA, 75 %, n=13, p=0.004; Dopac, 71 %, WT n=14, ML n=12, p=0.01; DA, 50 %, WT n=14, ML n=12, HVA, 85 %, WT n=14, ML n=13, p=0.0007). The concentration of 3MT in the striatum was significantly reduced in the *Magel2*-null (ML) mice. (3MT, 80 %, WT n=14, ML n=12, p=0.03). The ML2 mice had significantly less HVA in the midbrain (HVA, 88 %, WT n=15, ML n=13, p=0.05). The hindbrain of *Magel2*-null mice showed reduced levels of both NME and DA (NME, 47 %, WT n=12, ML n=11, p=0.003; DA, 63%, WT n=15, ML n=12, p=0.0186). There is an increased metabolic turnover suggesting an increase in inferred activity of the enzyme DBH, and of MAO in the hindbrain of *Magel2*-null mice (DBH, HYP, 154 %, n=12, p=0.02; MAO/COMT, HIND, WT n=13, ML n=12, p=0.003)

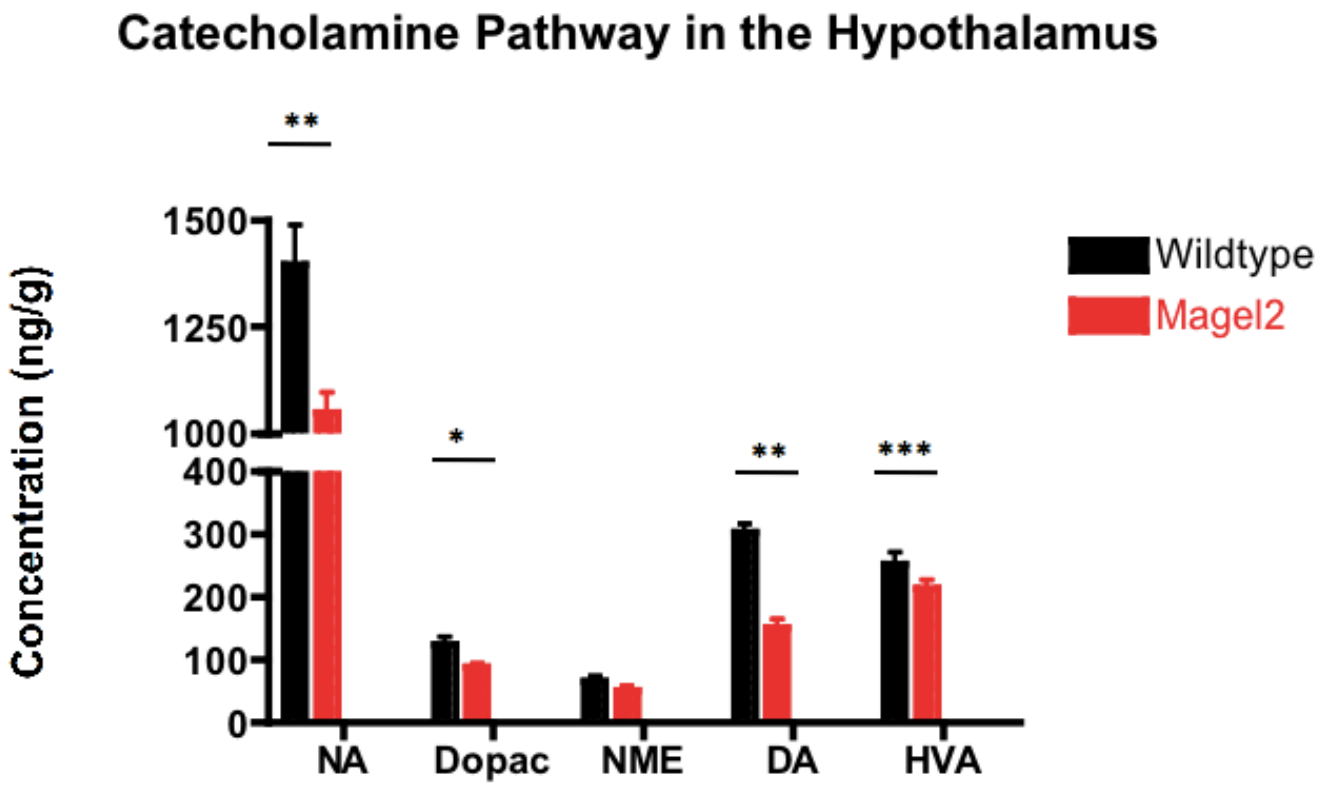

Figure 3.20. Catecholamines in the hypothalamus

HPLC quantification of dopamine metabolites in the hypothalamus. There is significantly less NA, dopac, DA, and HVA in the hypothalamic nuclei of *Magel2*-null mice. (NA 1.3-fold decrease, n=13 p=0.004; Dopac 1.4-fold decrease, WT n=14, ML2 n=12, p=0.01; DA 2-fold decrease, WT n=14, ML2 n=12, p=0.003; HVA 1.2-fold decrease, WT n=14, ML2 n=13, p=0.0007).

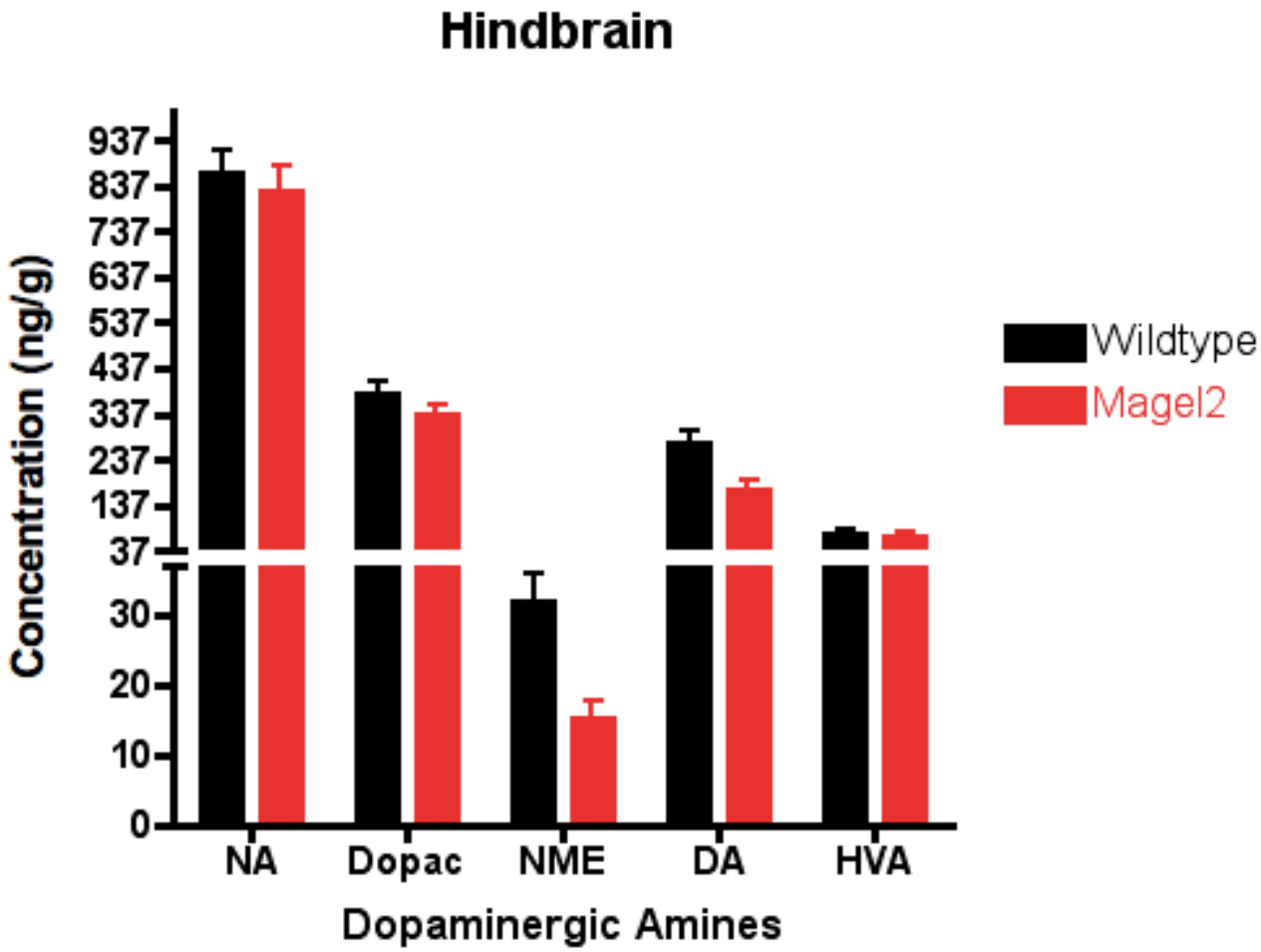

Figure 3.21. Dopaminergic amines in the hindbrain

HPLC analysis of dopamine metabolites in the hindbrain. There is significantly less dopamine (DA) and NME in the hindbrain of *Magel2*-null mice (NME 2.1-fold decrease, WT n=12, ML2 n=11, p=0.003; DA 1.6-fold decrease, WT n=15, ML2 n=12, p=0.02).

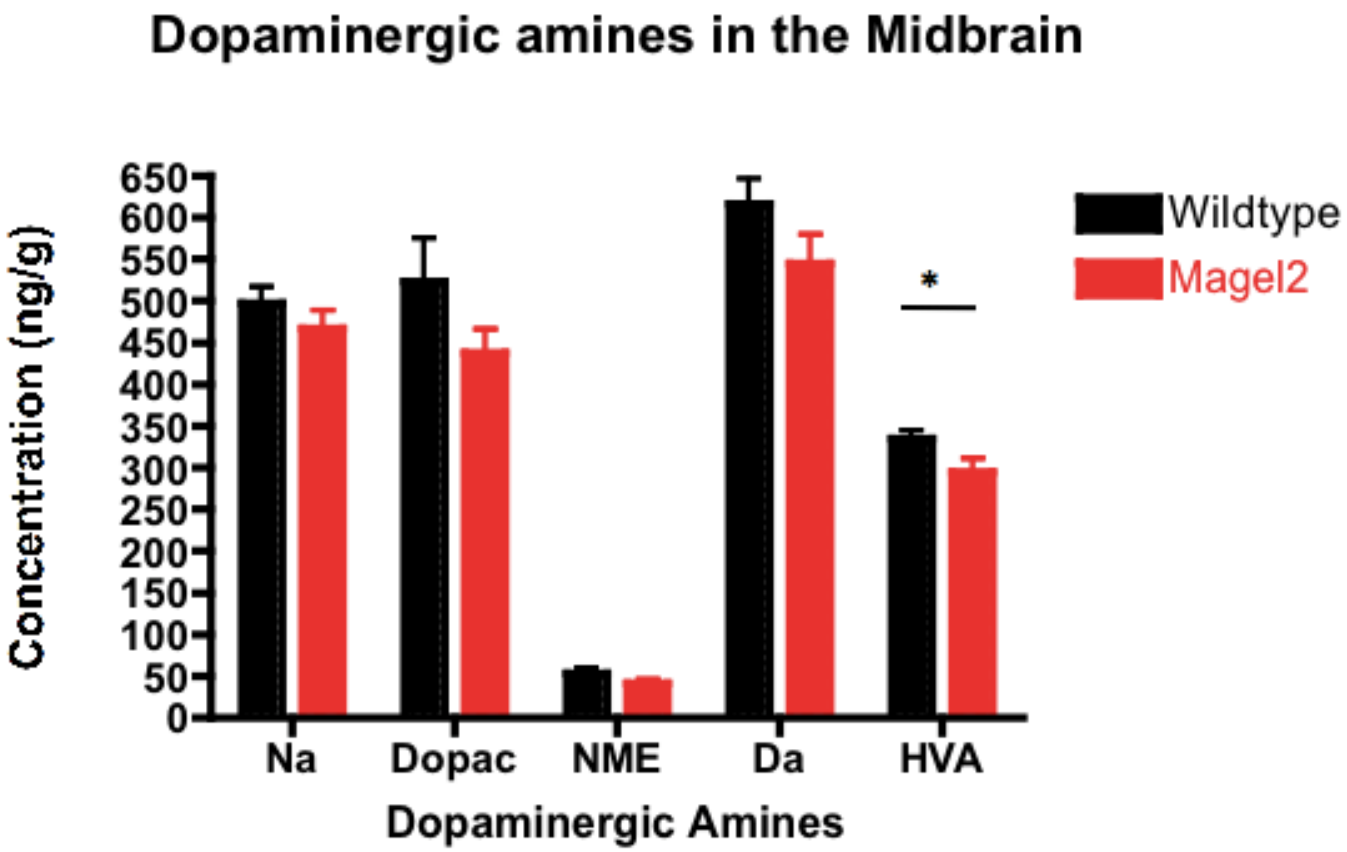

Figure 3.22. Dopaminergic amines in the midbrain

HPLC quantification of dopamine metabolites shows that there is significantly less homovanillic acid (HVA) in the midbrain of *Magel2*-null mice (HVA, 1.1-fold decrease, WT n=15, ML2 n=13, p=0.05).

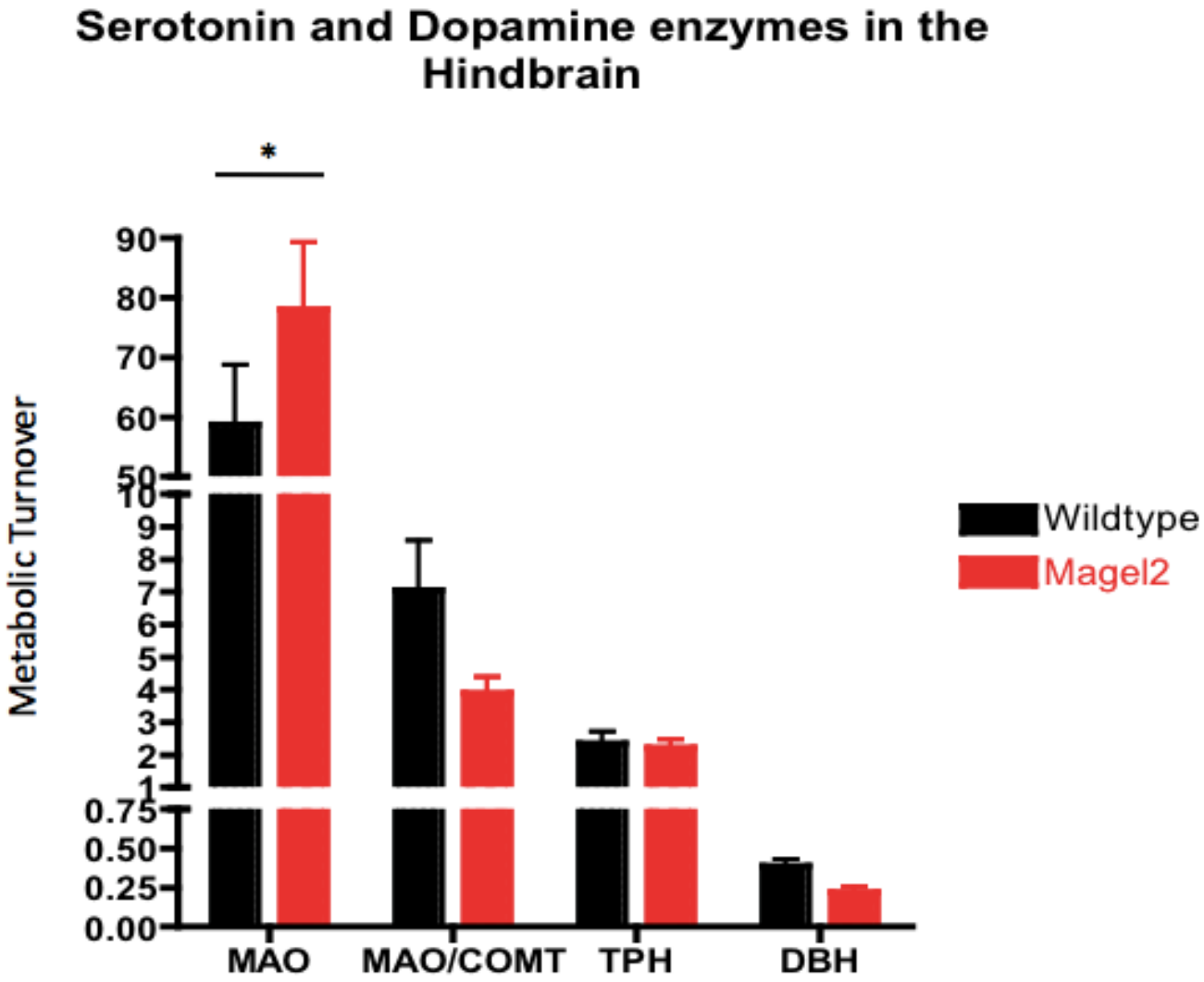

Figure 3.23. Metabolic turnover in the hindbrain

Using the HPLC quantification of the dopaminergic and serotonergic metabolites, the metabolic turnover at various steps in each pathway was assessed. This turnover is suggestive of the enzymatic activity and can be useful when determining what step is affected. The inferred activity of the enzyme monoamine oxidase, is significantly increased in the hindbrain of *Magel2*-null mice (ML2) when compared to WT littermates. (MAO, 1.8-fold increase, WT n=13, ML2 n=11 p=0.003).

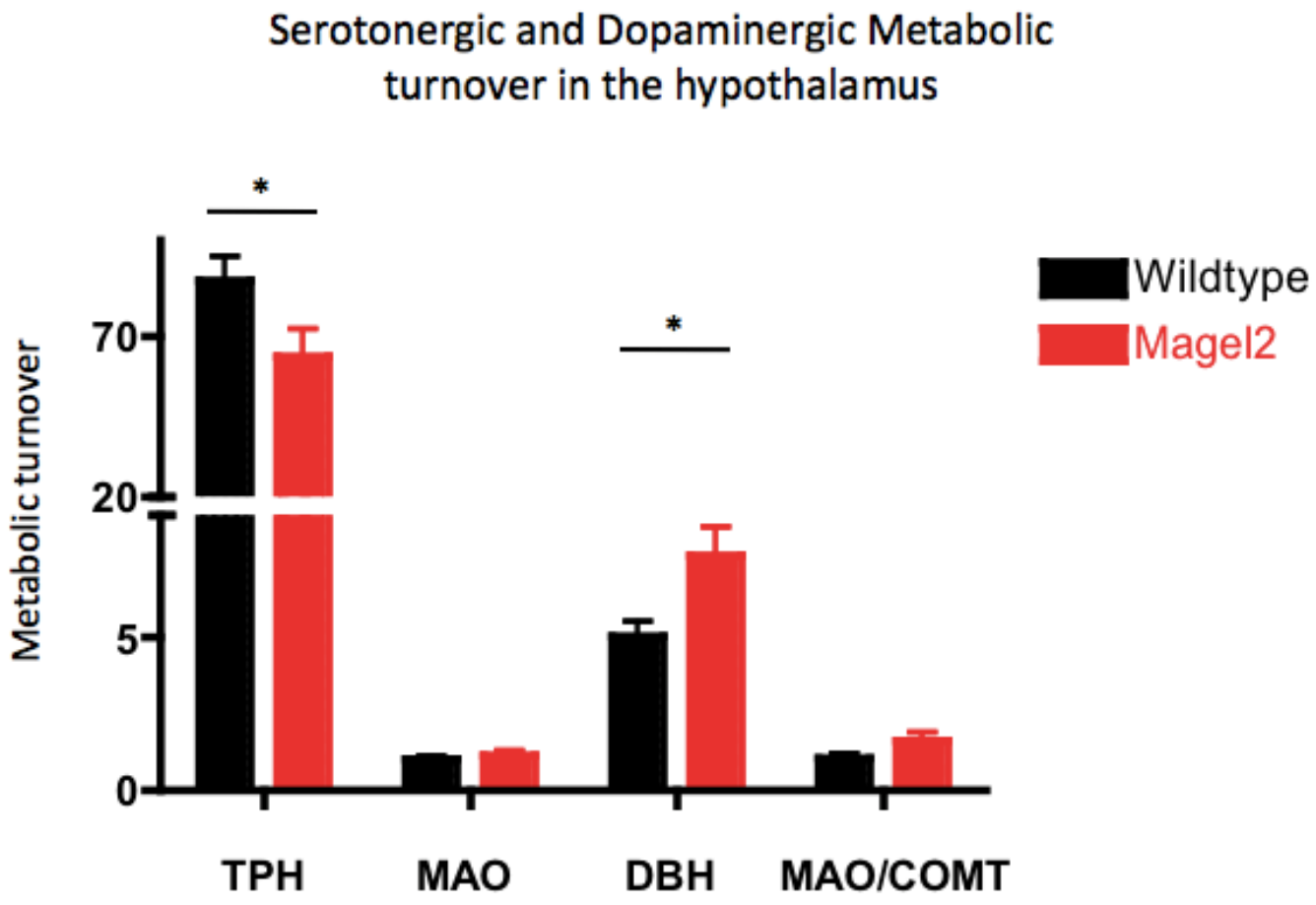

Figure 3.24. Metabolic turnover in the hypothalamus

Using the HPLC quantification of the dopaminergic and serotonergic metabolites, the metabolic turnover at various steps in each pathway was assessed. This turnover is suggestive of the enzymatic activity and can be useful when determining what step is affected. In the hypothalamus, there is significantly more DBH activity, and significantly less TPH activity in the *Magel2*-null mice (DBH, 1.5-fold increase, n=12, p=0.02; TPH 1.4-fold decrease in activity, n=11, p=0.05).

3.1.6. Ventricle area and dopaminergic cell size are intact in the *Magel2*-null mouse

Children with PWS have enlarged ventricles and an increased volume of CSF (Lukoshe, et al., 2013). Using coronal sections stained with thionine or tyrosine hydroxylase, the area of the third ventricle was measured using ImageJ software. There was no difference in area occupied by the third ventricle between the *Magel2*-null mice and the wildtype mice (Data not shown). This is consistent with MRI analysis of the *Magel2*-null mouse brain that did not show any difference in the size of the third ventricle.

AKT-induced morphological changes that occur in response to drug use, include a reduced size of the dopaminergic VTA-neurons (Russo et al., 2010). *Magel2*-null mice have abnormal physiological responses to exposure. We expect morphological differences corresponding to the abnormal behaviour and physiological responses to exposure observed in *Magel2*-null mice. Using the ImageJ software analysis of area count, the cell size of the dopaminergic neurons in the VTA were quantified. There was no difference in the size of VTA neurons in *Magel2*-null mice (Data not shown, WT n=6, ML n=4, ns).

3.2. Biochemical and physiological response to the exposure and withdrawal of high-fat diet

Within the mesolimbic dopamine system, immediate and long-term molecular changes occur in response to the exposure of natural rewards. These distinct molecular changes mediate the immediate effect of the reward, as well as induce long-term changes in synaptic morphology and gene expression that mediate the response to a subsequent exposure. It is our hypothesis that these molecular mechanisms are disrupted in our *Magel2*-null mouse model contributing to the observed phenotype. In order to test these changes, *Magel2*-null mice were exposed to, and withdrawn from, a HF-diet. The measurable molecular effects of exposure and withdrawal include an altered dopamine signaling profile, assessed by measuring TH levels, an altered stress response, and changes in expression of **Δ**FosB, and the activity of CREB. **Δ**FosB is a molecule involved in mediating the long-term effects, and the transcription factor CREB is responsible for the short-term effects of the exposure to a reward. Both the accumulation of **Δ**FosB and the phosphorylation of CREB are involved in the development of dependence and can be quantified in order to assess the molecular response to an exposure. A molecular stress response is also observed in response to the withdrawal of HF-diet. This stress-response can be quantified by measuring the phosphorylation of AKT and ERK within the nuclei of the reward pathway. We used various diets to assess these molecular changes within the mesolimbic reward nuclei. For this experiment three groups of mice were used, an

exposed group (28 days of HF-diet), a withdrawal group (28 days of HF-diet followed by a 24 hour return to standard chow), and a standard diet fed group used as a control.

Following the 28-day exposure to the HF-diet, both *Magel2*-null mice and WT mice gained a significant amount of weight indicating that both genotypes had been comparably exposed (Figure 3.25, WT 43 %, ML2 45 % weight gain, WT n=10, ML2 n=9, ns). The total weight gained was not significantly different between genotypes. However, the *Magel2*-null mice did have a delayed weight gain in response to the diet (Figure 3.26, 2.5-fold decrease in initial weight gain (day 1), WT n=10, ML2 n=9, p=0.01). This suggests that the Magel2-null mice had an initial aversion to the novelty of the HF-diet. This is supportive of previous findings indicating an attenuated response to novelty in *Magel2*-null mice. Ultimately, the increase in weight indicates that all the animals were sufficiently exposed to the HF-diet.

In response to the removal of a HF-diet, both genotypes lost a comparable amount of weight (Figure 3.28, WT 3.3% weight loss, ML2 2.8 % weight loss, WT n=5, ML2 n=4, ns). All the animals significantly reduced their food intake during the 24-hour return to standard chow (Figure 3.28, 6.2-fold decrease, n=9, $p<0.0001$). This indicates that both genotypes did undergo a comparable and significant behavioural withdrawal following the removal of the HF-diet.

3.2.1. The increase in tyrosine hydroxylase in animals withdrawn from a high-diet is lost in mice lacking *Magel2*

Dopamine signaling is central in mediating the response to natural and chemical rewards (drugs of abuse). Dopamine is responsible for producing the feeling of wanting when anticipating a reward and involved in the feeling of euphoria when actually receiving the reward. Like with chemical rewards, this dopaminergic response is observed with the exposure and the withdrawal of a HF-diet. By immunoblotting for tyrosine hydroxylase in mice either exposed or withdrawn from a HF-diet, we can get an idea of how the loss of Magel2 influences dopamine signaling in response to different dietary conditions. Tyrosine hydroxylase was used as a proxy measure for the level of dopamine signaling within the different nuclei of the reward pathway. We have demonstrated an increase in tyrosine hydroxylase in Magel2-null mice in the amygdala under standard feeding conditions. Holsen et al. (2006) have also demonstrated an increase in post-meal blood flow to the amygdala in individuals with PWS. This leads us to expect a similar result in the Magel2-null mouse model of PWS. We expect higher level of TH in the amygdala of *Magel2*-null mice compared to WT mice following the exposure of HF-diet. This would

indicate an increased drive for the reward both in anticipation of a reward before, and following the exposure.

In the amygdala, both wildtype and *Magel2*-null mice showed less TH in mice exposed to a HF-diet when compared to mice maintained on a standard chow diet (Figure 3.27, WT 42 % decrease, n=4, p=0.01, ML2 37 % decrease, n=4, p=0.01). The lower level of TH suggests a similar reduction in motivational behaviour in both genotypes following the exposure. There was no difference in the levels in between the HFD group and the control group in the VTA, the NAc, or the hypothalamus of either the wildtype or the *Magel2*-null mice. Previous work from our lab demonstrated reduced food intake in response to re-feeding following a complete fast in the *Magel2*-null mice (Mercer et al., 2013). This suggests a loss of response to the withdrawal of standard chow. We expected a similar loss of response to the withdrawal of HF-diet.

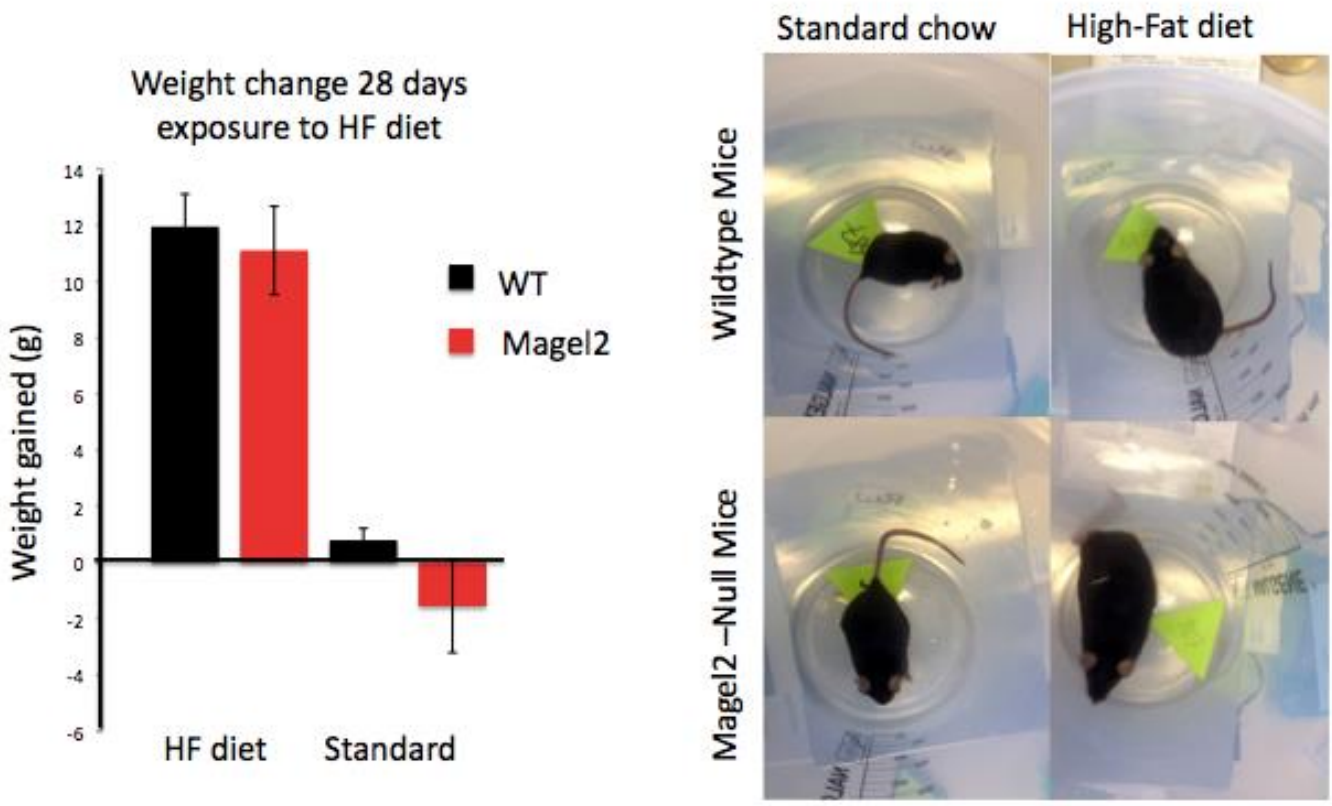

Figure 3.25. Weight gain in response to exposure of high-fat diet

Recorded weight change in response to the HF-diet. *Magel2*-null and WT mice both gained a significant amount of weight in response to the 28-day exposure of a HF-diet when compared to standard-diet fed littermates. (WT 143 %, ML2 145 % weight gain, WT n=10, ML2 n=9, ns).

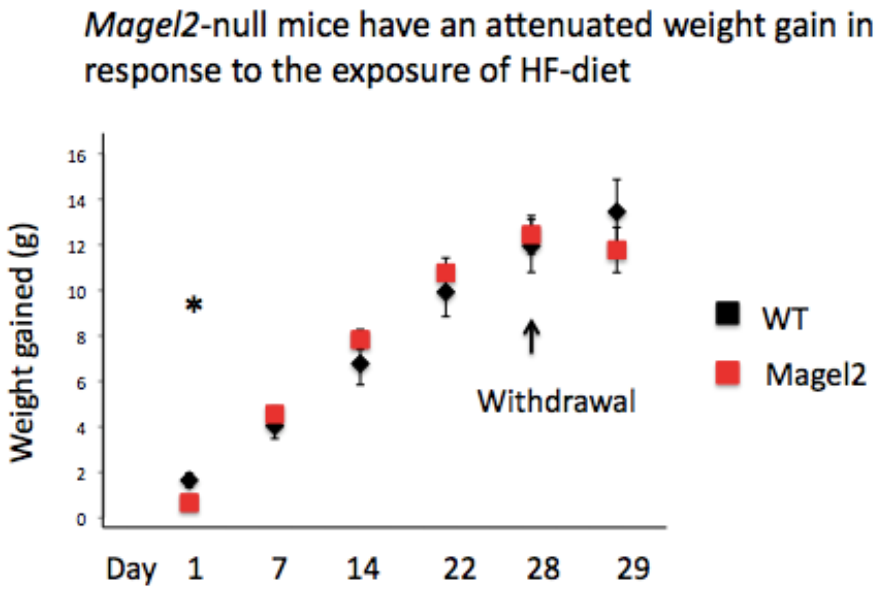

Figure 3.26. High-fat diet food intake

Recorded weight change in response to the HF-diet and withdrawal of HF-diet. *Magel2*-null and WT mice both gained a significant amount of weight with the 28-day exposure to a HF-diet (WT 143 %, ML2 145 % weight gain, WT n=10, ML2 n=9, ns). *Magel2*-null mice gained significantly less weight on day 1 (2.5-fold less weight gained, WT n=10, ML2 n=9, p=0.01).

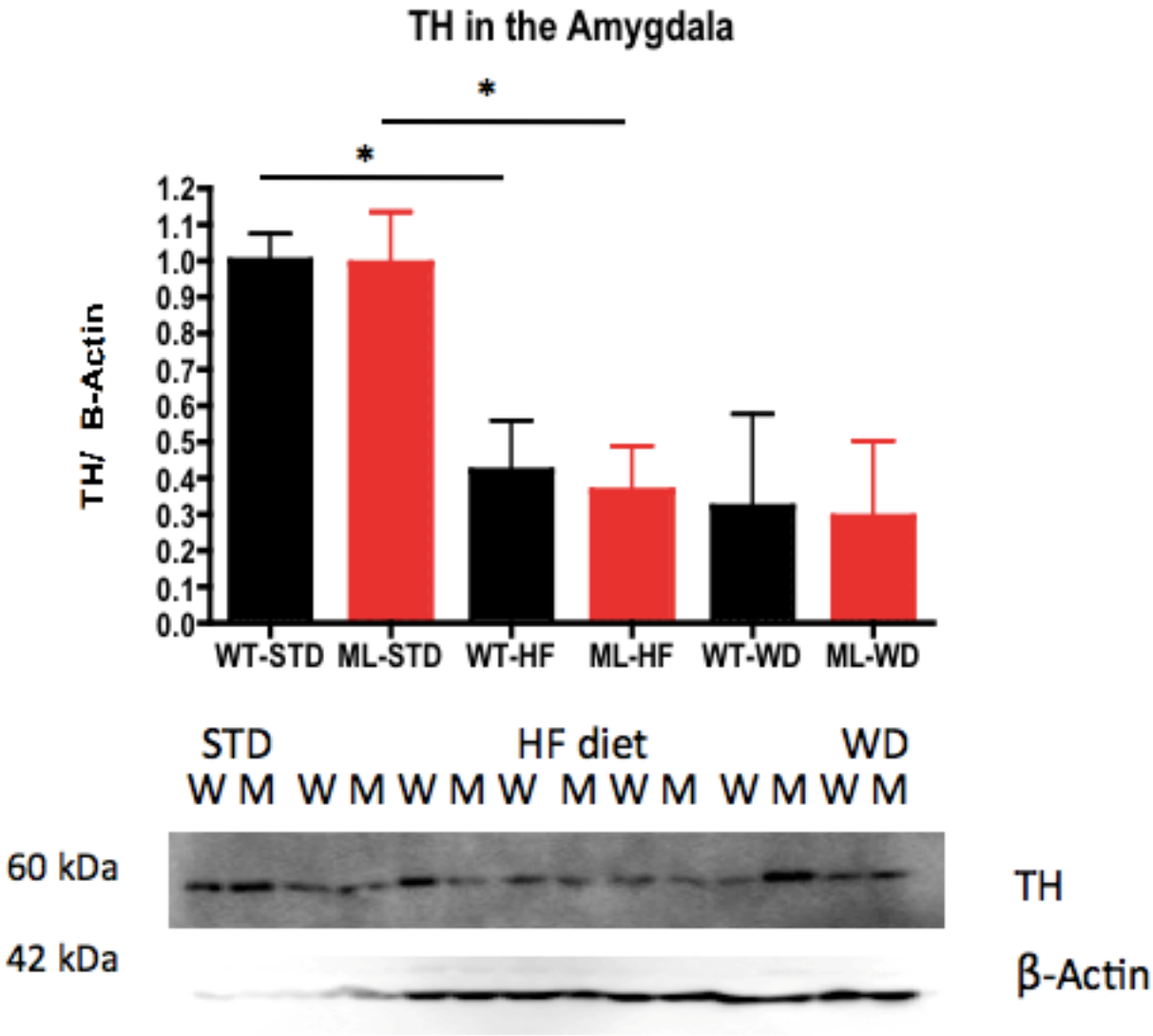

Figure 3.27. Tyrosine hydroxylase in the amygdala in response to changes in diet

Magel2-null mice (ML, M) and wildtype (WT,W) mice both have lower TH levels with the exposure to HF-diet, compared to mice fed a standard diet. Immunoblotting for TH normalized to **β**-Actin (WT 42 % decrease p=0.01, ML2 37 % decrease n=4, p=0.01).

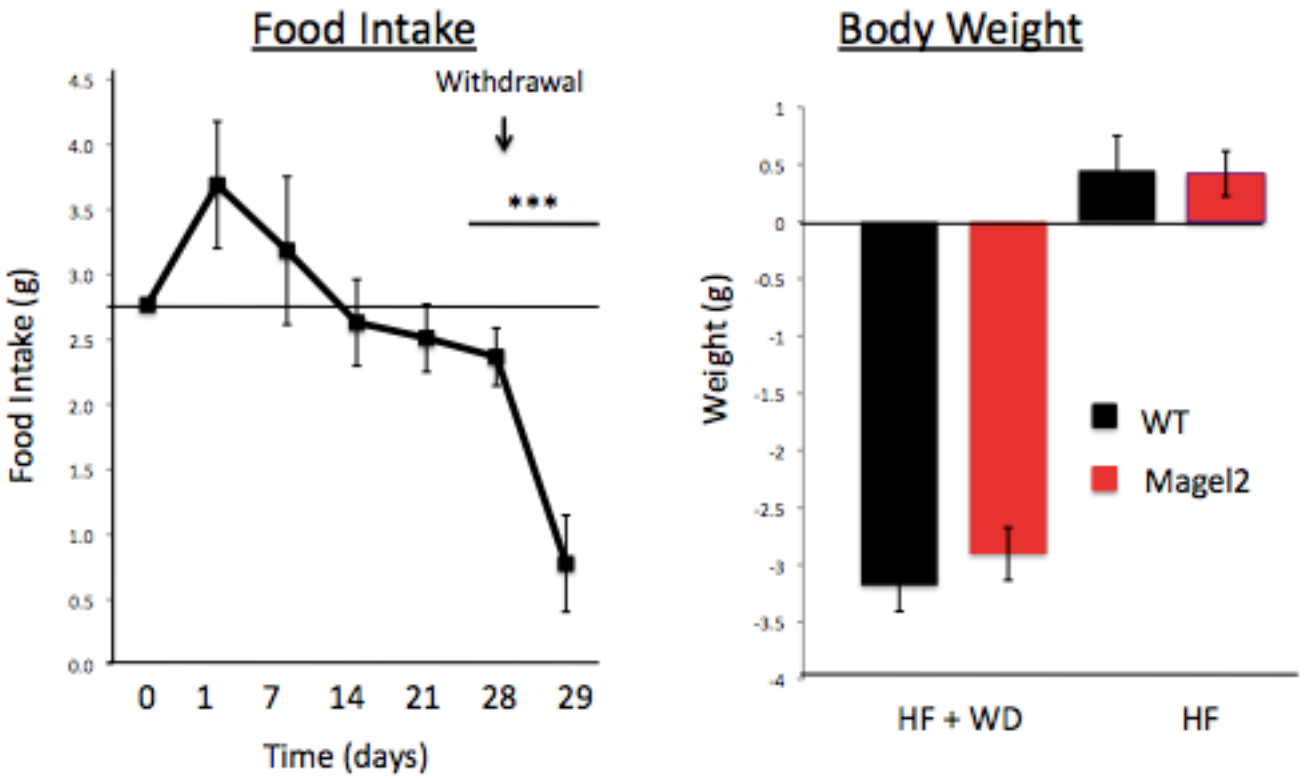

Figure 3.118. Weight loss and food intake in response to the withdrawal of the high-fat diet

Magel2-null and wildtype mice both lost a significant and comparable amount of weight in response to the 24-hour withdrawal of a HF-diet to standard chow. There was less food consumed in all the cages in response to the return to standard chow (6.2-fold decrease in food intake, n=9 $p<0.0001$; WT 3.3% weight loss, ML2 2.8 % weight loss, WT n=5, ML2 n=4, ns).

We observed a significant difference in TH levels in the hypothalamus in WT mice fed HFD compared to WT mice withdrawn from HFD (Figure 3.29, WT 2.6-fold increase in TH, n=4, p=0.005). This difference in hypothalamic tyrosine hydroxylase was not observed in *Magel2*-null mice, suggesting the loss of a response to the removal of the reward. The level of TH in the VTA was also influenced by the withdrawal of HF-diet. Both the *Magel2*-null and the WT mice had lower levels of TH in the VTA (Figure 3.30). This loss of dopamine activity in the midbrain suggests that both genotypes exhibited a comparable anhedonic response to the loss of the HF reward. This response was measured in the nucleus accumbens and the amygdala, where no detectable differences in TH levels were observed in either the wildtype or the *Magel2*-null mice (Figure 3.27 & Figure 3.31).

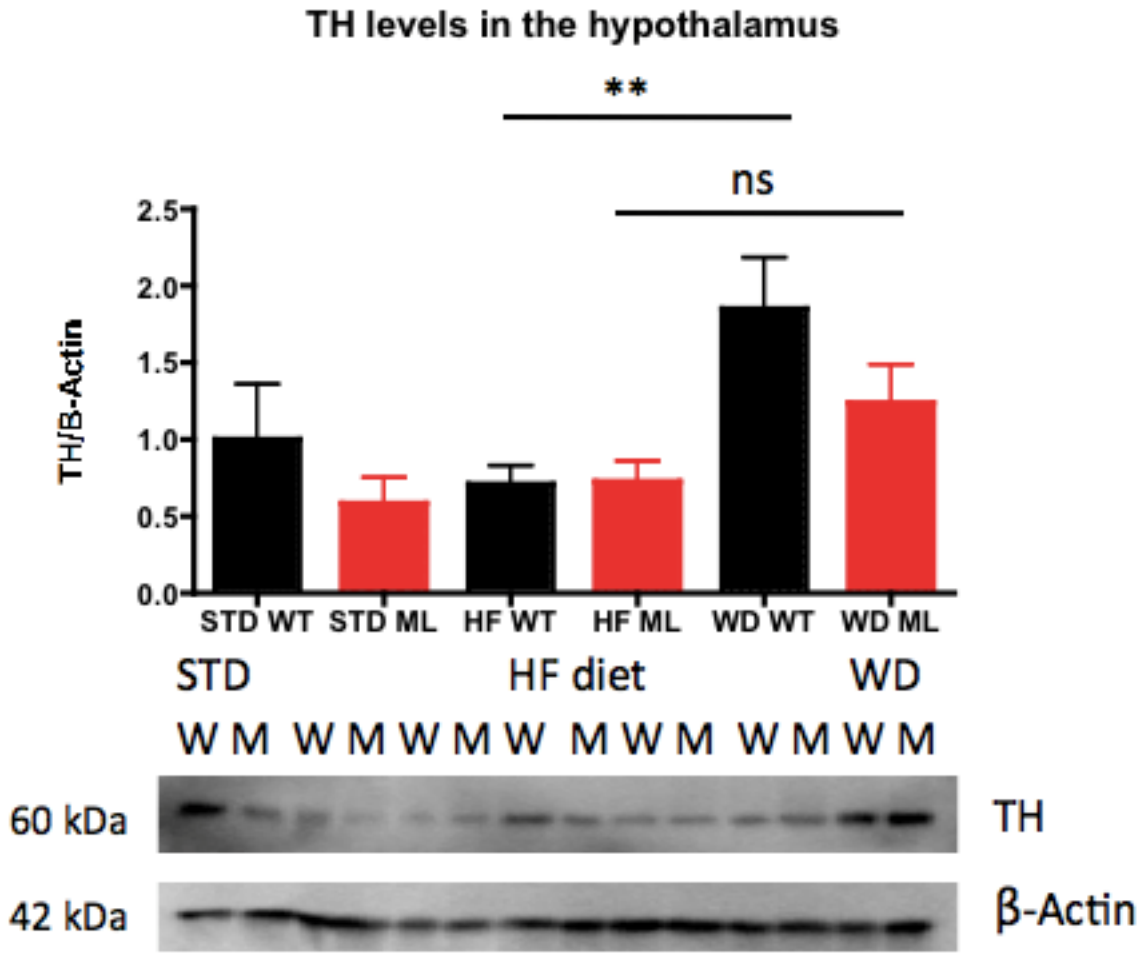

Figure 3.29. Tyrosine hydroxylase in response to the exposure and withdrawal of high-fat diet in the hypothalamus

Wildtype mice (WT, W) have significantly more TH protein in the hypothalamus when withdrawn from a HF-diet compared to mice fed a HFD but not withdrawn. HFD *Magel2*-null mice (ML, M) did not demonstrate a significant difference in TH protein compared to *Magel2*-null mice withdrawn from a HF-diet for 24 hours (WT, 2.6-fold increase in TH with W/D, n=5 p=0.005, ML2, n=4, ns).

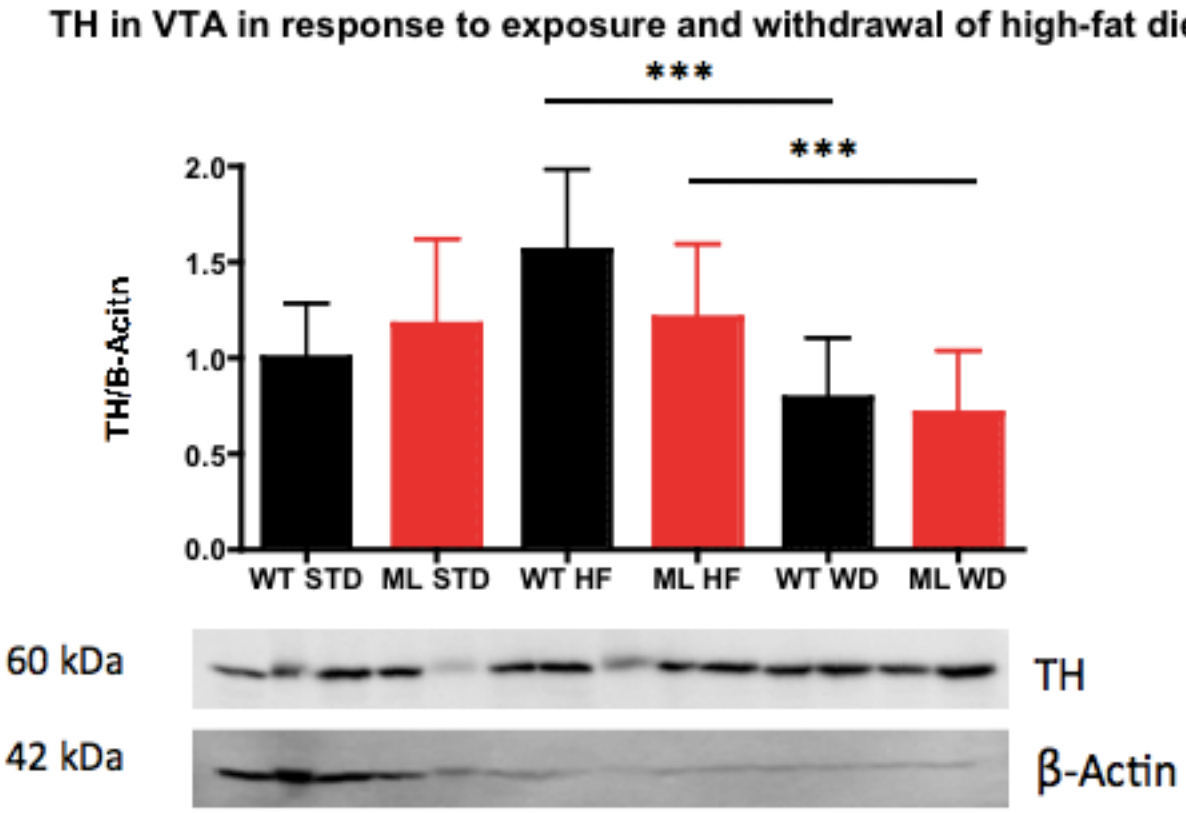

Figure 3.30. Tyrosine hydroxylase in the ventral tegmental area in response to the exposure and the withdrawal of high-fat diet

Both *Magel2*-null mice and WT mice withdrawn from a HFD have significantly less TH when compared to the HFD group. There was no difference between genotypes.

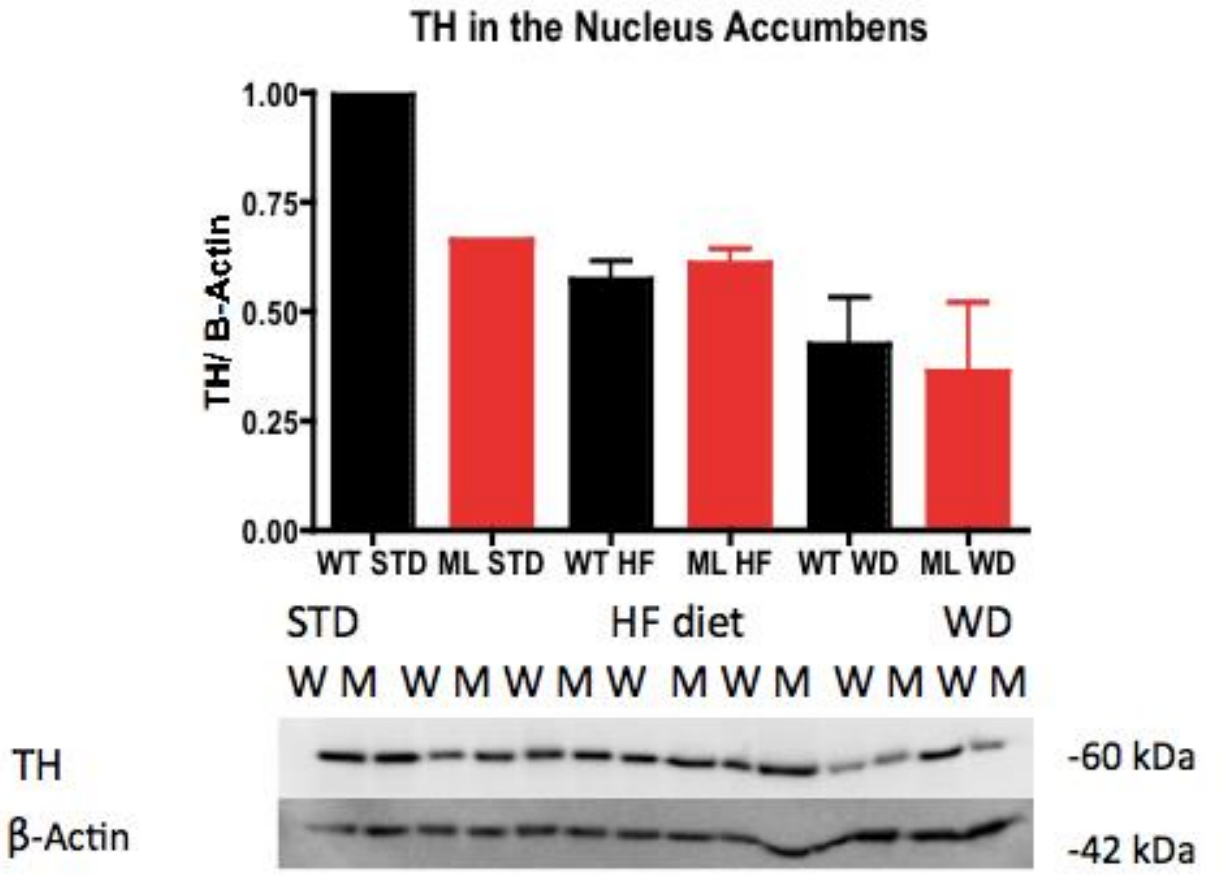

Figure 3.31. Tyrosine hydroxylase in the nucleus accumbens in response to the exposure and withdrawal of high-fat diet

There was no detectable difference in the TH protein level of either *Magel2*-null mice or WT mice for either the HFD exposed group of the HFD-withdrawal group.

3.2.2. *Magel2*-null mice have less activated AKT in the midbrain upon withdrawal of a high-fat diet

Along with altered dopamine signaling, we would also expect to see a stress response to the removal of a palatable food. ERK is involved in a variety of cellular processes including the synaptic adaptations involved in the development of a drug-dependence and the acute stress response to the removal of the drug. Activation of ERK has been demonstrated in several reward nuclei in response to the withdrawal of ethanol, cocaine, morphine, and high-fat diet (Lu et al., 2006; Schumann & Yaka, 2009; Cao et al., 2005). Activity of the AKT pathway is also involved in mediating the withdrawal response. The cellular morphology of dopaminergic neurons within the VTA is influenced by the exposure of drugs of abuse via an AKT-dependent mechanism to modify the reward experienced (Russo et al., 2006). Along with mediating a stress response AKT activity in the VTA is also implicated in social defeat and sucrose preference (Krishnan et al., 2008). We expect a reduced phosphorylation response of ERK and AKT in response to the withdrawal of a HF-diet in *Magel2*-null mice, this would support the attenuated feeding responses observed in fasted/re-fed *Magel2*-null mice. In order to assess the stress response on the removal of the diet, the phosphorylation of AKT was measured in tissue punches from the various nuclei of the reward pathway (Figure 3.14).

I was unable to measure a difference in phosphorylated-AKT in the hypothalamus or the nucleus accumbens in HFD withdrawn mice. In the VTA there was significantly less pAKT in the *Magel2*-null mice withdrawn from HFD compared to those fed HFD (Figure 3.32, $p=0.03$, $n=4$). This indicates a blunted stress response to the loss of reward. This is consistent with the re-feeding behaviour and the initial hesitation to feed, which could suggest that the HF-diet carries less of a reward value for the *Magel2*-null mice.

Along with AKT activity, the phosphorylation of ERK was measured following the withdrawal of HF-diet. There was no observable difference in the level of active ERK1/2 in the NAc or the VTA of either genotype (Figure 3.32, data not shown). There was a lot of variability between samples that could have arisen from several stress inducing events independent of the withdrawal. The mice were housed in groups and gained significant visceral fat that complicated the sacrifice procedure. The order of sacrifice and the speed of death, due to the increased visceral fat could all factor in to the stress response of the animal.

Another measurable response to the withdrawal of HF-diet is the phosphorylation of CREB. We would again expect a blunted response in the *Magel2*-null mice. In the amygdala, we found an exaggerated increase in the phosphorylation of CREB in the *Magel2*-null mice withdrawn from the HF-diet (Figure

3.33, 2.4-fold increase, n=4, p=0.05). Like the previous finding in the amygdala that demonstrate an increase in tyrosine hydroxylase in mice exposed to a HF-diet compared to mice maintained on standard chow, this increase in pCREB indicates an exaggerated molecular response to the changes in diet. There was no observable difference in CREB activity in the PFC or the VTA, or the NAc (Figure 3.32, data not shown). Between WT mice removed from the HF-diet and returned to standard chow and those maintained on HFD, there was a significant difference in CREB activity in the hypothalamus (Figure 3.34, n=4 p=0.04). This increase in activity was not significant in the *Magel2*-null mice.

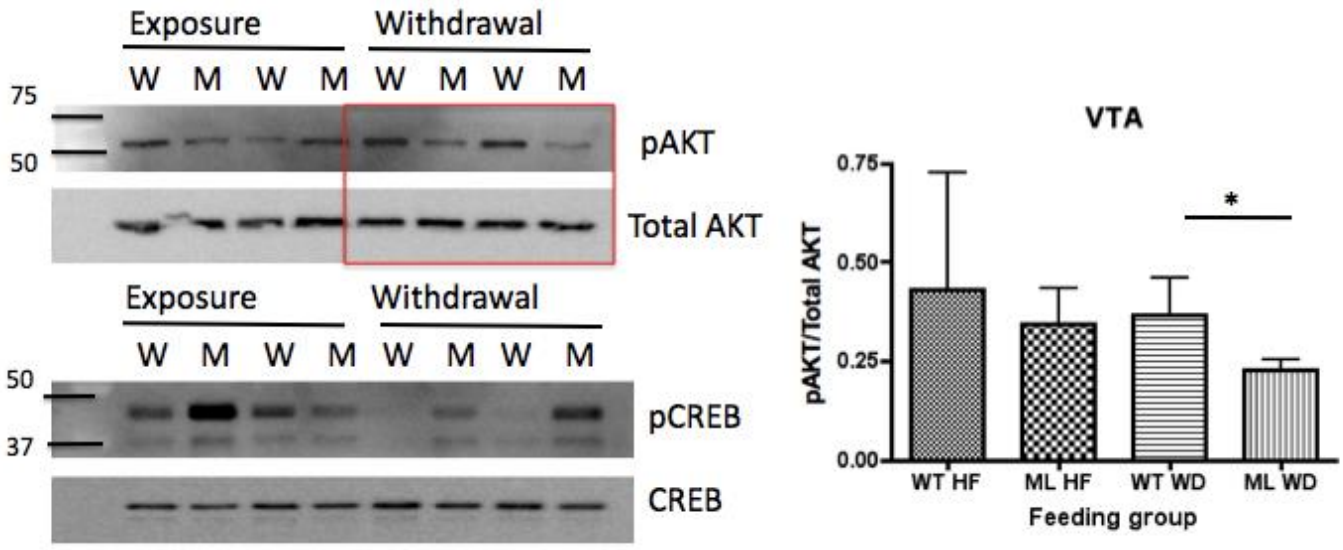

Figure 3.32. Molecular responses in the ventral tegmental area in mice exposed and withdrawn from a high-fat diet.

The phosphorylation of CREB, and AKT in the VTA tissue punches was determined through immunoblot analysis. There is significantly less phospho-AKT in the VTA of *Magel2*-null mice compared to WT mice following the WD of HF-diet. (40 % pAKT in the *Magel2*, p=0.03, n=4).

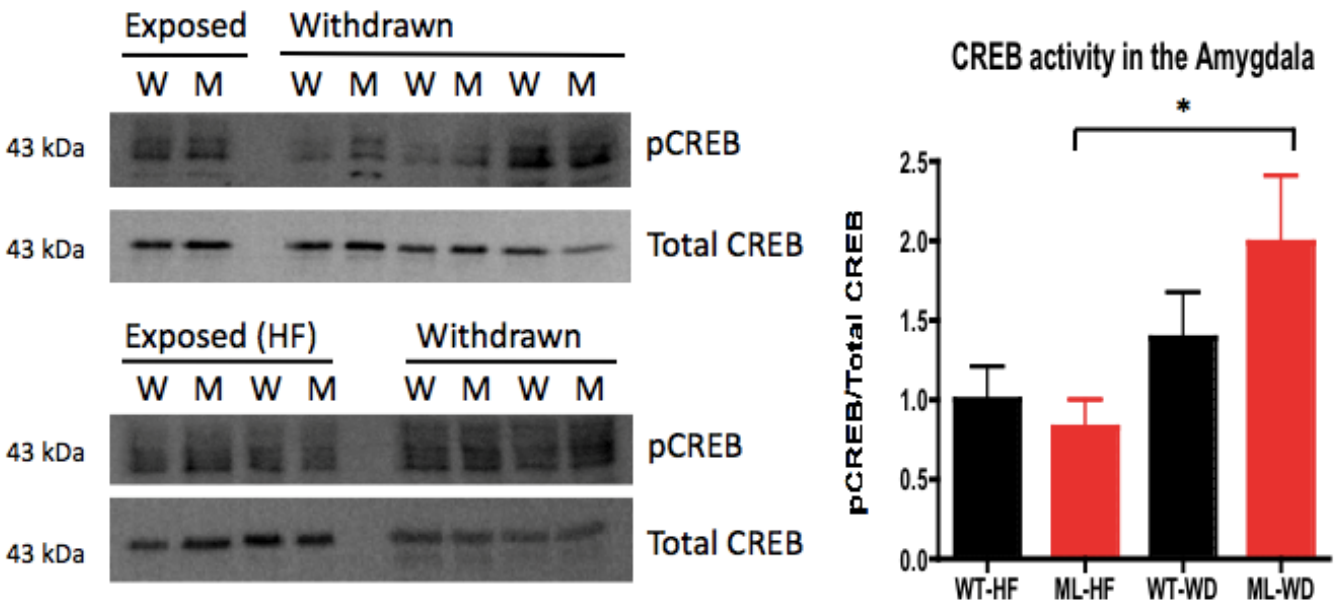

Figure 3.33. Phosphorylated CREB in the Amygdala

In the amygdala there was a significant increase in the phosphorylation of CREB in response to the withdrawal of a HF-diet. This was not observed in the wildtype mice. (ML2, 2.4-fold increase, n=4, p=0.05).

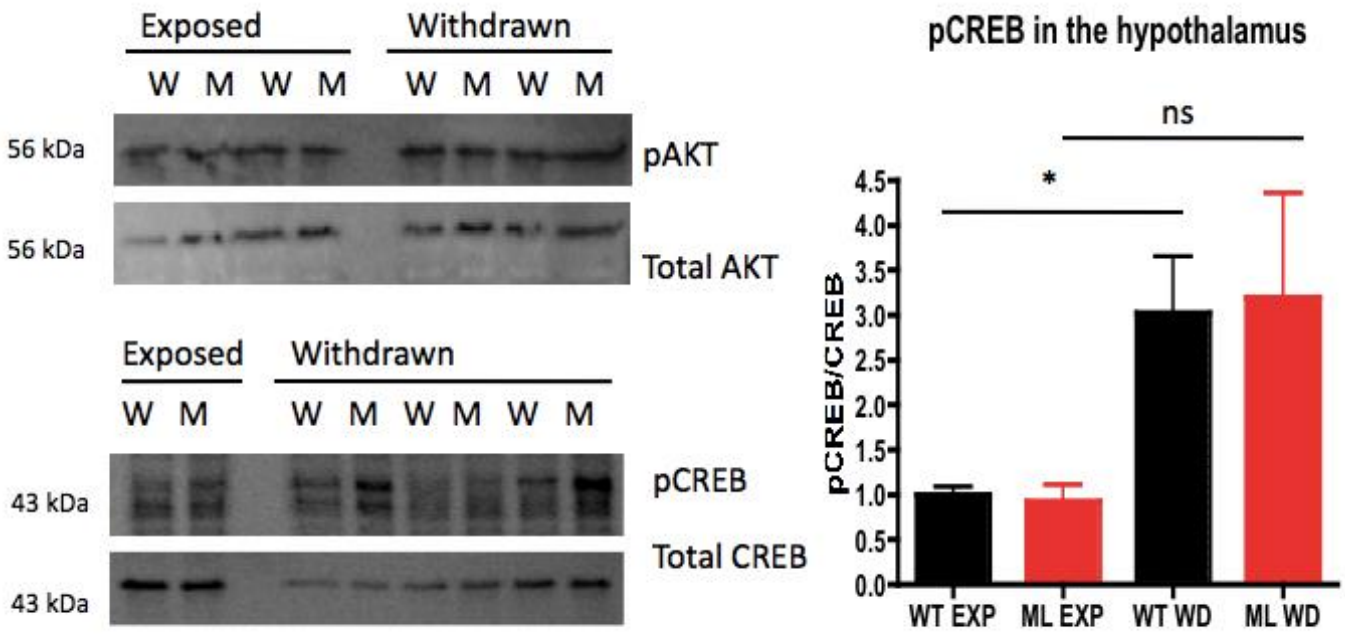

Figure 3.34. Phosphorylated CREB and AKT in the hypothalamus in response to the withdrawal of high-fat diet

A significant increase in the phosphorylation of CREB is observed in the hypothalamus of Wildtype (WT,W) mice following the withdrawal of HF-diet. There was no significant difference in the phosphorylation of CREB in the *Magel2*-null mice (ML, M) (WT, n=4, p=0.04; ML2, ns). There was no significant difference in the phosphorylation of AKT in the hypothalamus in response to the 24 hr withdrawal of a HFD in either genotype.

3.2.3. Immunoblotting for ΔFosB did not prove useful in assessing the response to chronic exposure of a high-fat diet

It has previously been demonstrated by Nestler et al. in 2001 that, like with chronic exposure to drugs of abuse, the chronic exposure of HF-diet can produce molecular changes in the dopamine reward pathway. These changes can be used as molecular markers of an addictive phenotype. These molecular addiction markers include the accumulation of **Δ**FosB in the nucleus accumbens. There is an attenuated short-term response to the exposure of cocaine and HF-diet, however the chronic exposure has not been assessed in the *Magel2*-null mice. We expected to find a reduced accumulation of **Δ**FosB in the nucleus accumbens that would indicate an impaired addiction response similar to the short-term addiction-response observed. After immunoblotting for **Δ**FosB in the nucleus accumbens, I found no significant difference in the way *Magel2*-null and wildtype mice respond to the 28-day exposure to a HF-diet (data not shown).

3.2.4. *Magel2*-null mice have less striatal dopamine with the exposure to a high-fat diet

The exposure to a high-fat diet over the course of 28 days alters the mesolimbic dopamine profile. HPLC was used to analyze the levels of dopamine and serotonin metabolites in the three different feeding groups including; high-fat, high-fat withdrawn, and standard fed mice. Similar to the loss of response observed with immunoblotting for TH and for stress and addiction markers, we expect that the *Magel2*-null mice will have a blunted response to the exposure and withdrawal of the HF-diet.

With exposure to the HF-diet we observed significant changes in the levels of NA, HVA and the inferred enzymatic activity of DBH in the WT striatum (Figure 3.35, HVA, 1.2-fold increase, WT n=19, ML2 n=18, p=0.05; NA, 2-fold decrease, WT n=19, ML2 n=17, p=0.02; DBH, 1.9-fold decrease in activity, WT n=19, ML2 n=17, p=0.04). The decrease in NA and DBH activity suggests that dopamine is being broken down differently than under standard conditions. The increase in HVA levels also suggests an altered metabolic profile with HF-diet. *Magel2*-null mice lack both of these difference between feeding groups. The altered dopamine synthesis/breakdown pathway in response to the change in diet is lost in the *Magel2*-null mice. *Magel2*-null mice also had a 1.5-fold decrease in noradrenaline in the hypothalamus of HF-fed mice, when compared to HF-fed littermates (Figure 3.36, n=13, p=0.01). This reduced NA level in the exposed group was followed by an exaggerated increase in NA in mice withdrawn from a HF-diet (1.2 fold increase, n=13, p=0.04). This response was not observed in the wildtype mice. In response to the withdrawal of HF-diet, wildtype mice demonstrate a significant increase in the inferred MAO enzymatic activity, which was not seen in the *Magel2*-null mice (WT 2.4-fold increase, n=13, p=0.004). Despite

having observed a difference in the serotonin metabolites under standard feeding conditions, there was no significant serotonergic response to either the exposure or withdrawal of a HF-diet in either genotype.

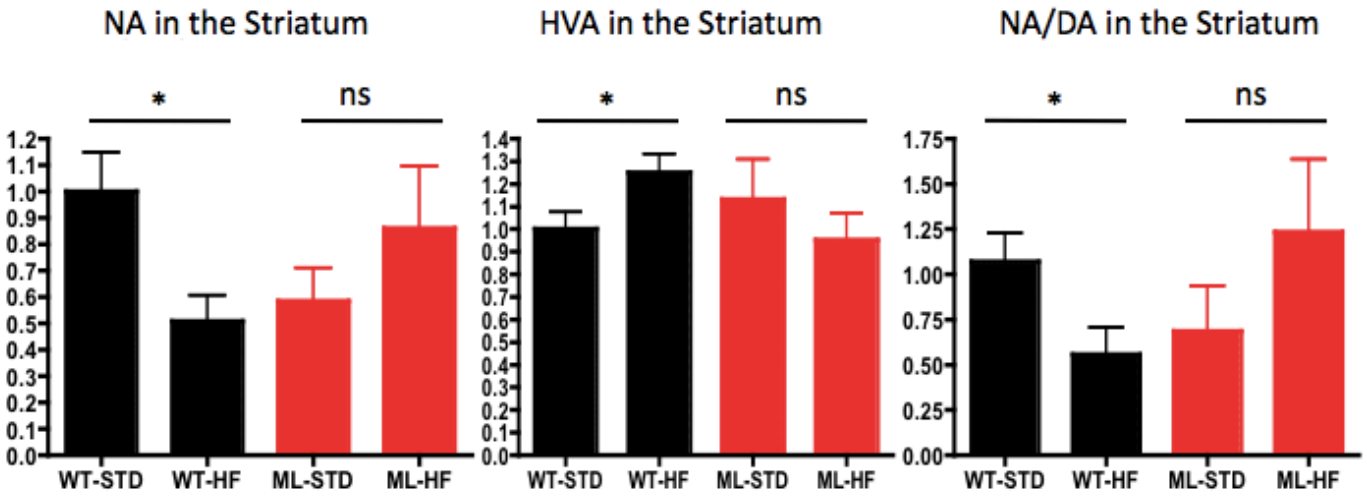

Figure 3.35. Dopamine metabolites in response to the exposure of a high-fat diet

Magel2-null mice (ML) have a loss of response to the withdrawal of a HF-diet in the striatum. Significant decreases in DBH activity and NA levels were observed in the WT mice following the exposure to a HF-diet. This response was not observed in the *Magel2*-null mice. An increase in striatal HVA was also observed in the WT mice in response to the exposure of a HF-diet, and not the *Magel2*-null mice. (HVA, 1.2-fold increase, WT n=19, ML2 n=18, p=0.05; NA, 2-fold decrease, WT n=19, ML2 n=17, p=0.02; DBH, 1.9 fold decrease in activity, WT n=19, ML2 n=17, p=0.04).

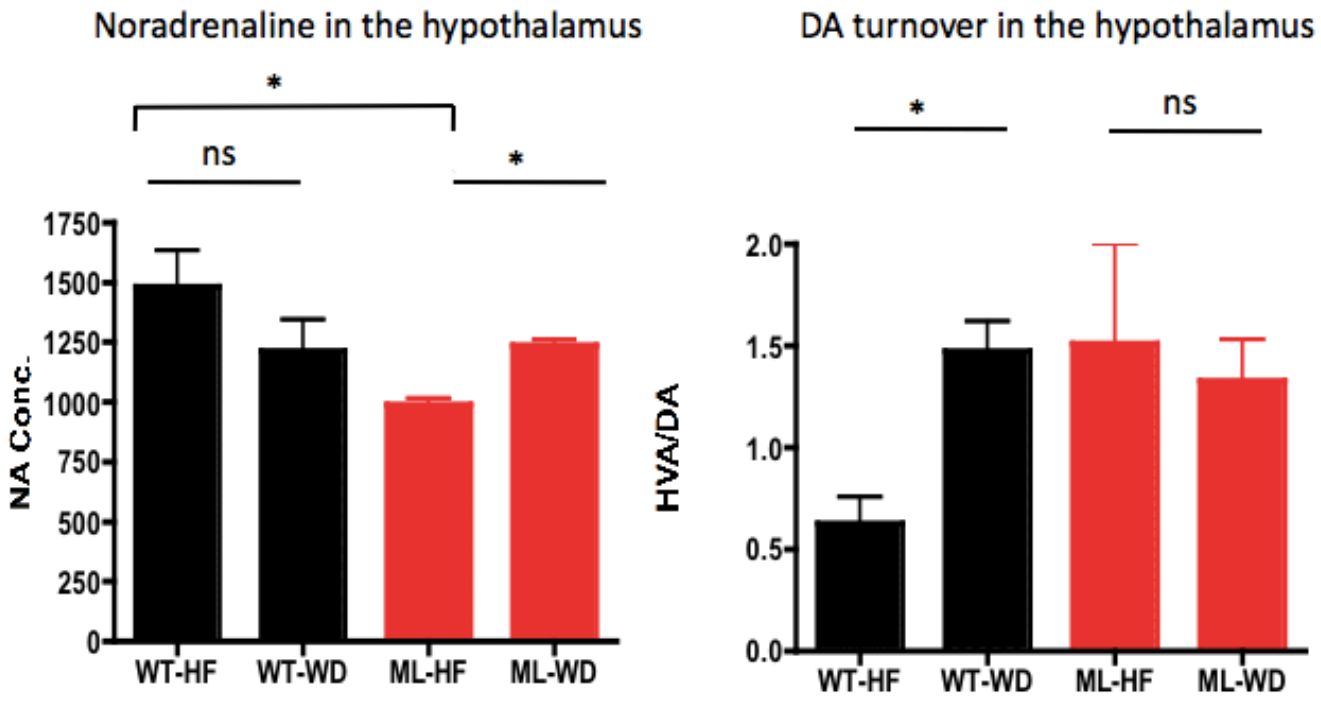

Figure 3.36. Diet-induced differences in the hypothalamus

Magel2-null mice have significantly less NA in the hypothalamus in response to the chronic exposure of HF-diet, when compared to WT littermates. (HF-diet; 1.5-fold less NA in ML2, n=13, p=0.01). *Magel2*-null mice have an exaggerated increase in NA in response to the withdrawal of HF-diet, compared to the HF-diet group. This response is not observed in the WT littermates (ML2, 1.2-fold increase, n=13, p=0.04; WT, ns). Wildtype mice have a significant increase in MAO activity upon withdrawal that is not observed in the *Magel2*-null mice (MAO, WT, 2.4-fold increase, n=12 p=0.004; ML2, ns).

3.3. Binge-feeding behaviour

3.3.1. *Magel2*-null mice have an attenuated binge-feeding response

Binge feeding was assessed using a limited access model that was developed by Halpern et al. (2013). This involved exposing the animals to a HF-diet daily for one hour. This experiment is designed to cause increased feeding of the HF-diet over the course of several days. The hyperphagia observed in PWS, along with the abnormal anticipation of the dark cycle previously observed in *Magel2*-null mice, suggests that they may have an exaggerated binge feeding response to the limited exposure. We expected that *Magel2*-null mice exposed to a limited access diet would have an initial hesitation to feed followed by an exaggerated binge feeding response.

Similar to the chronic exposure trial, *Magel2*-null mice do demonstrate an initial hesitation to feed on the HF-diet. This is consistent with *Magel2*-null mice behaviour surrounding novel objects, and previous feeding experiments using novel food items. Over the ten days of limited exposure, *Magel2*-null mice consistently demonstrated significantly less food intake when compare to their WT littermates (Figure 3.37). *Magel2*-null mice have a decreased binge-feeding response. This is consistent with the reduced TH observed in the hypothalamus in response to the chronic exposure of HF-diet and the HPLC data that indicated a lack of response to the exposure of HF-diet in striatal dopamine signaling. *Magel2*-null mice have previously demonstrated reduced locomotive activity in response to the acute exposure of cocaine (Luck et al., in press, Figure 1.4), and *Magel2*-null mice also exhibit an abnormal response to novel foods (Bischof et al., 2007). This blunted response to the acute and chronic exposure of a natural reward (HF-diet) and the attenuated response to the acute exposure of cocaine suggest that *Magel2*-null mice have an impairment in not only the motivation to find a reward but also an impairment in experiencing the hedonia associated with the reward.

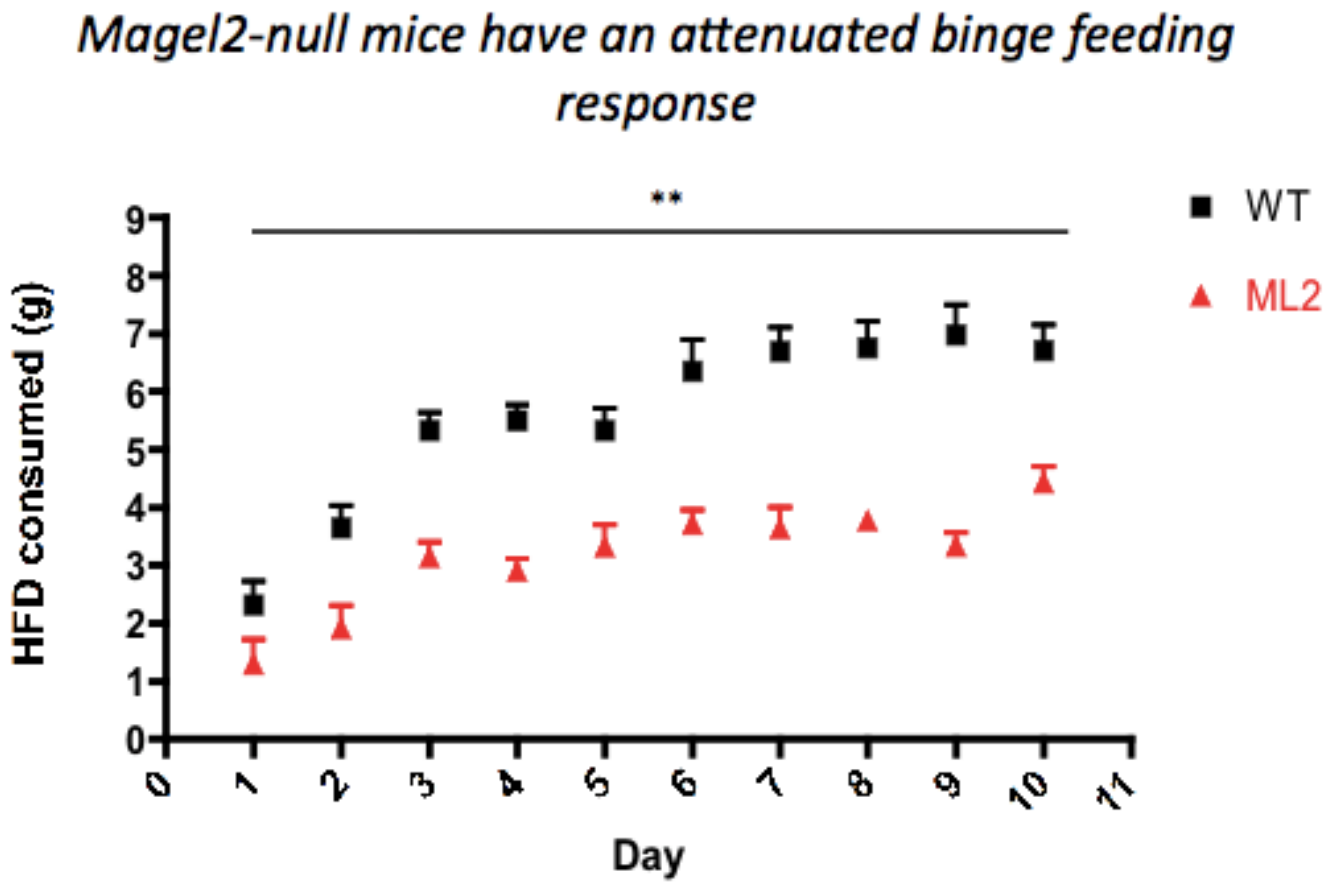

Figure 3.37. Limited exposure to high-fat diet

Magel2-null mice consistently eat less of the HF food compared to WT mice during the limited exposure experiment (WT n=6, ML n=6, p=0.001).

3.4. We were unable to quantify leptin receptor activation in the ventral tegmental area

Magel2-null mice have previously shown impaired leptin signaling in the hypothalamus (Mercer et al., 2013). Through western blot analysis and IHC we expect to see less phosphorylation of STAT3. STAT3 is phosphorylated following the activation of the LepR and can be used as a marker for a cellular response to extracellular leptin. We expect the same blunted response previously observed in the hypothalamus of adult mice to be present in the VTA, influencing the hedonic feeding system. We were unable to reproduce a quantifiable response to an IP injection of leptin. This was done through IHC staining for pSTAT3 and through immunoblotting for pSTAT3 (data not shown).

Chapter 4: Discussion

4.1. *Magel2*-null mice have a loss in baseline dopamine production within the hypothalamic nuclei

Magel2-null mice demonstrated fewer dopaminergic neurons in the A14 region of the hypothalamus. The dopaminergic neurons in the periventricular nucleus (A14) of the hypothalamus project to the supraoptic nucleus (SON) and the intermediate lobe of the pituitary (Goudreau et al., 1992; Vulpen et al., 1999). Dopaminergic input from the periventricular nucleus to the intermediate lobe of the pituitary functions to regulate the secretion of **α**-melanocyte-stimulating hormone (**α**-MSH) from pituitary melanotrophic cells (Goudreau et al., 1992). Alpha-MSH is an anorexigenic peptide involved in stimulating energy expenditure and limiting food intake (Mercer et al., 2013). Alpha-MSH is also produced in the arcuate nucleus of the hypothalamus by cells that express pro-opiomelanocortin (POMC) (Mercer et al., 2013). The loss of TH+ cells in the A14 nuclei could result in a decrease in **α**-MSH being secreted from the intermediate pituitary and a subsequent increase in food intake that could potentially contribute to the *Magel2*-null phenotype. The A14 region of the hypothalamus also sends projections to the supraoptic nucleus (SON) of the hypothalamus where the release of specific hormones, namely oxytocin and vasopressin, is regulated (Vulpen et al., 1999). The loss of dopaminergic cells in the periventricular nucleus (A14) could indirectly influence both the secretion of **α**-MSH and oxytocin through the SON and the intermediate lobe of the pituitary (Figure 4.1). The loss of dopaminergic output from the PeVN could lead to the loss of oxytocin and **α**-MSH, both anorexigenic molecules. This loss could be influencing the energy imbalance in the *Magel2*-null mice.

Magel2-null mice have an increased sensitivity to the effects of an MTII which is a melanocortin receptor agonist (Mercer et al., 2013). This hypersensitivity could be secondary to a reduction in dopaminergic stimulation from the periventricular nucleus, indicated by the loss of TH+ cells. This decrease in TH+ cells in the periventricular nucleus could also help explain the impaired hypothalamic oxytocin levels in individuals with PWS, and in other mouse models of PWS.

We did not observe a difference in the number of dopaminergic cells in the midbrain through IHC cell counting, or through TH western blot analysis of midbrain tissue. The distribution of dopaminergic neurons in the periventricular nucleus of the hypothalamus has been shown to be sexually dimorphic (Simerly et al., 1985). I used both sexes and this could have influenced the A14 and A15 quantification in the *Magel2*-null

mice. It would be useful in the future to repeat this quantification separating the mice into male and female groups. This would elucidate any sex-specific effects if the loss of *Magel2* on the number of dopaminergic neurons in the A14 region of the hypothalamus.

We did not observe a difference in baseline tyrosine hydroxylase in the VTA of *Magel2*-null mice. From the physiological phenotype and the attenuated response to cocaine observed in *Magel2*-null mice, we expected a loss of midbrain dopamine. The lack of an observed loss in midbrain dopamine suggests that the cause for the attenuated response to cocaine may be downstream of the VTA. This could, for example, be at the synaptic interface between the VTA and the post-synaptic cells. There was no observed difference in TH protein levels downstream of the VTA in the NAc. The lack of a difference in midbrain, and striatal tyrosine hydroxylase could be the lack of sensitivity of the methods used. It is possible that the potential difference in DA signaling is too small to be detected through IHC cell counting or TH immunoblot analysis. It is also possible that the tissue samples that were used for this quantification are too variable, or included too much tissue outside of the midbrain. It would be useful in the future to directly measure DA transmission and striatal DA binding.

A linescan analysis of TH-IHC was also used to address tyrosine hydroxylase reaching the target nuclei. ImageJ software that measures the average pixel intensity of a linescan was used to determine a possible difference in synaptic dopamine. There was a wide range of pixel intensities across each individual image and between images from the same sample. This made it difficult to measure any small changes in the level of TH at the synapse. To get a better indication of how synaptic dopamine is influenced by the loss of *Magel2,* this experiment may require a larger sample size or a more specific measure of synaptic dopamine and its post-synaptic receptors. In the western blot analysis of the midbrain target nuclei the amygdala does show a difference in the level of TH, but this is not observed with our quantification of TH in immunostained sagittal sections. It is possible that the tissue punch assay incorporated a larger portion of the amygdala allowing the small differences of each TH+ neuron to be additive and therefore detectable. It is also possible that the difference in TH staining was not detected due to the specific location within the amygdala that the images were taken. In order to get a better picture of how post-synaptic dopamine reception is affected by the loss of *Magel2*, I would suggest that future experiments focus on post-synaptic receptor availability or the response to specific dopamine receptor antagonists.

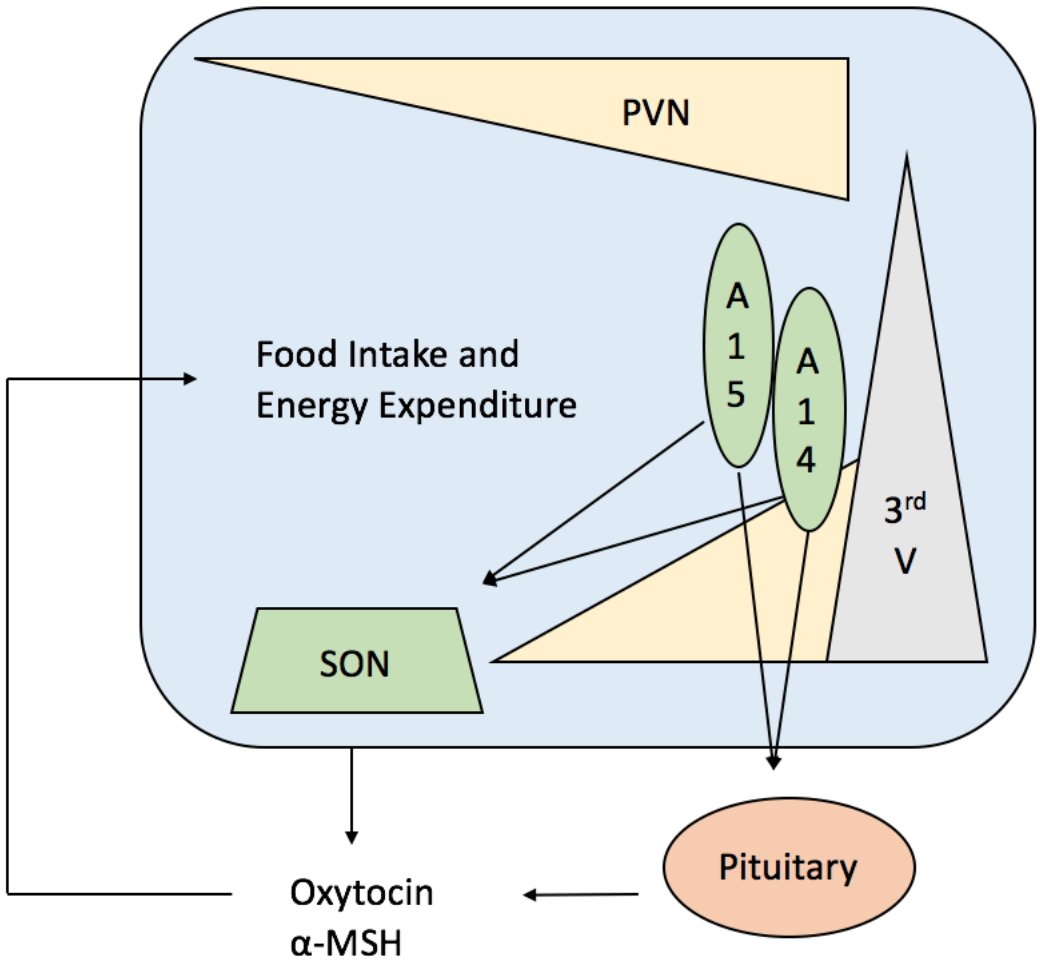

Figure 4.1. Periventricular dopamine projections

The A14 and A15 groups of dopaminergic cells in the periventricular nucleus project to the supraoptic nucleus (SON) of the hypothalamus and the intermediate lobe of the pituitary gland to regulate the release of oxytocin, vasopressin and **α**-MSH. The loss of *Magel2* is associated with fewer dopaminergic neurons in the A14 region of the hypothalamus. This could potentially have downstream effects on the supraoptic nucleus and subsequent production of oxytocin and **α**-MSH.

4.2. The loss of *Magel2* leads to an increase in amygdalar dopamine signalling

HPLC analysis has previously demonstrate a reduced level of hypothalamic dopamine metabolites in mice lacking *Magel2*. Despite this reduction in hypothalamic dopamine, there is an apparent increase in dopamine metabolites in the mesolimbic nuclei responsible for motivational behaviour. *Magel2*-null mice have increased TH levels in the amygdala under baseline conditions. In the amygdala, dopamine plays an important role in learning the value of a reward, fear conditioning, motivating an animal to obtain a reward, and place preference (Darvas et al., 2010). *Magel2*-null mice do show a loss of fear in response to the smell of bobcat urine and an abnormal behavioural response to novel environments suggesting a disruption in amygdalar dopamine signaling. The amygdala is also responsible for both motivational and emotionally driven behaviours, which have been shown to be disrupted in individuals with PWS.

The PWS behaviour profile and the exaggerated fMRI activation of the amygdala following a meal suggests a disruption in dopamine signaling to the amygdala of individuals with PWS (Holsen et al., 2006). An increased amygdalar dopamine signaling is also observed following the withdrawal of drugs of abuse in drug users. This increase in extracellular dopamine influences the intensity of the drug-seeking behaviour during the withdrawal (Tran-Nguyen et al., 1998). The increased TH observed in our *Magel2*-null mice could be causing an increased motivation to feed. This result supports the inappropriate activation of the amygdala in individuals with PWS, and suggests an increase in dopaminergic activity in the amygdala could be contributing to the increased drive to feed observed in individuals with PWS.

The amygdala communicates directly with the hypothalamus, the NTS, the VTA, and the striatum (Anderberg et al., 2014). Abnormal dopamine signaling in the amygdala could influence feeding through abnormal feedback to the VTA or by mediating the activity of the hypothalamus or NTS directly. The increase in dopamine metabolites is an interesting finding considering the global loss of dopamine previously observed in whole brain samples of *Magel2*-null mice (Mercer et al., 2009). There is a finite level of DA in the central nervous system. Much of this dopamine is produced by cells in the midbrain that project to various reward nuclei including the amygdala. The increased DA signaling in the amygdala must be met with a loss of dopamine elsewhere in the brain, to account for the total level of dopamine being lower in *Magel2*-null mice. Immunoblotting for tyrosine hydroxylase in the remaining reward nuclei failed to show a significant difference. This is unexpected and also inconsistent with our finding of less periventricular dopaminergic neurons (Figure 3.4). It is possible that despite the loss of TH+ cells in the

PeVN, there is a comparable amount of TH being expressed from these cells. It is also possible that the loss of TH from these PeVN cells is too small to be detected in the hypothalamic tissue punches used for TH immunoblotting. This could be because the tissue punches used for this experiment included a lot of non-specific tissue that could dilute the sample and decreased the sensitivity of the assay. For example, in the amygdala the volume of tissue determines our ability to detect a difference; in 1 mm diameter tissue punches, *Magel2*-null mice have significantly more TH, whereas in 2 mm tissue samples, the difference fails to reach significance. The hypothalamus is a small structure with several different nuclei expressing tyrosine hydroxylase. Using smaller, more specific punches could allow us to detect the same changes as observed in the IHC quantification of the hypothalamus, and would be a good next step in corroborating these results.

4.3. *Magel2*-null mice have an abnormal distribution of glial and neuronal cell proteins

Magel2-null mice have abnormal levels of neuronal and glial protein markers. *Magel2*-null mice have a higher inferred neuron to glia ratio in the hypothalamus. This could be indicative of several things. There could be a skewed ratio of cell types, a neuron specific cell death, or an inflammatory response.

With the chronic exposure to drugs of abuse there is an altered expression profile of neurofilament proteins, this enables morphological changes to the synapse. These neurofilament-mediated structural changes alter the synaptic response to a subsequent exposure. Changes in the expression of genes involved in the plasticity of the synapse have previously been observed in response to the chronic exposure to drugs of abuse. These changes in hypothalamic gene expression occur primarily in the lateral hypothalamic area (Ahmed et al., 2005).

The increase in the neuronal marker 2H3 in the hypothalamus of *Magel2*-null mice could be the result of the chronic loss in hedonia. The observed loss in response to both natural and chemical rewards (cocaine) could have induced compensatory synaptic adaptations to sensitize the animal to a subsequent reward. It is also possible that the altered synapse indicated by the increased level of neurofilament could have induced a loss of experienced reward. Future experiments should focus on assessing the synaptic integrity in *Magel2*-null mice at different developmental time-points. This would allow us to assess if the loss of response to reward is driving morphological changes in the synapse, or if it is these morphological changes that are driving the attenuated reward experienced. Another potential future experiment would be to assess directly the morphological structure of the synapse. This could be done using microscopy to directly visualize and measure synaptic changes including the thickness and density of dendritic spines and

branches. It would also be useful to assess the cell composition directly. A cell-type count would allow us to determine if the neuron:glia ratio is what is being disrupted in the Magel2-null mice. This would also allow us the assess the cellular structure of the hypothalamic nuclei. For example the cell size of both neurons and glia, or the complexity of the neurons. It is possible there is an exaggerated neuronal outgrowth which would cause an increase in neurofilament.

We found a significant decrease in the thickness of axons projecting from the midbrain to the frontal cortex in *Mage2*-null mice. The loss of axonal calibre observed in the *Magel2*-null mice could influence the amount of dopamine reaching the prefrontal cortex. The loss of dopamine signaling in the PFC has been implicated in cognitive impairment and in the development of psychiatric illness (Seamans & Yang, 2004). It is neurofilament proteins that regulate axonal calibre. In the future, it would be useful to analyze the calibre of dopaminergic axons projecting to the hypothalamus where the level of the neurofilament protein 2H3 differs in the *Magel2*-null mice.

4.4. *Magel2*-null mice have a global reduction in biogenic metabolites involved in the synthesis of both dopamine and serotonin

Magel2-null mice have reduced levels of serotonin and dopamine throughout the reward pathway. This effect is greatest in the hypothalamus. The hypothalamic reduction in dopamine, serotonin, and their respective metabolites is to be expected considering that the hypothalamus is not only the region of highest *Magel2* expression, but also that many of the baseline differences within the reward pathway are primarily found in the hypothalamus.

Abnormalities in the serotonin levels are consistent with previous results from our lab (Mercer et al., 2009). Serotonin abnormalities also observed in OCD, and autism suggesting that the abnormal levels of serotonin and its metabolites throughout the reward pathway might be influencing the animal's behaviour. The loss of Magel2 in humans with PWS might also be influencing the compulsive and ritualistic behaviours that are often observed. The trend towards higher levels of tryptophan in *Magel2*-null mice, and the lower levels of 5HIAA and trend towards lower 5HT, suggests that there is an impairment in the conversion of tryptophan to serotonin. Individuals with PWS show an increase in 5HIAA in CSF suggesting that the loss of serotonin could potentially be from an increased breakdown of serotonin into 5HIAA. Fluctuations in 5HIAA have been observed in humans in response to changes in season, and in humans suffering from autism. Changes in CSF levels of 5HIAA have been associated with certain

behaviours including impulsivity, aggression, and self-injurious behaviour (Samuelsson et al., 2006; Chatzittofis et al., 2013; Zajicek et al., 2000). It would be useful to measure the social behaviour of the *Magel2*-null mice to determine any serotonergic-mediated behavioural abnormalities that could link the *Magel2*-null mouse model to the human condition.

Measuring CSF levels of 5HIAA in the *Magel2*-null mice might be more useful when comparing our results to findings from humans with PWS. Our findings are consistent with previous work from the Wevrick lab demonstrating reduced levels of catecholamines and indolamines throughout the reward pathway of *Magel2*-null mice. Previously, Mercer et al., (2009) demonstrated that embryonic *Magel2*-null mice do not have significant differences in the concentrations of dopamine and serotonin metabolites. It has yet to be determined if this difference in biogenic amine concentration is the result of the transition from one state of disease to another, or if it is the reduction of these amines that drives the transition from a failing-to-thrive state to a state of increased food seeking behaviour. It would be useful to measure the levels of dopaminergic and serotonergic amines during a time more critical to this transition. HPLC data at an earlier developmental time point would also be useful to compare to the results in the adult mice. A better understanding of the transitional phenotype in a our mouse model could pinpoint a critical time-point for therapeutic intervention.

4.5. *Magel2*-null mice show a consistent loss of response throughout the dopamine reward pathway on a behavioural, physiological and a molecular level

Magel2-null mice have a loss in molecular response to the removal of a HF-diet. This is demonstrated in various reward nuclei through both western blot analysis and HPLC analysis. Immunoblots of tissue that had undergone the withdrawal of a HF-diet demonstrated several molecular changes including an increase in hypothalamic TH and reduced levels of amygdalar TH. This increase in tyrosine hydroxylase, indicative of an increase in dopamine production, is lost in the *Magel2*-null mice. HPLC also demonstrated an exaggerated increase in noradrenaline in response to the removal of the diet in the hypothalamus in *Magel2*-null mice. Both of these results show that within the hypothalamus there is an abnormal ratio of dopamine and noradrenaline with the loss of Magel2 driving the synthesis of NA in response to the withdrawal of a HF-diet. Hypothalamic NA has been shown to increase in response to the acute withdrawal of water, but not with food (Luttinger & Seiden, 1981). It is possible that the loss of Magel2 causes a similar response to the removal of a HF-diet.

Along with direct changes in dopamine production, there are several molecular changes that are blunted in the brains of *Magel2*-null mice. These include a blunted phosphorylation of AKT in response to the withdrawal of HF-diet and an exaggerated phosphorylation of CREB in the amygdala. In the amygdala, the phosphorylation of CREB drives the expression of several genes including NPY. In the amygdala specifically, the expression of NPY causes a reduced anxiety-like response in rats (G. Wand, 2005). This suggests that upon withdrawal of a HF-diet, *Magel2*-null mice exhibit an attenuated emotionally anxious response to the withdrawal. This is consistent with behavioural data demonstrating that upon the return of chow following a withdrawal, *Magel2*-null mice have an attenuated re-feeding response. In the future it would be useful to assess the anxiety behaviour and social behaviour of the *Magel2*-null mice following the withdrawal of a HF-diet. This would allow us to connect the increased phosphorylation of CREB in the amygdala to a profile of anxiety-induced behavioural responses.

4.6. The abnormal response to limited exposure of high-fat diet

Magel2-null mice show an impaired binge-feeding response to the limited exposure of a HF-diet. This attenuated binge-feeding response observed in the *Magel2*-null mice is consistent with the reduced response to re-feeding previously observed in our lab. This is also consistent with the previous finding that *Magel2*-null mice have an attenuated feeding response when given HF-diet chronically (Bischof et al., 2007). In the same study, Bischof et al. (2007) determined that the feeding patterns of *Magel2*-null mice were abnormal in relation to the light cycle. It is possible that revisiting this binge feeding experiment exposing the mice to the HF-diet closer to the initiation of the dark cycle or during the dark cycle could provide a different result when assessing binge feeding in a nocturnal model with circadian rhythm abnormalities.

It is possible that *Magel2*-null mice do have an increased drive to feed indicated by an increase in amygdalar dopamine signalling. This increased motivation could be paired with a diminished experienced reward demonstrated by a reduced level of striatal dopamine transmission. It may be useful to expose the animals to a palatable diet for a more limited time to separate the motivational behaviour from the experienced reward.

This binge-feeding paradigm assessed the addictive-like behaviour surrounding HF-diet. The behavioural and neurochemical responses to binging on high-fat differs from the addictive behaviour observed with the exposure of high-sugar diet (Avena et al., 2009). It may be useful to repeat this binge-

feeding experiment in our mouse model using a limited exposure to a high-sugar diet as opposed to high-fat. The *Magel2*-null mice have previously demonstrated abnormal feeding with the initial exposure, and chronic exposure to this HF-diet. The high-sugar limited exposure model is able to induce behavioural and neurochemical opioid-like withdrawal response, whereas the limited exposure of a HF-diet is unable to induce a withdrawal-like response (Avena et al., 2009). Sugar-bingeing would be a useful future experiment in investigating the dopamine-reward pathway of the *Magel2*-null mice.

4.7. Challenges and limitations

Throughout the characterization of the mesolimbic reward pathway in our mouse model of Prader-Willi Syndrome we ran into several challenges. In quantifying the dopamine producing cells of the reward nuclei the TH+ cells in the LHA were not included. This was due to the sparse distribution of this specific subset of cells that complicated the identification of the TH+ signal. The LHA plays an integral role for the communication between the midbrain and the central hypothalamus. The LHA contains receptors for leptin, orexins, and **α**-MSH, and communicates directly with the VTA and the arcuate nuclei to regulate food intake and energy expenditure (Saper & Lowell, 2004). The inability to quantify this subset of neurons is a limiting factor in our understanding of the effect that the loss of *Magel2* has on the dopamine reward pathway.

For the experiments involving the biochemical responses to different diets, I was unable to detect several of the molecular changes that have previously been reported in mice following the exposure and withdrawal of a HF diet. This could be due to the variability between samples. This variability is a consequence of the methods used and could be due to either dissection error, or variability in the order of euthanasia which could have initiated a stress response of its own. These responses include an accumulation of **Δ**FosB in response to the chronic exposure, the phosphorylation of CREB in some of the reward nuclei, and the failure to consistently demonstrate a molecular stress-response indicated by the phosphorylation of ERK and AKT. When reporting a lack of response this variability should be taken into consideration. The lack of response is an important finding, however, this should be viewed critically when interpreting these findings. The consistent loss of response observed within the reward pathway of *Magel2*-null mice does suggest an attenuated response to the changes in diet.

Some of the effects of HF-diet on the dopamine reward pathway can only be observed at various developmental time-points. The observed loss of response to both the administration of cocaine and the exposure to a HF-diet were both determined in adult mice. It may be useful to repeat the exposure to HF-

diet in mice at different developmental time-points. The transitional nature of the PWS/Magel2 phenotype suggests there could be a switch in the dopamine response of the *Magel2*-null animals. Performing this experiment on a younger animal could be a useful next step to understanding how and when the dopamine-reward pathway loses its sensitivity in the *Magel2*-null mouse. This could be useful when considering different age-specific interventions for individuals suffering from PWS and other forms of binge feeding.

Leptin signaling is important in regulating feeding. *Magel2*-null mice have shown impaired leptin signaling. The inability to quantify leptin signaling in the LHA and the VTA was a huge limitation in interpreting the results of this project.

4.8. Future Directions

An important next step for this research would be to understand the downstream effects of these findings. In the PVN we found reduced numbers of dopaminergic neurons. Understanding if the dopaminergic innervation of the intermediate pituitary is being affected by this loss would be valuable in determining the importance of this finding. Understanding how pituitary **α**-MSH is affected in our mouse model could also provide insight into how this system could be manipulated to repair feeding.

Due to the sparse distribution of the dopaminergic neurons in the lateral hypothalamic area (LHA), I was unable to determine the number of TH+ cells. The LHA plays a crucial role in the communication between the hedonic and the homeostatic feeding pathways. An important future direction of this research would be to determine the effect the loss of *Magel2* has on dopamine production and leptin signaling within the LHA.

Another limitation to this research was the inability to determine leptin signaling in the VTA of our *Magel2*-null mice. Leptin signaling in the VTA allows the peripheral energy state to directly influence dopamine signaling. The leptin signaling in the VTA is important for modifying the dopaminergic output of these TH+, LepR+ cells. Leptin signaling in the amygdala is also important for modifying feeding behaviour as these leptin sensitive cells are responsible for the conditioned taste aversion to certain foods.

Leptin signaling has been demonstrated to be impaired in the arcuate nuclei of *Magel2*-null mice (Mercer et al., 2013). Midbrain leptin signaling is responsible for communication between the homeostatic and hedonic feeding systems. The major dopamine output of leptin receptor-positive neurons in the VTA is the amygdala (Leshan et al., 2010). Abnormalities have been observed in the amygdala of both *Magel2*-null mice and individuals with PWS. Investigating the leptin signaling response in both the VTA and the amygdala would offer an explanation for the attenuated dopamine response observed in *Magel2*-null mice.

This information would give a clearer picture of the pathology of PWS, and would be essential for determining specific target sites for potential therapies.

4.9. Conclusions

In conclusion, we have identified several differences in the reward pathway of *Magel2*-null mice that have not previously been identified. The loss of *Magel2* reduces the animal's ability to respond to natural rewards. The lower baseline activity within the reward pathway demonstrated by the HPLC results, the decreased axonal calibre, and the attenuated response to the limited exposure HF-diet, all suggest that there is a loss of dopamine signaling in the *Magel2*-null mice. An increase in amygdalar TH, suggests that midbrain dopaminergic neurons could be preferentially signaling to the amygdala at the expense of dopamine signaling to other areas of the reward pathway.

Magel2-null mice show an increase in tyrosine hydroxylase in the amygdala indicated by the increase in TH protein. The increased TH and intact amygdalar dopamine profile, determined through HPLC analysis, demonstrates intact or even exaggerated dopamine signaling to the amygdala. This is consistent with the fMRI results in individuals with PWS indicating an increase in motivational behaviour surrounding food. This increased motive is paired with the loss of experienced reward indicated by: the loss of biochemical response to the exposure and withdrawal, the attenuated behavioural response to the limited exposure of HF-diet, and the loss of locomotive response to a cocaine injection. These results suggest an increase in the "wanting" state and a loss in the "liking" state, or the state of actually experiencing a reward. Our mice have also previously shown a decreased locomotive response to the exposure to cocaine indicative of an impaired striatal dopamine response (Luck et al., in press). This impaired response that is measured by locomotive activity could also influence the euphoria associated with a cocaine injection. If the dopamine reward response is affected to the same extent that locomotion was, this would support an increased baseline wanting followed by a blunted response to both receiving a reward and the removal of a reward. This indicates an increased drive to feed and the loss of a satiety response once the food item, or drug, has been consumed.

In 1985, Louilot et al. demonstrated that the dopaminergic signal reaching the nucleus accumbens is influenced by the strength of the dopamine signal sent to the amygdala. In behavioural terms, the experienced "wanting" influences the experienced "liking". There is an absolute level of dopamine and its metabolites in the neurons of the A10 nuclei at a given time. The VTA consists of a subset of neurons that

produce dopamine, the A10 nuclei, a portion of these dopamine-producing cells also express leptin receptors. The group of cells in the VTA expressing both tyrosine hydroxylase and leptin receptors, preferentially signals to the amygdala, over the nucleus accumbens (Louilot et al., 1985). Leptin modulates the activity of these neurons limiting the dopamine transmission to the motivation centre (AMY) in response to physiological satiety (Figure 4.2).

I propose that in our *Magel2*-null mouse model there is a loss of leptin sensing in these neurons causing an increased dopamine signaling to the amygdala at the expense of striatal DA-signaling. This switch from dopamine reaching the striatum to dopamine reaching the amygdala is explained by the loss of reward and the increase in motivation observed in both our mouse model and individuals with PWS. A leptin-insensitivity-induced switch from striatal to amygdalar signaling could contribute to the increased level of TH in the amygdala, and could also help explain the abnormal dopamine responses in the striatum following the exposure and the withdrawal of HF-diet. The diversion of TH from the nucleus accumbens to the amygdala would also help explain the abnormal fear conditioning observed in the *Magel2*-null mice.

I was unable to quantify VTA neurons expressing both TH and activated leptin receptors indicated by the phosphorylation of the downstream protein STAT3. Our lab has previously shown the loss of response to leptin in the arcuate nucleus of the hypothalamus of adult *Magel2*-null mice. Arcuate leptin signaling was also shown to be intact in pre-weaned *Magel2*-null mice indicating that this insensitivity develops over time (Pravdivyi, 2015). This suggests that it is possible that midbrain leptin signaling is also impaired during development.

A gradual switch from dopamine reaching the nucleus accumbens to dopamine being diverted to the amygdala would help explain why the learned rewarding property of food in PWS is intact. For example, with an initial exposure, individuals learned the reward value of a certain item. The subsequent loss of leptin signaling and the inappropriate rerouting of dopamine signaling to the amygdala would cause not only the loss of reward experience, but also an increased incentive value to obtain subsequent reward. This could potentially lead to the hyperphagic phenotype observed in PWS.

A progressive loss of midbrain-leptin receptor activation would also explain why drug/HF-diet-naïve adult *Magel2*-null mice have a blunted response to HF-diet and cocaine. An interesting next-step would be to first quantify the leptin receptor TH+ cells in the adult midbrain and amygdala, and to reassess the physiological and biochemical responses to exposure, to determine if/when this response is lost throughout development. This could be done using *Magel2*-null mice at an earlier developmental stage, and repeating the exposure in adults who have had an initial exposure to the reward early in life and are not naïve to the

reward. Due to the sparse distribution of dopaminergic neurons in the LHA, I was unable to quantify the number of dopamine-producing cells. Quantifying both the number of TH+ cells and the number of LepR+ cells that response to leptin would be useful in understanding the extent of the leptin receptor desensitization that occurs throughout the development of the *Magel2*-null mouse.

The level of tyrosine hydroxylase staining in the amygdala and the striatum did not show any difference in the *Magel2*-null mice. This was done under baseline conditions. In the future it may be useful to quantify the relative dopamine reaching each nuclei as opposed to an absolute TH signal. This would allow us to determine if the midbrain neurons of the *Magel2*-null mice are preferentially signaling to one nuclei.

In conclusion, the loss of Magel2 does influence feeding behaviour on both the molecular and the behavioural level. The loss of Magel2 also influences dopaminergic tone throughout the nuclei of the reward pathway contributing to the PWS-like phenotype observed in *Magel2*-null mice.

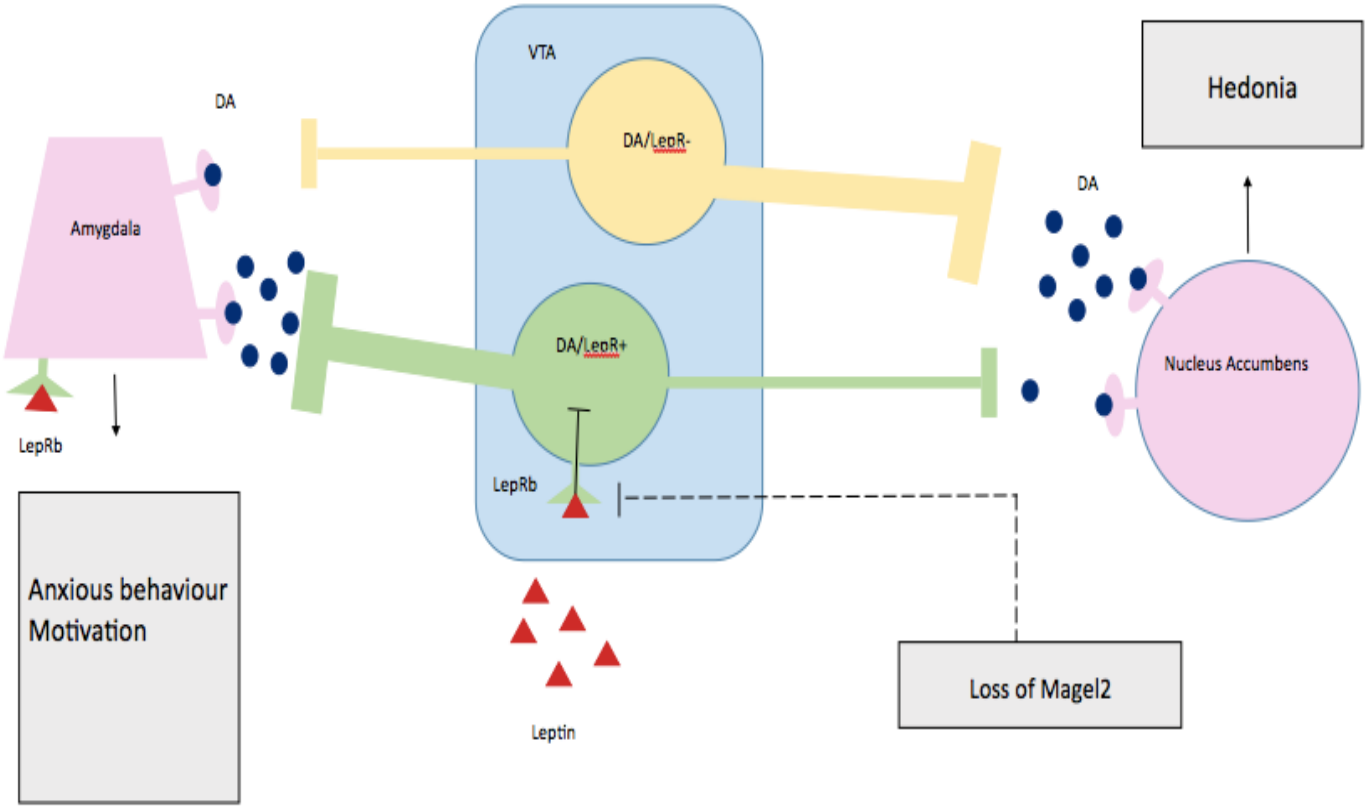

Figure 4.2. Proposed action of Magel2 on the dopamine transmission of midbrain dopamine neurons

Leptin receptors in the VTA are localized on DA neurons that preferentially signal to the amygdala. Activation of the leptin receptor inhibits this dopaminergic transmission. Magel2's influence on the leptin receptor could have downstream effects on the balance between striatal and amygdalar DA signaling

References

Ahmed, S. H., Lutjens, R., van der Stap, L. D., Lekic, D., Romano-Spica, V., Morales, M., et al. (2005). Gene expression evidence for remodelling of lateral hypothalamic circuitry in cocaine addiction. (Vol. 102 (32), pp. 11533-11538). *Proceedings of the National Academy of Science of the United States of America.*

Akefeldt, A., Ekman, R., Gillberg, C., & Mansson, J. E. (1998). Cerebrospinal fluid monoamines in Prader-Willi syndrome. (Vol. 12, pp. 1321-1328). *Biological Psychiatry.*

Alcaro, A., Huber, R., & Panksepp, J. (2007). Behavioural functions of the mesolimbic dopaminergic system: an affective neuroethological perspective. (Vol. 56 (2), pp. 283-231). *Brain Res Rev*.

Avena, N. M., & Bocarsly, M. E. (2012). Dysregulation of brain reward systems in eating disorders: Neurochemical information from animal models of binge eating, bulimia nervosa, and anorexia nervosa. (Vol. 63, pp. 87-96). *Neuropharmacology*.

Avena, N. M., Rada, P., & Hoebel, B. G. (2009). Sugar and Fat Bingeing have notable differences in addictive-like behaviour. (Vol. 139 (3), pp. 623-628). *The Journal of Nutrition*.

Baladi, M. G., Horton, R. E., Owens, W. A., Daws, L. C., & France, C. P. (2015). Eating high fat chow decreases dopamine clearance in adolescent and adult male rats but selectively enhances the locomotor stimulating effects of cocaine in adolescents. (Vol. 18 (7), pp. 1-11). International Journal of *Neuropsychopharmacology.*

Baroncini, M., Jissendi, P., Balland, E., Besson, P., Pruvo, J. P., Francke, J. P., et al. (2012). MRI atlas of the human hypothalamus. (Vol. 59 (1), pp. 168-180). *NeuroImage.*

Barrot, M., Olivier, J. D. A., Perotti, L. I., DiLeone, R. J., Berton, O., Eisch, A. J., et al. (2002). CREB activity in the nucleus accumbens shell controls gating of behaviour responses to emotional stimuli (Vol. 99 (17), pp. 11435-11440). *PNAS.*

Barsh, G. S., Farooqi, S., & O'Rahilly, S. (2000). Genetics of body-weight regulation. (Vol. 404, pp. 644-651). *Nature.*

Beaulieu, J. M., & Gainetdinov, R. R. (2011). The physiology, signaling and pharmacology of dopamine receptors. (Vol. 63, pp. 182-217). *Pharmacological Reviews.*

Beitner-Johnson, D., Guitart, X., & Nestler, E. J. (1992). Neurofilament proteins and the mesolimbic dopamine system: common regulation by chronic morphine and chronic cocaine in the rat ventral tegmental area. (Vol. 12 (6), pp. 2165-2176). *The Journal of Neuroscience.*

Bischof, J. M., Stewart, C. L., & Wevrick, R. (2007). Inactivation of the mouse Magel2 gene results in growth abnormalities similar to Prader-Willi syndrome. (Vol. 16, pp. 2713-2719). *Human Molecular Genetics.*

Bittel, D. C., Kibiryeva, N., Dasouki, M., Knoll, J. H. M., & Butler, M. G. (2006). A 9-year-old male with a duplication of chromosome 3p25.3p26.2: Clinical report and gene expression analysis. (Vol. 140A (6), pp. 573-579). *American Journal of Medical Genetics.*

Boccaccio, I., Glatt-Deeley, H., Watrin, F., Roeckel, N., Lalande, M., & Muscatelli, F. (1999). The human MAGEL2 gene and its mouse homologue are paternally expressed and mapped to the Prader-Willi region. (Vol. 8 (13), pp. 497-505). *Human Molecular Genetics.*

Cadoudal, T., Buleon, M., Sengenes, C., Diene, G., Desneulin, F., Molinas, C., et al. (2014). Impairment of adipose tissue in Prader-Willi Syndrome rescued by growth hormone treatment. (Vol. 38, pp. 1234-1240). *International Journal of Obesity.*

Camerino, C. (2009). Oxytocin thinks globally and acts locally: The oxytocinergic regulation of bone mass. (Vol. 6, pp. 295-300). *IBMS BoneKEy.*

Cao, J. L., He, J. H., Ding, H. L., & Zeng, Y. M. (2005). Activation of the spinal ERK signaling pathway contributes naloxone-precipitated withdrawal in morphine-dependent rats. (Vol. 118 (3), pp. 336-349). *Pain.*

Cardinal, R. N., Parkinson, J. A., Hall, J., & Everitt, J. (2002). Emotion and motivation: the role of the amygdala, ventral striatum, and prefrontal cortex. (Vol. 26 (3), pp. 321-352). *Neuroscience & Behavioural Reviews.*

Cassidy, S. B. (1997). Prader-Willi Syndrome. (Vol. 34, pp 917-923). *Journal of Medical Genetics.*

Cassidy, S. B., Mckillop, J. A., & Morgan, W. J. (1990). Sleep disorders in Prader-Willi syndrome. (Vol. 4(1). *Dysmorphology and clinical genetics.*

Cassidy, S. B., Schwartz, S., Miller, J. L., & Driscoll, D. J. (2012). Prader-Willi Syndrome. (Vol. 14, pp. 10-26). *Genetics in Medicine.*

Chamberlain, R. S., & Herman, B. H. (1990). A novel biochemical model linking dysfunctions in brain melatonin, proopiomelanocortin peptides, and serotonin in autism. (Vol. 28 (9), pp. 773-193). *Biological Psychiatry.*

Chatzittofis, A., Nordstrom, P., Hellstrom, C., Arver, S., Asberg, M., & Jokinen, J. (2013). CSF 5-HIAA cortisol and DHEAS levels in suicide attempters. (Vol. 23 (10), pp. 1280-1287). *European Neuropsychopharmacology.*

Chen, K. Y., Muniyappa, R., Abel, B. S., Mullins, K. P., Staker, P., Brychta, R. J., et al. (2015). RM-493, a melanocortin-4 receptor (MC4R) agonist, increases resting energy expenditure in obese individuals. (Vol. 100 (4), pp. 1639-1645). *J Clin Endocrinol Metab.*

Clarke, D. J., Boer, H., Whittington, J., Holland, A., Butler, J., & Webb, T. (2002). Prader-Willi Syndrome, compulsive and ritualistic behaviours: the first population based survey. (Vol. 180 (4), pp. 358-362). *The British Journal of Psychiatry.*

D'Ardenne, K., Ashel, N., Luka, J., Lenartowicz, A., Nystrom, L. E.,, & Cohen, J. D. (2012). Role of prefrontal cortex and the midbrain dopamine system in working memory updating. (Vol. 109 (49), pp. 19900-19909). *Proceedings of the National Academy of Sciences.*

Darvas, M., Fadok, J. P., & Palmiter, R. D. (2010). Requirement of dopamine signaling in the amygdala and striatum for learning and maintenance of a conditioned avoidance response. (Vol. 18, pp. 136-143). *Learning Memory.*

Davis, J. F., Tracy, A. L., Schurdak, J. D., Tschop, M. H., Lipton, J. W., Clegg, D. J., et al. (2008). Exposure to elevated levels of dietary fat attenuates psychostimulant reward and mesolimbic dopamine turnover in the rat. (Vol. 122 (6), pp. 1257-1263). *Behavioural Neuroscience.*

Deblon, N., Veyrat-Durebex, C., Bourgoin, L., Caillon, A., Bussier, A. L., Petrosino, S., et al. (2011). Mechanisms of the anti-obesity effects of oxytocin in diet-induced obese rats. (Vol. 6 (9), e25565. *PLoS ONE.*

DeMarcantonio, M. A., Darrow, D. H., Gyuricsko, E., & Derkay, C. S. (2010). Obstructive sleep disorders in Prader-Willi syndrome: The role of surgery and growth hormone. (Vol. 74, pp. 1270-1272). *International Journal of Pediatric Otorhinolaryngology.*

Didden, R., & Sigafoos, J. (2001). A review of the nature and treatment of sleep disorders in individuals with developmental disabilities. (Vol. 22 (4), pp. 255-272). *Research in Developmental Disabilities.*

DiLeone, R., Taylor, J. R., & Picciotto, M. R. (2012). The drive to eat: Comparisons and distinctions between mechanisms of food reward and drug addiction. (Vol. 15, pp. 1330-1335). *Nature Neuroscience.*

Dolen, G., Darvishzadeh, A., Huang, K. W., & Malenka, R. C. (2013). Social reward requires coordinated activity of nucleus accumbent oxytocin and serotonin. (Vol. 501, pp. 179-184). *Nature.*

Dombret, C., Nguyen, T., Michaud, J. L., Hardin-Pouzet, H., Bertrand, M. J., & De Backer, O. (2012). Loss of Maged1 results in obesity, deficits of social interaction, impaired sexual behaviour and severe alteration of mature oxytocin production in the hypothalamus. (Vol. 21, pp. 4703-4717). *Human Molecular Genetics.*

Dong Kyu Jin. (2011). Systematic review of the clinical and genetic aspects of Prader-Willi syndrome. (Vol. 54, pp. 55-63). *Korean Journal of Pediatrics.*

Doyle, J. M., Gao, J., Yang, M., & Potts, P. R. (2010). MAGE-RING protein complexes comprise a family of E3 ubiquitin ligases. (Vol. 39 (6), pp. 963-974). *Molecular Cell.*

Dubois, L., Kyvik, K. O., Girard, M., Tatone-Tokuda, F., Perusse, D., Hjelmborg, J., et al. (2012). Genetic and Environmental Contributions to Weight, Height, and BMI from Birth to 19 Years of Age: An International Study of Over 12,000 Twin Pairs. (Vol. 7 (2), e30153). *PLoS ONE.*

Dykens, E. M. (2000). Contaminates and unusual food combinations: What do people with Prader-Willi Syndrome choose? (Vol. 38, pp. 163-171). *Mental Retardation.*

Dykens, E. M., Lee, E., & Roof, E. (2011). Prader-Willi syndrome and autism spectrum disorders: an evolving story. (Vol. 3, pp. 225-237). *Journal of Neurodevelopmental Disorders.*

El-Merahbi, R., Loffler, M., Mayer, A., & Sumara, G. (2015). The roles of peripheral serotonin in metabolic homeostasis. (Vol. 589, pp. 1728-1734). *FEBS Letters.*

Elsworth, J. D., & Roth, R. H. (1997). Dopamine synthesis, uptake, metabolism, and receptors: Relevance to gene therapy of parkinson's disease. (Vol. 144, pp. 4-9). *Experimental Neurology.*

Farooqi, I. S., & O'Rahilly, S. (2005). Monogenic obesity in humans. (Vol. 56, pp. 443-458). *Annu Rev Med.*

Farooqi, S., & O'Rahilly S. (2013). Genetics of obesity in humans. (Vol. 27 (7), pp. 710-718). *Endocrine Reviews.*

Figlewicz, D. P., Evans, S. B., Murphy, J., Hoen, M., & Baskin, D. G. (2003). Expression of receptors for insulin and leptin in the ventral tegmental area/substantia nigra (VTA/SN) of the rat. (Vol. 964, pp. 107-115). *Brain Research.*

Flier, J. S. (2004). Obesity Wars: Molecular progress confronts an expanding epidemic. (Vol. 116 (2), pp. 337-550). *Cell.*

Fountain, M. D., Schaaf, C. P. (2016). Prader-Willi Syndrome and Schaaf-Yang Syndrome: Neurodevelopmental diseases intersecting at the MAGEL2 gene. (Vol. 4 (1), pp. 2). *Diseases.*

Frank, G. K. W., Reynolds, J. R., Shott, M. E., Jappe, L., Yang, T. T., Tregellas, J. R., et al. (2012). Anorexia Nervosa and obesity are associated with opposite brain reward response. (Vol. 37, pp. 2031-2046). *Neuropsychopharmacology.*

Franklin, K., & Paxinos, G. (2008). The mouse brain in stereotaxic coordinates, compact, 3rd edition. (pp. 1-256). *Academic Press.*

Fried, I., Wilson, C. L., Morrow, J. W., Cameron, K. A., Behnke, E. D., Ackerson, L. C., et al. (2001). Increased dopamine release in the human amygdala during performance of cognitive tasks. (Vol. 4, pp. 201-206). *Nature Neuroscience.*

Fulton, S., Pissios, P., Manchon, R. P., Stiles, L., Frank, L., Pothos, E. N., et al. (2006). Leptin regulation of the mesolimbic dopamine pathway. (Vol. 51 (6), pp. 811-822). *Neuron.*

Funahashi, H., Yada, T., Suzuki, R., & Shioda, S. (2003). Distribution, function, and properties of leptin receptors in the brain. (Vol. 224, pp. 1-27). *International Review of Cytology.*

Gayrard, V., Thiery, J. C., & Tillet, Y. (1995). Efferent projections from the retrochiasmatic area to the median eminence and to the pars nervosa of the hypophysis with special reference to the A15 dopaminergic cell group in the sheep. (Vol. 281, pp. 561-567). *Cell & Tissue Research.*

Gearhardt, A. N., Yokum, S., Orr, P. T., Stice, E., Corbin, W. R., & Brownell, K. D. (2011.). Neural correlates of food addiction. (Vol. 68 (8), pp. 808-816). JAMA *Psychiatry.*

Georgescu, D., Zachariou, V., Barrot, M., Mieda, M., Willie, J. T., Eisch, A. J., et al. (2003). Involvement of the lateral hypothalamic peptide orexin in morphine dependance and withdrawal. (Vol. 23 (8), pp. 3106-3111). *The Journal of Neuroscience.*

Gilessen-Kaesbach, G., Robinson, W., Lohmann, D., Kaya-Westerloh, S., Pssarge, E., & Horstemke, B. (1995). Genotype-phenotype correlation in a series of 167 deletion and non-deletion patients with Prader-Willi syndrome. (Vol. 96, pp. 638-643). *Human Genetics.*

Goudreau, J. L., Lindley, S. E., Lookingland, K. J., & Moore, K. E. (1992). Evidence the hypothalamic periventricular dopamine neurons innervate the intermediate lobe of the rat pituitary. (Vol. 56, pp. 100-105). *Neuroendocrinology.*

Greggi, T., Martikos, K., Lolli, F., Bakaloudis, G., Di Silvestre, M., Cioni, A., et al. (2010). Treatment of scoliosis in patients affected with Prader-Willi syndrome using various techniques. (Vol. 5, pp. 1-11). *Scoliosis.*

Halpern, C. H., Tekiwal, A., Santollo, J., Keating, J. G., Wolf, J. A., Daniels, D., Bale, T. L. (2013). Amelioration of binge eating by nucleus accumbens shell deep brain stimulation in mice involves D2 receptor modulation. (Vol. 33.17, pp 7122-7129). *The Journal of Neuroscience.*

Hannibal, J. (2002). Neurotransmitters of the retino-hypothalamic tract. (Vol. 309 (1), pp. 73-88). *Cell and Tissue Research.*

Helbing-Zwanenburg, B., Kamphuisen, H. A. C., & Mourtazaev, M. S. (1993). The origin of excessive daytime sleepiness in the Prader-Willi syndrome. (Vol. 37, pp. 533-541). *Journal of Intellectual Disability Research.*

Ho, A. Y., & Dimitropoulos, A. (2010). Clinical management of behavioural characteristics of Prader-Willi syndrome. (Vol. 6, pp. 107-118). *Neuropsychiatric Disease and Treatment.*

Holsen, L. M., Savage, C. R., Martin, L. E., Bruce, A. S., Lepping, R. J., Ko, E., et al. (2012). Importance of reward and prefrontal circuitry in hunger and satiety: Prader-Willi Syndrome vs. simple obesity. (Vol. 36, pp. 638-647). *International journal of obesity.*

Holsen, L. M., Zarcone, J. R., Brooks, W. M., Butler, M. G., Thompson, T. I., Ahluwalia, J. S., et al. (2006). Neural mechanisms underlying hyperphagia in Prader-Willi syndrome. (Vol. 14, pp. 1028-1037). *Obesity.*

Howland, R. H. (2015). Aspergillus, angiogenesis, and obesity: The story behind Beloranib. (Vol. 53 (3), pp. 13-16). *Psychopharmacology.*

Jentsch, J. D., Olausson, P., Nestler, E. J., & Taylor, J. R. (2002). Stimulation of protein kinase a activity in the rat amygdala enhances reward-related learning. (Vol. 52 (2), pp. 111-118): *Biological Psychiatry.*

Jin, D. K. (2011). Systematic review of the clinical and genetic aspects of Prader-Willi Syndrome. (Vol. 54 (2), pp. 55-63). *Korean Journal of Pediatrics.*

Kenny, P., J. (2011). Common cellular and molecular mechanisms in obesity and drug addiction. (Vol. 12, pp. 638-651). *Nature Reviews Neuroscience.*

Kim, E. M., O'Hare, E., Grace, M. K., Welch, C. C., Billington, C. J., & Levine, A. S. (2000). ARC POMC mRNA and PVN alpha-MSH are lower in obese relative to lean zucker rats. (Vol. 862, pp. 11-16). *Brain Research.*

Koenig, K., Klin, A., & Schultz, R. (2004). Deficits in social attribution ability in Prader-Willi Syndrome. (Vol. 34 (5), pp. 573-582). *Journal of Autism and Developmental Disorders.*

Kozlov, S. V., Bogenpohl, J. W., Howell, M. P., Wevrick, R., Panda, S., Hogenesch, J. B., et al. (2007). The imprinted gene Magel2 regulates normal circadian output. (Vol. 39, pp. 1266-1272). *Nature Genetics.*

Krishnan, V., Han M. H., Mazei-Robison, M., Iniguez, S. D., Ables, J. L., Vialou, V., et al. (2008). AKT signaling within the ventral tegmental area regulates cellular and behavioural responses to stressful stimuli. (Vol. 64 (8), pp. 691-700). *Biological Psychiatry.*

Kweh, F. A., Miller, J. L., Sulsona, C. R., Wasserfall, C., Atkinson, M., Shuster, J. J., et al. (2015). Hyperghrelinemia in Prader-Willi syndrome begins in infancy long before the onset of hyperphagia (Vol. 167A, pp. 69-79). *American Journal of Medical Genetics Part A.*

Lam, D. D., Garfield, A. S., Marston, O. J., Shaw, J., & Heisler, L. K. (2010). Brain serotonin system in the coordination of food intake and body weight. (Vol. 97, pp. 84-91). *Pharmacology, Biochemistry and Behaviour.*

Lau, D. C. W., Douketis, J. D., Morrison, K. M., Hramiak, I. M., Sharma, A. M., & Ur, E. (2007). 2006 Canadian clinical practice guidelines on the management and prevention of obesity in adults and children [summary]. (Vol. 176, pp. S1-S13). *CMAJ.*

Lee, S., Kozlov, S., Hernandez, L., Chamberlain, S. J., Brannan, C. I., Stewart, C. L., et al. (2000). Expression and imprinting of MAGEL2 suggest a role in Prader-willi syndrome and the homologous murine imprinting phenotype. (Vol. 12, pp. 1813-1819). *Human Molecular Genetics.*

Leinninger, G. M. (2011). Lateral thinking about leptin: A review of leptin action via the lateral hypothalamus. (Vol. 104, pp. 572-581). *Physiology & Behaviour.*

Leinninger, G. M., Jo, Y. H., Leshan, R. L., Louis, G. W., Yang, H., Berrera, J. G., et al. (2009). Leptin acts via leptin receptor-expressing lateral hypothalamic neurons to modulate the mesolimbic dopamine system and suppress feeding. (Vol. 10, pp. 89-98). *Cell Metabolism.*

Leshan, R. L., Opland, D. M., Louis, G. W., Leinninger, G. M., Patterson, C. M., Rhodes, C. J., et al. (2010). Ventral tegmental area leptin receptor neurons specifically project to and regulate cocaine- and amphetamine-regulated transcript neurons of the extended central amygdala. (Vol. 30 (16), pp. 5713-5723). *The Journal of Neuroscience.*

Lobstein, T., Baur, L., & Uauy, R. (2004). Obesity in children and young people: a crisis in public health. (Vol. 5, pp. 4-85). *Obesity Reviews.*

Louilot, A., Simon, H., Taghzouti, K., & Le Moal, M. (1985). Modulation of dopaminergic activity in the nucleus accumbens following facilitation or blockade of the dopaminergic transmission in the amygdala: a study by in vivo differential pulse voltammetry. (Vol. 346 (1), pp. 141-145). *Brain Research.*

Lu, L., Koya, E., Zhai, H., Hope, B. T., & Shaham, Y. (2006). Role of ERK in cocaine addiction. (Vol. 29 (12), pp. 695-703). *Trends in Neuroscience.*

Lukoshe, A., White, T., Schmidt, M. N., van der Lugt, A., & Kokken-Koelega, C. (2013). Divergent structural brain abnormalities between different genetic subtypes of children with Prader-Willi syndrome. (Vol. 5, pp. 1-11). *Journal of Neurodevelopmental Disorders.*

Luttinger, D., Seiden, L. S. (1981). Increase hypothalamic norepinephrine metabolism after water deprivation in the rat. (Vol. 208, pp. 147-165). *Brain Research.*

Maejima, Y., Iwasaki, Y., Yamahara, Y., Kodaira, M., Sedbazar, U., & Yada, T. (2011). Peripheral oxytocin treatment ameliorates obesity by reducing food intake and visceral fat mass. (Vol. 3 (12), pp. 1169-1177). *Aging (Albany NY).*

Maglieri, K. A., DeLeon, I. G., Rodriguez-Catter, V., & Sevin, B. M. (2000). Treatment of covert food stealing in an individual with Prader-Willi Syndrome. (Vol. 33, pp. 615-618). *Journal of Applied Behavioural Analysis.*

Mercer, R. E., Kwolek, E. M., Bischof, J. M., van Eede, M., Henkelman, R. M., & Wevrick, R. (2009). Regionally reduced brain volume, altered serotonin neurochemistry, and abnormal behaviour in mice Null for the Circadian Rhythm Output Gene Magel2. (Vol. 150 (8), pp. 1085-1099). *American Journal of Medical Genetics Part B.*

Mercer, R. E., Michaelson, S. D., Chee, M. J. S., Atallah, T. A., & Wevrick, R. (2013). Magel2 is required for leptin-mediated depolarization of POMC neurons in the hypothalamic arcuate nucleus in mice. (Vol. 9 (1), pp. 1-10). *PLOS Genetics.*

Miller, J. (2015). Dr. Miller phase 2 oxytocin trial webinar. *PWSA(USA).*

Miller, J. L., Lynn, C. H., Discoll, D. C., Goldstone, A. P., Gold, J. A., Kimonis, V., et al. (2012). Nutritional phases in Prader-Willi syndrome. (Vol. 155A, pp. 1040-1049). *American Journal of Medical Genetics.*

Miller, J. L., Strong, T. V., & Heinemann, J. (2015). Medication trials for hyperphagia and food-related behaviours in Prader-Willi syndrome. (Vol. 3(2), pp. 78-85). *Disease.*

Mimee, A., Kuksis, M., & Ferguson, A. V. (2014). Alpha-MSH exerts direct postsynaptic excitatory effects on the NTS neurons and enhances GABAergic signaling in the NTS. (Vol. 262, pp. 70-82). *Neuroscience.*

Moran, T. H. (2000). Cholecystokinin and satiety: current perspectives. (Vol. 16, pp. 858-865). *Nutrition.*

Muscatelli, F., Abrous, D. N., Massacrier, M., Boccaccio, I., Le Moal, M., Cau, P., et al. (2000). Disruption of the mouse Necdin gene results in hypothalamic and behavioural alterations reminiscent of the human Prader-Willi syndrome. (Vol. 9, pp. 3101-3110). *Human Molecular Genetics.*

Neel, J. V. (1999). The "Thrifty Genotype" in 1998. (Vol. 57, pp. S2-9). *Nutrition reviews.*

Nestler, E. J. (2001). Molecular basis of long-term plasticity underlying addiction. (Vol. 2, pp. 119-128). *Nature Reviews Neuroscience.*

Nestler, E. J. (2004). Molecular mechanisms of drug addiction. (Vol. 47, pp. 24-32). *Neuropharmacology.*

Nestler, E. J. (2005). Is there a common molecular pathway for addiction? (Vol. 8 (11), pp. 1445-1449). *Nature Neuroscience.*

Nestler, E. J., Barrot, M., DiLeone R. J., Eisch, A. J., Gold, S. J., & Monteggia, L. M. (2002). Neurobiology of depression. (Vol. 34 (1), pp. 13-25). *Neuron.*

Nestler, E. J., & Carlezon, W. A. (2006). The mesolimbic dopamine reward circuit in depression. (Vol. 59 (12), pp. 1151-1159). *Biological Psychiatry.*

Nogueiras, R., & Seeley, R. J. (2012). Our evolving understanding of the interaction between leptin and dopamine system to regulate ingestive behaviours. (Vol. 1, pp. 8-9). *Molecular Metabolism.*

O'Rahilly, S., & Farooqi, I. S. (2006). Genetics of obesity. (Vol. 361, pp. 1095-1105). *Phil. Trans. R. Soc. B.*

Olson, V. G., Zebetian, C. P., Bolanos, S., Edwards, S., Barrot, M., Eisch, A. J., et al. (2005). Regulation of drug reward by cAMP Response Element-Binding Protein: Evidence for two functionally distinct subregions of the ventral tegmental area. (Vol. 24 (23), pp. 5553-5562). *The Journal of Neuroscience.*

Opland, D. M., Leinninger, G. M., & Myers, M. G. J. (2010). Modulation of the mesolimbic dopamine system by leptin. (Vol. 1350, pp. 65-70). *Brain Research.*

Ott, V., Finlayson, G., Lehnert, H., Heitmann, B., Heinrichs, M., Born, J., et al. (2013). Oxytocin reduces reward-driven food intake in humans. (Vol. 62 (10), pp. 3418-3425). *Diabetes.*

Parent, M., Bush, D., Rauw, G., Master, S., Vaccarino, F., Baker, G. (2001). Analysis of amino acids and catecholamines, 5-hydroxytryptamine and their metabolites in brain areas in the rat using in vivo microdialysis.(Vol. 23 (1), pp. 11-20). *Methods.*

Pravdivyi, I., Ballanyi, Colmers, W. F., Wevrick, R. (2015). Progressive postnatal decline in leptin sensitivity of arcuate hypothalamic neurons in the Magel2-null mouse model of Prader-Willi Syndrome. (Vol. 24(15), pp. 4276-4283). *Human molecular genetics.*

Ribeiro, A. C., Sawa, E., LeSauter, I. C., LeSauter, J.,, Silver, R., & Pfaff, D. W. (2007). Two forces for arousal: Pitting hunger versus circadian influences and identifying neutrons responsible for changes in behavioural arousal. (Vol. 104 (50), pp. 20078-20083). *PNAS.*

Russo, S. J., Dietz, D. M., Dumitriu, D., Morrison, J. H., Malenka, R. C., & Nester, E. J. (2010). The addicted synapse: mechanisms of synaptic and structural plasticity in nucleus accumbens. (Vol. 33 (6), pp. 267-276). *Trends in Neuroscience.*

Sabatier, N., Leng, G., & Menzies, J. (2013). Oxytocin, feeding, and satiety. (Vol. 4, pp. 1-10). *Frontiers in Endocrinology.*

Samuelsson, M., Jokinen, J., Nordstrom, A. L., & Nordstrom, P. (2005). CSF 5-HIAA, suicide intent and hopelessness in the prediction of early suicide in male high-risk attempters. (Vol. 113, pp. 44-47). *Psychiatry.*

Saper, C. B., & Lowell, B. B. (2014). The Hypothalamus. (Vol. 24 (23), pp. 1111-1116). *Current Biology.*

Schaaf, C. P., Gonzalex-Garay, M. L., Xia, F., ., Potocki, L., Gripp, K. W., Zhang, B., et al. (2013). Truncating mutations of MAGEL2 cause Prader-Willi phenotypes and autism. (Vol. 45, pp. 1405-1408). *Nature Genetics.*

Schumann, J., & Yaka, R. (2009). Prolonged withdrawal from repeated noncontigent cocaine exposure increases NMDA receptor expression and ERK activity in the nucleus accumbens. (Vol. 29 (21), pp. 6955-6963). *The Journal of Neuroscience.*

Seamans, J. K., & Yang, C. R. (2004). The principal features and mechanisms of dopamine modulation in the prefrontal cortex. (Vol. 74 (1), pp. 1-58). *Progress in Neurobiology.*

Shen, H. (2015). Neuroscience: The hard science of oxytocin. (Vol. 522 (7557), pp. 410-412). *Nature.*

Shiraishi, T., Oomura, Y., Sasaki, K., & Wayner, M. J. (2000). Effects of leptin and orexin-A on food intake and feeding related hypothalamic neurons. (Vol. 71, pp. 251-261). *Physiology & Behavior.*

Shoemaker, A., Proietto, J., Abuzzahab, M. J., Markovic, P., Malloy, J., & Kim, D. D. (2015). Randomized, double-blind, placebo controlled 4 week proof of concept trial of Beloranib resulted in rapid and significant weight loss in patients with hypothalamic-injury associated obesity. (Vol. 53, pp. LBS-095). *Endocrine Society's 97th annual meeting and expo.*

Simerly, R. B., Swanson, L. W., Handa, R. J., & Gorski, R. A. (1985). Influence of perinatal androgen on the sexually dimorphic distribution of tyrosine hydroxylase-immunoreactive cells and fibres in the anteroventral periventricular nucleus of the rat. (Vol. 40, pp. 501-510). *NeuroEndocrinology.*

Small, D. M., Jones-Gotman, M., & Dagher, A. (2003). Feeding-induced dopamine release in dorsal striatum correlates with meal pleasantness ratings in healthy human volunteers. (Vol. 19 (4), pp. 1709-1715). *Neuroimage.*

Soni, S., Whittington, J., Hollend, A. J., Webb, T., Maina, E., Boer, H., et al. (2007). The course and outcome of psychiatric illness in people with Prader-Willi syndrome: implications for management and treatment. (Vol. 51, pp. 32-42). *Journal of Intellectual Disability Research.*

Squires, L. N., Jakubowski, J. A., Stuart, J. N., Rubakhin, S. S., Hatcher, N. G., Kim, W. S., et al. (2006). Serotonin catabolism and the formation and fate of 5-hydroxyindole thiazolidine carboxylic acid. (Vol. 281 (19), pp. 13463-13470). *The Journal of Biological Chemistry.*

Stevenson, D. A., Heinemann, J., Angulo, M., Butler, M. G., Loker, J., Rupe, N., et al. (2007). Gastric rupture and necrosis in Prader-Willi Syndrome. (Vol. 45 (2), pp. 272-274). *Journal of Pediatric Gastroenterology.*

Succu, S., Sanna, F., Cocco, C., Malis, T., Boi, A., L., F. G., et al. (2008). Oxytocin induces penile erection when injected into the ventral tegmental area of male rats: role of nitric oxide and cyclic GMP. (Vol. 28 (4), pp. 813-821). *European Journal of Neuroscience.*

Swaab, D. F., Purba, J. S., & Hofman, M. A. (1995). Alterations in the hypothalamic paraventricular nucleus and it's oxytocin neurons (putative satiety cells) in Prader-Willi Syndrome: a study of five cases. (Vol. 80 (2), pp. 573-579). *The Journal of Clinical Endocrinology & Metabolism.*

Symons, F. J., Butler, M. G., Sanders, M. D., Feurer, I. D., & Thompson, T. (1999). Self-Injurious behaviour and Prader-Willi Syndrome: Behavioural forms and body locations. (Vol. 104 (3), pp. 260-269). *American Journal on Mental Retardation.*

Takayanagi, Y., Kasahara, Y., Onaka, T., Takahashi, N., Kawada, T., & Nishimori, K. (2008). Oxytocin receptor-deficient mice developed late-onset obesity. (Vol. 19 (9), pp. 951-955). *Neuroreport.*

Tennese, A. A., & Wevrick, R. (2011). Impaired hypothalamic regulation of endocrine function and delayed counter-regulatory response to hypoglycemia in Magel2-null mice. (Vol. 152 (3), pp. 967-978). *Endocrinology.*

Tiles, Y. (1995). Distribution of neurotransmitters in the sheep brain. (Vol. 49, pp. 199-220). *Journal of Reproduction and Fertility.*

Tran-Nguyen, L. T. L., Fuchs, R. A., Coffey, G. P., Baker, D. A., O'Dell, L. E., & Neisewander, J. L. (1998). Time-dependent changes in cocaine-seeking behaviour and extracellular dopamine levels in the amygdala during cocaine withdrawal. (Vol. 19 (1), pp. 48-59). *Neuropsychopharmacology.*

Van Vulpen, E. H. S., Yang, C. R., Nissen, R., & Renaud, L. P. (1999). Hypothalamic A14 and A15 catecholamine cells provide the dopaminergic innervation to the supraoptic nucleus in rat: a combined retrograde tracer and immunohistochemical study. (Vol. 93 (2), pp. 675-680). *Neuroscience.*

Volkow, N. D., Wang, G. J., Baler, R. D. (2011). Reward, dopamine and the control of food intake: implications for obesity. (Vol. 15 (1), pp. 37-46). *Trends in Cognitive Sciences.*

Wand, G. (2005). The anxious amygdala: CREB signalling and the predisposition to anxiety and alcoholism. (Vol. 115 (10), pp. 2697-2699). *J. Clinical Investigation.*

Wang, G. J., Geliebter, A., Volkow, N. D., Telang, F. W., Logan, J., Jayne, M. C., et al. (2011). Enhanced striatal dopamine release during food stimulation in binge eating disorder. (Vol. 19 (8), pp. 1601-1608). *Obesity.*

Willie, J. T., Chemelli, R. M., Sinton, C. M., & Yanagisawa, W. (2001). To eat or to sleep? Orexin in the regulation of feeding and wakefulness. (Vol. 24, pp. 429-458). *Neuroscience.*

Wren, A. M., Small, C. J., Ward, H. L., Murphy, K. G., Dakin, C. L., Taheri, S., et al. (2000). The novel hypothalamic peptide ghrelin stimulates food intake and growth hormone secretion. (Vol. 141 (11), pp. 4325-4328). *Endocrinology.*

Yamanaka, A., Beuckmann, C. T., Willie, J. T., Hara, J., Tsujino, N., Mieda, M., et al. (2003). Hypothalamic orexin neurons regulate arousal according to energy balance in mice. (Vol. 38 (5), pp. 701-713). *Neuron.*

Zajicek, K. B., Price, C. S., Shoaf, S. E., Mehlman, P. T., Suomi, S. J., Linnoila, M., et al. (2000). Seasonal variation in CSF 5-HIAA concentrations in male rhesus macaques. (Vol. 22, pp. 240-250). *Neuropsychopharmacology.*